Modification of angiogenesis
to abrogate abdominal aortic aneurysm growth

-

Modifikation von Angiogenese um das Wachstum
abdominaler Aortenaneurysmen zu beeinflussen

Doctoral thesis for a doctoral degree
at the Graduate School of Life Sciences,
Julius-Maximilians-Universität Würzburg,

Section Biomedicine

submitted by

Albert Franz Jakob Busch

from

Weiden i.d. Opf.

Würzburg **2020**

Submitted on: **March 31st 2020**

Members of the Thesis Committee

Chairperson: **Prof. Dr. Peter Heuschmann, Würzburg**

Primary Supervisor: **Prof. Dr. Christoph Otto, Würzburg**

Supervisor (Second): **Prof. Dr. Andreas Rosenwald, Würzburg**

Supervisor (Third): **Prof. Dr. Lars Maegdefessel, München**

Date of Public Defence:

Date of Receipt of Certificates:

"Let it burst"

Albert Einstein to his doctors in 1950 upon secondary expansion of his 1948 operated on aneurysm
He died on April 11th 1955

Out of the deep wish –
to, despite any personal ambition,
never stop listening and paying attention
to your patients, colleagues and especially beloved ones

The doctoral candidate is a board-certified Vascular Surgeon (BLAEK)
and
a Fellow of the European Board of Vascular Surgeons, FEBVS (UEMS)

He holds a medical doctorate (Dr. med.) from the University of Würzburg
and
a postdoctoral lecture qualification (Habilitation) from the Technical University Munich

Table of contents

1.   Thesis in an abstract

Introduction: Abdominal aortic aneurysm (AAA) is a pathological saccular enlargement most often of the infrarenal aorta. Eventual rupture is fatal, making preemptive surgical therapy upon a diameter threshold of >50mm the treatment of choice. The pathophysiology, especially the initial trigger aortic remodeling is still largely unknown. However, some characteristic features involved in aneurysm growth have been established, such as medial angiogenesis, low-grade inflammation, vascular smooth muscle cell (VSMC) phenotype switch, extracellular remodeling, altered hemodynamics and an eventual humoral immune answer. Currently, no medical treatment options are available. RNA therapeutics and drug repurposing offer new possibilities to overcome this shortage. Using such to target angiogenesis in the aneurysm wall and investigate their potential mechanisms is the aim of this thesis.

Material and Methods: We test our hypothesis by targeting the long non-coding RNA H19 and re-use the anti-cancer drug Lenvatinib in two murine inducible AAA models and one preclinical large animal model in the $LDLR^{-/-}$ pig. Furthermore, a $H19^{-/-}$ mouse is included to verify the results. AAA and control samples from a human biobank along with a primary human cell culture are used to verify results ex vivo by qPCR, WesternBlot, live cell imaging, histo- and immunohistochemistry along with gene array analysis, RNA knockdown, pull-down- and promotor assays.

Results: H19 is significantly upregulated in AAA mice models and its knockdown limited aneurysm growth. It is well known that H19 interacts with several transcription factors. We found that cytoplasmic interaction between H19 and hypoxia-inducible factor 1-alpha (HIF1α) increased apoptosis in cultured SMCs associated with sequential p53 stabilization. In contrast, the knockdown of H19 was associated with markedly decreased apoptotic cell rates. Our data underline that HIF1α was essential in mediating the pro-apoptotic effects of H19.

Secondly, Lenvatinib was applied both systemically and locally by endovascular means in mice with an established AAA. The drug significantly halted aneurysm growth and array analysis revealed myosin heavy chain 11 (MYH11) as the most differentially regulated target. This was shown to be up regulated after Lenvatinib treatment of primary AAA smooth muscle cells suggesting a salvage mechanism to obtain a contractile phenotype based on gene expression and immunohistochemistry. The same results were shown upon a local endovascular Lenvatinib-coated balloon angioplasty in the established aneurysmatic lesion of a novel atherosclerotic $LDLR^{-/-}$ Yucatan minipig model. Decreased phosphorylation of extracellular-signal regulated kinases 1-2 (ERK1-2) is the downstream effect of Lenvatinib-specific blockage of the vascular endothelial growth factor receptor (VEGFR2).

Conclusion: Taking into account the heterogeneity of the disease, inhibition of VSMC phenotype switch, extracellular remodeling and angiogenesis seem promising targets in some if not all AAA patients. Together with surveillance and surgical therapy, these new non-invasive treatment strategies would allow for a more personalized approach to treat this disease.

1. Die Arbeit auf einer Seite

Einleitung: Das abdominale Aortenaneurysma (AAA) ist eine Erweiterung der infrarenalen Aorta. Die größte Gefahr ist eine Ruptur, sodass eine präemptive chirurgische Ausschaltung ab 50mm Durchmesser empfohlen wird. Insbesondere die initialen Triggermechanismen zur AAA Entstehung sind weiterhin unklar. Einige charakteristische Eigenschaften des Aneurysmawachstums sind z.B. Angiogenese in der Media, *low-grade* Entzündung, die *vascular smooth muscle cell* (VSMC) Phänotyp-Änderung, Remodelling der extrazellulären Matrix, eine veränderte Hämodynamik und eine humorale Immunantwort. Gegenwärtig sind neben den chirurgischen, keine medikamentösen Therapiealternativen vorhanden. RNA-Therapien und *drug repurposing* könnten dies ändern. Ziel dieser Arbeit ist die Beeinflussung der Angiogenese, um das Wachstum von AAAs zu verändern.

Material und Methoden: Um diese Hypothese zu überprüfen wurden zwei verschiedene Ansätze verfolgt: Inhibition der long non-coding RNA H19 und die Verwendung von Lenvatinib in zwei Mausmodellen mit induzierbarem AAA und einem präklinischen Großtiermodell im $LDLR^{-/-}$ Schwein. Zusätzlich wurden Versuche in einer $H19^{-/-}$ Maus durchgeführt. AAA und Kontrollen aus einer humanen Biobank in Kombination mit der Verwendung einer primären Zellkultur aus AAA Patientenproben, wurden mittels qPCR, WesternBlot, *live cell imaging*, Histo- und Immunhistochemie sowie *Microarray* Analysen und RNA *knockdown* untersucht.

Ergebnisse: Wir zeigen, dass experimenteller knockdown von H19, mittels *antisense* Oligonukleotiden (LNA-GapmeRs) in vivo das AAA Wachstum signifikant einschränkt. In vitro reduziert dieser *knockdown* deutlich die Apoptoserate von menschlichen aortalen VSMCs. Mittels *array* Analyse wurde *hypoxia-inducible factor 1-alpha* (HIF1α) als Zielgen identifiziert. Zytoplasmatische Interaktion zwischen H19 und HIF1α führt zu einer Stabilisierung von p53. Dieser Mechanismus konnte auch in $H19^{-/-}$ Mäusen bestätigt werden, die nach AAA Induktion kein Aneurysma entwickelten.

Zweitens konnte Lenvatinib sowohl bei systemischer, wie auch bei lokaler Applikation in Mäusen mit etabliertem AAA deren Wachstum signifikant einschränken. In einer *Microarray* Analyse wurde hier *myosin heavy chain 11* (MYH11) als am deutlichsten verändertes Gen identifiziert. In primären humanen AAA Zellen war dies nach Lenvatinib Behandlung deutlich hochreguliert und deutet damit einen Erhalt des kontraktilen VSMC Phänotyps an. Der gleiche Effekt konnte im Großtiermodell nach lokaler endovaskulärer Behandlung mit einem Lenvatinib-*coated balloon* in einem neuen $LDLR^{-/-}$ Yucatan minipig Modell gezeigt werden. Reduzierte Phophorylierung von ERK1-2 ist das Ergebnis der Lenvatinib-spezifischen Blockade von *vascular endothelial growth factor receptor* (VEGFR2).

Schlussfolgerung: Zieht man die Heterogenität der Erkrankung AAA in Betracht, ist die Inhibition von VSMC Phänotyp Änderung, Remodelling der Matrix und Angiogenese möglicherweise ein guter Mechanismus um die Aneurysmen einiger Patienten zu behandeln. Diese neuen Ansätze werden möglicherweise in Kombination mit Überwachung und chirurgischer Therapie einen personalisierten Ansatz in der Therapie erlauben.

2. Introduction

2.1. The abdominal aortic aneurysm

The abdominal aortic aneurysm (AAA) is best defined as a diameter enlargement of 1.5 fold of the normal age- and sex-matched diameter.[1] With this being rather complicated, an aorta up to 15mm in diameter is considered to be of normal size, 15 – 30mm as ectasia and >30mm as aneurysmatic (**fig.1**). These numbers might differ slightly in women and Asian populations, having a lower mean baseline aortic diameter.[2]

Fig.1: 3D reconstructions from CT-angiograms: Different types of abdominal aortic aneurysms with different parts of the aorta being dilated are shown (source: own material from our department).

Once exceeding 30mm in diameter, the course of each patient's aneurysm is very distinct and difficult to predict. Some might grow rapidly over a short timeframe, whereas some might never grow any further.[3] On average an AAA would grow approx. 2.2mm/year in both men and women, increased by continued smoking and eventually decreased in the presence of diabetes.[4] However, with increasing diameter, the growth rate expands in a non-linear way from approx. 1.3 mm at 30mm diameter to approx. 3.6mm annual growth at 50mm.[5]

Based on these numbers, the well accepted European and US guidelines recommend annual ultrasound control of a known AAA and eventual CT-follow up for thoracic or thoraco-abdominal aneurysms before reaching a surgical threshold (**s. 2.1.2.**).[6, 7]

2.1.1. Epidemiology

Although aneurysmatic dilation can occur at any vessel and especially any part of the aorta, it is the abdominal aorta where approx. 80% of all aneurysms are seen.[8] This is followed by aneurysms of the ascending aorta (8%) and then descending aortic (4%) and thoraco-abdominal aortic (4%) aneurysms.[8] About 1% of aneurysms described and eventually operated on are seen in the visceral and peripheral arteries. The most frequent pathology here is the popliteal artery aneurysm which accounts for 4 out of 5 non-aortic aneurysms, followed by the hepatic and splenic artery aneurysms, only very rarely seen in daily practice.[9-11]

Additionally, a generalized vessel phenotype prone to aneurysm formation has been proposed several times with patients showing aneurysms at different localizations, yet no clear genetic link or consistent phenotype has been found.[12, 13]

For exact numbers of AAA patients please see **2.1.4.3**.

2.1.2. Clinical relevance

AAAs are usually clinically silent and often detected coincidently on abdominal ultrasound or CT angiography. The imminent threat of an aortic aneurysm is rupture, most often into the retroperitoneum (**fig.2A**), only rarely into the abdominal cavity, the vena cava or the small intestine. Symptoms or signs of an intact AAA, if present, are mainly pain or tenderness on palpation, localized to the AAA or radiating to the back or to the genitals. Symptoms may be related to complications, either by compression of nearby organs or distal embolism.[6] About 10% of patients admitted for AAA are supposed to be symptomatic.[14] Symptomatic AAAs compared to elective non-symptomatic AAAs have worse long-term survival, especially in women and 2fold increased risk of perioperative mortality.[15, 16] However, urgent repair is indicated due to a supposed prodromal state of rupture in these patients.[6] Whereas e.g. increased peak wall stress in aneurysms of such patients could be proven, no direct link to an increased rupture risk is currently available.[17, 18]
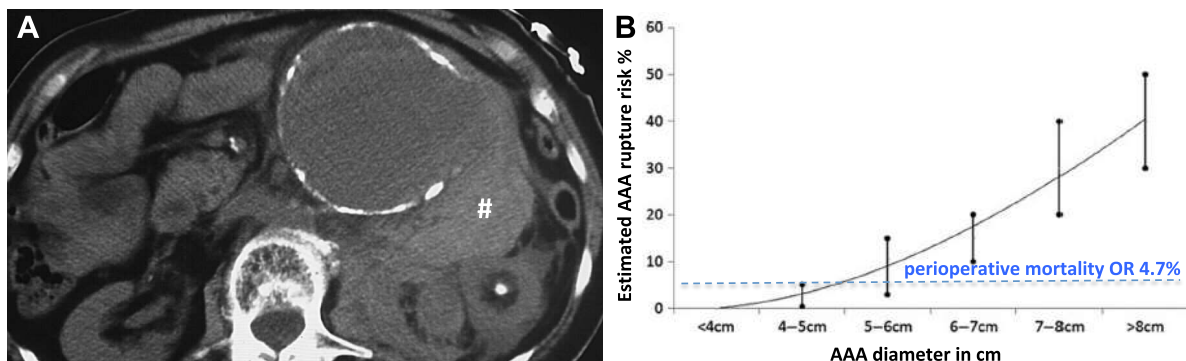
Fig.2: Ruptured AAA. CT-angiography showing an AAA with retroperitoneal rupture **(A)**. Note the interrupted aortic aneurysm wall and the large retroperitoneal hematoma **(#)** (author's own material). The annual risk of rupture increases with AAA diameter **(B)**. Currently the cut-off for surgical repair is based on comparison with the perioperative mortality from open repair (OR) (blue line) (graph modified from Chaikof et al.[19]).

For rupture, the signs are usually more dramatic (hemodynamic collapse, pallor, abdominal and/or back pain, abdominal distension, and rarely primary aorto-enteric or arterio-venous fistula). As mentioned above, the average growth rate increases non-linear with diameter, also increasing the risk of rupture (**fig.2B**).[6] Therefore, the cut-off for pre-emptive surgical repair is calculated in comparison to the risk of perioperative death undergoing open repair. Hence, the 2019 European and the 2017 US guidelines for AAA treatment recommend repair of non-symptomatic elective cases in men at 55mm diameter and in women at 50-54mm diameter.[6, 19] Naturally, for ruptured AAA immediate repair is recommended and for symptomatic AAA urgent repair within 24-72hours is recommended.

2.1.3. AAA pathogenesis

2.1.3.1. The non-aneurysmatic infrarenal aorta

The normal infrarenal aorta is a so-called elastic type artery and consists of three distinct layers: the intima, the media and the adventitia (**fig.3A/fig.4A**).

The intima is a thin layer comprising the internal elastic membrane, a thin subendothelial space with collagens type I, III and XVIII and finally the endothelium as a single cell layer with crucial barrier function allowing undisturbed blood flow. The latter is also the first to respond in case of vascular injury.[20] Endothelial cells (EC) have a high plasticity and various metabolic and signaling functions. Hence endothelial dysfunction is defined as an altered phenotype with impaired vasoreactivity and an eventual thrombogenic surface.[21]

The media consists of a varying number of 20-50 layers of helically interwoven elastic fibers made of elastin. Elastic fibers and fibrillar collagen comprise approx. 50% of the dry weight of larger arteries.[22] In between are the vascular smooth muscle cells (VSMCs) in single layers. This combination allows the aorta to exert its "Windkessel" function to propulse the blood volume and pulse wave ejected from the left ventricle with every heartbeat.[20, 23] Up to approx. 30 units of elastic layer and VSMC layer, sufficient oxygen supply is provided by diffusion from the luminal blood. Everything above requires vasa vasorum for nutritional supply.[20] The normal contractile apparatus of a VSMC consists of a variety of specific proteins dominated by α-smooth muscle actin and myosin as well as vimentin, desmin and others.[24] In addition to their contractile function, VSMCs have a high plasticity, especially in response to eventual damage or stress.[25, 26]

The adventitia contains fibroblasts, some elastic fibers and collagen type I and III. Here is where private vessels (vasa vasorum), vessel nerves and lymphatic vessels lie.[20] Naturally, the adventitia is a vascular surgeon's best friend, since this is the only layer remaining after a thrombendarterectomy has been performed to resect e.g. stenosis in a heavily calcified vessel.

This very orderly anatomy is subject to severe changes as observed in AAA specimen (**fig.3A/B/fig.4**). These observations described in detail below are, however, limited by the restricted access to tissue samples from advanced stages of disease. Since patients with ectasia or small aneurysms never get operated on, not much is known

about the specific hallmarks of such early disease. Additionally, the initial trigger of aneurysm formation remains elusive and can only be speculated on (**s.2.1.3.9.**).
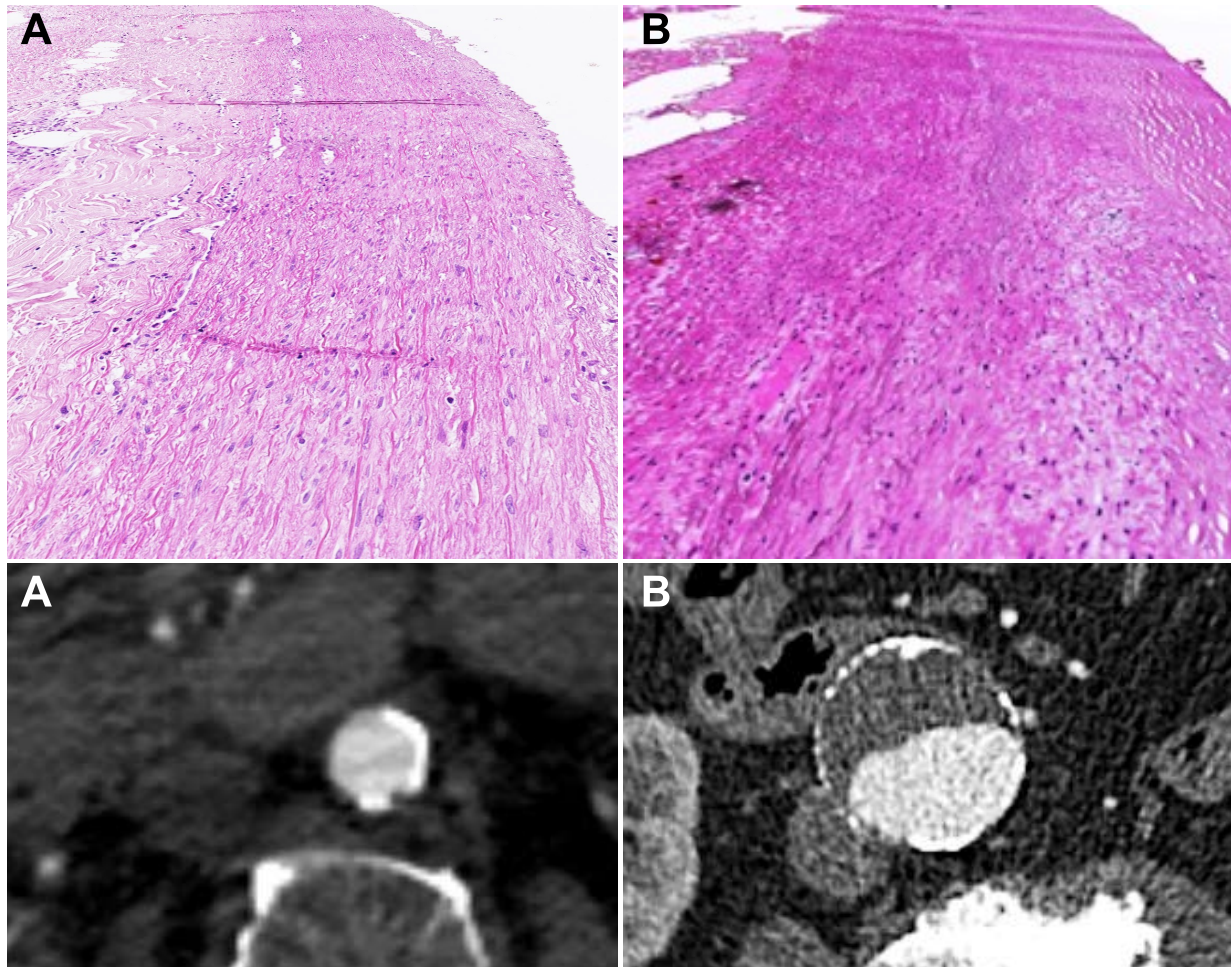
Fig.3: Comparison of normal aorta and AAA: The non-aneurysmatic infrarenal aorta **(A)** has a contained structure with approx. 28 layers of elastic fibers with VSMC in between (upper row). No intraluminal thrombus (ILT) and some calcification of the aortic wall is seen on CT-angiography (lower row). In AAA **(B)**, the aneurysm wall shows a more diffuse organization of the layers with less cells and more extracellular matrix content (upper row). On CT, the circumference is unevenly covered with ILT (lower row). (source: own material from laboratory and clinical unit)

2.1.3.2. Fibrosis

Fibrosis, e.g. collagen deposition of the aortic wall, is a key feature of AAA and has led to a grading based on fibrosis and inflammation by Rijbroek et al. in 1994.[27] These changes are however seen with great variance between individuals, but seem to be independent of AAA diameter or sex.[24, 28, 29]

The adventitia can also be the site of an important fibroblastic reaction, probably driven by transforming growth factor β (TGFβ), leading to collagen accumulation, and thus delaying the risk of rupture.[1] Fibroblasts play a critical role in the adventitial response and secrete procollagen-1.

Such fibrosis, however, usually remains limited to the aortic wall and does not affect the surrounding retroperitoneum.[28] The typical collagen I/III predominance in the normal aortic wall is altered towards deposition of different types of mature and

premature collagens with hence a deficit in crosslinking.[30] While elastin is fragmented or absent, the amount of collagen increases and the number VSMCs, as well as their phenotypic function, changes significantly, rendering the above described mechanical aortic function towards a stiffer tube.[31, 32] Again, this composition of the extracellular matrix and VSMCs seems to be independent of diameter (**fig.4B**).[33]

However, changes differ depending on the amount of thrombus coverage of the aortic wall.[34]

2.1.3.3. Intraluminal thrombus formation

The intraluminal thrombus (ILT) is a biologically active compartment with a laminated structure, containing several layers of fibrin clot, underlying a fresh, red hematic luminal layer containing undegraded cross-linked fibrin and an actively fibrinolysed abluminal layer.[1] A multitude of canaliculi allows passive and active transport between the ILT and the aortic wall.[35] The luminal layer is highly biologically active and releases free hemoglobin and fibrin formation secondary to platelet and thrombin activation (**fig.4D**). Tissue-plasminogen activator and plasminogen and neutrophils are also trapped here (**s.2.1.3.9.**).[36] These proteins in combination with the neutrophil enrichment are considered to be the major source of active matrix metalloproteinases (MMPs), elastase and other serine proteases and correlate positively with thrombus volume.[37, 38] The amount of proteases and plasma proteins found within the aortic wall correlates strongly with AAA growth.[39] Haller et al. have demonstrated that smaller AAAs with less ILT layers rupture earlier than bigger aneurysms where the aortic wall is farther away from the biologically active luminal layer.[40] Concordantly, higher oxidative stress in the aortic wall has been linked to thinner thrombus coverage.[41] In general, a declining gradient of active enzymes from inner to outer layers must be considered.[42] Higher circulating levels of fibrin degradation products such as D-Dimers in AAA patients suggest a constant fibrinolysis at the thrombus site.[43]

From a mechanical view, the ILT, apart from its biological role (s. above) must be considered a viscoelastic element mediating peak wall stress aneurysm growth.[44, 45] Approx. 30% of the thrombus are fluids, making it a porous diluted structure (biphasic solid-fluid material).[46, 47] Thus, hemodynamics on the aortic wall vary depending on the amount of thrombus (**fig.4C**).[34] The ILT and the aneurysm wall harbor the blood pressure difference from intraluminal (e.g,100 mmHg) and the interstitial pressure in the adventitia (10 mmHg).[40] Of note, up to 5% of AAAs do not show any ILT. Vice versa, the thrombus apposition depends on hemodynamics and is unevenly distributed over the AAA circumference.[48]

2.1.3.4. Altered hemodynamics

Hemodynamic forces relevant to AAA pathogenesis are wall shear stress (WSS), the tangential force exerted by moving blood along the axis of flow, hydrostatic pressure, the perpendicular force acting on the vascular wall and relative wall strain (RWS), the circumferential stretch of the vessel wall exerted by cyclic luminal pressure changes and the resulting tensile stress (**fig.4C**).[49]

The physiological centrifugal convection in the aorta is disturbed in AAA due to the ILT, the lack of endothelium, elastic fiber degradation and a high amplitude of pulsatility due to dilatation.[50] The latter might be influenced by iliac outflow, e.g. due to stenosis or major amputation, causing aneurysm bulging and tortuosity.[51, 52] In experimental studies, simulation of blood flow was used as one out of many parameters to predict directional growth of AAAs.[53] Such hemodynamics interact closely with the ILT and vice versa, ILT thickness depends on wall shear stress.[54]

The hemodynamic alterations described must be considered in combination with the above-described local changes in the aortic wall. Especially reduced distal aortic elasticity, in combination with augmented pressure due to pulse wave reflections from the aortic bifurcation and other downstream arteries, may increase wall strain and aneurysm susceptibility.[49] Many of the following cellular effects have been shown to be altered under the influence of varying hemodynamics.

Interestingly, Suh et al. published on preliminary data on how exercise-induced alteration of blood flow might stabilize AAA growth.[55]

2.1.3.5. Proteolysis vs. synthesis

In a non-aneurysmatic aorta, there is a physiological balance with an equilibrium of proteolytic and synthetic enzymes orchestrating a turnover of cells and extracellular matrix (ECM).[56] However, this balance is gradually changed in AAA with supremacy of proteolytic enzymes and cells.[37]

The phenotypic switch of VSMCs has a crucial role in this. Losing their contractile abilities, they show secretory properties concerting the proteolytic nature of macrophages, neutrophils and mast cells.[57] MMPs, produced by neutrophils are the main effector of this imbalance (**fig.4E**) (reviewed in detail[37]). Naturally, their counterparts, tissue inhibitors of MMP (TIMPs), are to dampen the effect, but these are significantly reduced in the aneurysm wall.[58] Further proteases, released during AAA formation, include cathepsins stored in mast cell granules.[59] In addition to the above-mentioned oxidative stress from the luminal layer of the ILT, neutrophil myeloperoxidase creates further reactive oxygen species within the aneurysm wall.[60] These are also activators of MMPs.

MMP2 and 9 are the two most critical players in AAA development. MMP2 is predominantly derived from VSMCs and fibroblasts, whereas MMP9 is predominantly derived from macrophages and to a lesser extent neutrophils.[37] Macrophages are recruited mostly from circulating monocytes, however, recently this has been challenged by the concept of trans-differentiation of e.g. VSMCs to macrophages.[61, 62] Exposure to elastin breakdown products has been shown to trigger phenotype switching towards the M1 phenotype, considered pro-inflammatory.[24, 63]

2.1.3.6. Humoral immune answer

T- and B-cells are found in abundance in the aortic wall.[24, 64] Since B-cell clonality is observed, extensive research has been conducted to provide an exogenous (**s.2.1.3.9.**) or intrinsic pathogen (e.g. oxidized low density lipoprotein) triggering this.[65]

In a minority of cases, lymphoid follicle-like structures are seen in the adventitia with T-cell subpopulations, B-cells, dendritic cells and macrophages accumulating. This is referred to as vascular associated lymphatic tissue (VALT), however, its role in AA is unclear (**fig.4G**).[66, 67]

AAA tissues also contain large amounts of immunoglobulin protein and IgG extracted from human AAAs exhibits immune-reactivity with aortic wall matrix proteins.[68] Recently, our group demonstrated that absence of IgG results in an increased severity of aneurysm formation in mice.[69] The triggers of adaptive immunity in AAAs are unknown and immune responses against aortic wall structural components may arise secondary to long-standing inflammation and connective tissue destruction through proteolytic exposure of neo-epitopes.[68] While some active forms of complement factors are seen, the role of the complement cascade in AAA remains largely unknown.[70]

Conflicting experimental results suggest both a pro-inflammatory component of this innate immune answer – but even more important, a macrophage mitigating clearance of inflammation, eventually promoting tissue healing (modified from[68]).[71]
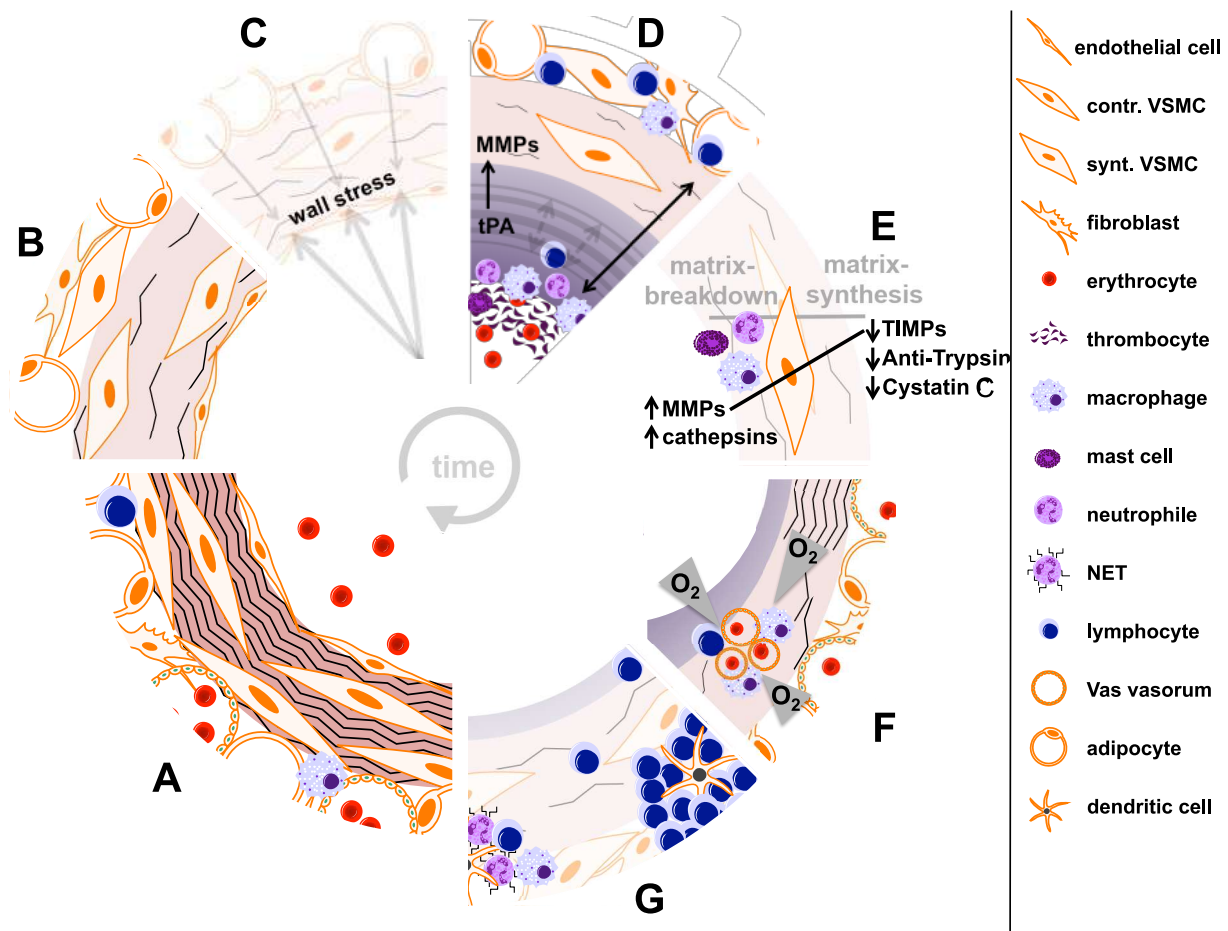
Fig.4: AAA Pathomechanisms: The normal aortic wall **(A)** changes its morphology over time upon AAA formation. Samples from open repair show distinct pathologic features: medial disruption and fragmentation of elastic fibers with fibrosis and wall thickening **(B)**; rarefication of VSMCs and the elastic units along with calcification changing hemodynamics **(C)**; ILT formation in most aneurysms with a layered structure and an enzymatically active luminal surface **(D)**; proteolytic imbalance with MMP up-regulation orchestrated by VSMCs, macrophages and mast cells **(E)**; hypoxic micromilieu with adventitial and medial neoangiogenesis allowing homing of inflammatory cells in the media **(F)**; infiltration of B-/T-cells with formation of tertiary lymphoid structures **(G)**; (modified from Busch et al.

2018[72]) (tPA=tissue-type plasminogen activator; MMP=matrix metalloproteinase; TIMP=tissue inhibitor of MMP; VSMC=vascular smooth muscle cell; NET=neutrophil extracellular trap;)

2.1.3.7. Angiogenesis

In 1995, Holmes et al. first reported on medial neovascularization in abdominal aortic aneurysms as a histopathologic marker of AAA, increased in comparison to patients with occlusive disease.[73]

Our group has previously demonstrated that the thickness of the aneurysm wall depends on the amount of inflammation, the number of CD34 positive cells and vessels increases with wall thickness.[24] Increased expression of hypoxia inducible factor 1α (HIF1α) as reported by others and us suggests a hypoxic micromilieu in the thickening aneurysm wall with vascular endothelial growth factor (VEGF) and its receptors (mainly VEGFR1 and R2) mediating further downstream mechanisms.[74, 75] HIF1α is supposed to be secreted mainly by adventitial fibroblasts and VSMCs (**fig.4F**).[76, 77] Alterations in the HIF-pathway have also been suggested to be crucial for other disease entities involving the arterial vessel wall.[78]

Additionally, there is similar data for ascending and thoracic aortic aneurysms.[79, 80] Recently, angiogenesis has been tracked by non-invasive imaging techniques using specific MRI tracers and has been suggested to be important for rupture risk prediction.[81, 82] On an experimental background, blockage of VEGF has been shown to decrease aneurysm growth in mouse models.[83]

Of note, little is known about lymphangiogenesis in AAA. Immunohistochemical studies identified inflammation-dependent infiltration of lymphatic vessels in the media and adventitia probably resulting in insufficient lymph drainage.[84, 85]

2.1.3.8. Aneurysm and atherosclerosis

Atherosclerosis to a greater or minor extent is observed in almost every AAA patient and the associated diseases like coronary artery disease and carotid artery disease, as well as, peripheral arterial occlusive disease (PAOD) are observed more frequently in this cohort.[86, 87] Hence, vascular surgery textbooks typically classify the origin of aneurysms with one category being "idiopathic/atherosclerotic".

Thus, it is justified to look for similarities in both conditions. However, AAA is observed in patients with different degrees of atherosclerosis and not every patient with severe infrarenal sclerotic lesions suffers from AAA – on the contrary, some might even experience aortic occlusion. In addition, many different aortic diseases, such as dissection, penetrating ulcer or intramural hematoma are independently associated with the degree of atherosclerosis and typical high risk factors for both diseases vary considerably.[88, 89]

Atherosclerosis is commonly considered a disease of the intima, since the early stages of the disease are seen here.[90] AAA on the other hand is considered a disease of the media based on the early changes observed in animal models since human early stage material is missing (**s.2.2.**).[1, 70]

Similarly, VSMC phenotype switch (**s.2.1.3.2.**) is observed in both diseases, however, probably to a different extent and with heterogeneous clonality.[25, 91] Concordantly, the role of T- and B-lymphocytes, observed in both atherosclerotic and dilated aortas, is a matter of discussion.[90] Experimental screening studies comparing tissue or plasma samples from patients with the respective disease have also found inflammatory processes or markers as the least common denominator.[92-94] Considering the variability of inflammatory processes and the plethora of inflammatory markers, this data can on the other hand also be interpreted to mark AAA and atherosclerosis as different entities.[89] In a small study, McMillan et al. found higher MMP9 plasma levels in AAA patients compared to PAOD patients and healthy volunteers.[95] Shireman et al. found differing levels of tissue-type and urokinase-type plasminogen activator (tPA/uPA) (**s.2.1.3.9.**).[96]

2.1.3.9. Speculations on the origin of AAA

Why does the majority of aneurysms occur at the infrarenal part (**s.2.1.1.**) of the aorta? The answer to this question remains largely elusive and open for speculation.

Since no gene with e.g. tissue-specific expression was identified to be responsible for AAA formation (s.2.1.3.10.), the next consideration is the special hemodynamic situation at the aortic bifurcation continuing to the iliac vessels. A variety of studies have suggested disturbed flow at the aortic bifurcation, probably in combination with previous atherosclerosis leading to endothelial "micro damage" propagating medial disruption.[97, 98] Such flow conditions could also cause an initial ILT formation according to Virchow's triad.[99]

Again, a central role falls probably to VSMCs. Experimental data from animals and human tissues suggest a unique phenotype of the aortic VSMC in comparison to others, eventually causing early elastin disruption enhanced by accidental macrophage homing.[100, 101] This uniqueness is also reflected by the origin of cells in this specific part of the aorta. The infrarenal aorta is derived from the splanchnic mesoderm in comparison to the aortic bulb (second heart field), the aortic arch (cardiac neural crest) and the descending and visceral segment of the aorta (somatic mesoderm.[102] This comes with a distinct responsiveness to various stimuli, such as TGFβ signaling, early in embryogenesis, but also later during adult life.[103, 104]

However, primary triggers might also appear via private vessels and e.g. extravasation of inflammatory agents or cells.[56] This might e.g. be the origin of bacterial antigens triggering a low-grade inflammation speculated to be responsible for aortic dilation as exogenous weak pathogens.[1] In the past, various bacterial pathogens such as *C. pneumoniae, P. gingivalis* or *S. mutans* have been described but could never be proven.[105, 106]

Another theory is a transient local proteolytic imbalance causing initial tissue destruction. This might happen in the endothelium or in the media. In the endothelium, cleavage of human plasmin or collagen XVIII (part of the infrarenal aortic basement membrane) would lead to the enzymatically active cleavage products angiostatin and endostatin resulting in endothelial cell (EC) apoptosis and inflammation.[107-109]

2.1.3.10. Risk factors associated with AAA

Nicotine consumption, dyslipidemia, male gender, age >65 years, genetic predisposition and possibly also Caucasian descent are established risk factors for AAA formation.[1, 6] These originate from big retrospective association studies and only very rarely have a biological background regarding AAA.

As such, diabetes mellitus, in the absence of positive association often called "aneurysm-protective", causes glycosylation of the ECM proteins and thus an increased stability of the aortic wall. This effect was particularly seen in patients under metformin (**s.2.1.5.**).[110, 111]

Genetic predisposition means an increased prevalence in a first- and second-degree relative of an AAA patient. A brother or son might have a 2fold increased risk of also developing an aneurysm.[112, 113] Genome wide association studies (GWAS) have identified a couple of risk alleles, such as LDLR, LRP1, DAB2IP, DCKNB-AS1 or CNTN3 in AAA individuals, however a universal candidate actually causing the disease could never be verified.[114-118] The disease must therefore be considered polygeneic.[119] Exemptions are patients with genetic diseases resulting in a weakened aortic wall as seen in Marfan, Ehlers-Danlos or Loeys-Dietz syndrome, eventually presenting with aortic aneurysms.[120-122]

Nicotine has been identified as risk factor with the highest odd's ratio for AAA development.[123] Molecular mechanisms include an impaired endothelial nitric oxide synthesis and production of MMPs and α1-anti-trypsin, hence pro-proteolytic processes. It is highly probable that smoking is a more detrimental risk factor in women than in men, perhaps modulated by the effect of smoking on reproductive function in women.[70, 124] Additionally, in both sexes, continued smoking accelerates aneurysm growth above the normal rate of 2.5mm/year in aneurysms 4-5cm in diameter.[125]

As described above, the likelihood of having an AAA increases with age, making age an independent risk factor. Additionally, longer telomere lengths were shown to be associated with a decreased risk of AAA.[126] Low HDL, independent of total cholesterol, is associated with the presence of AAA.[127] As precursor in the 5-lipoxygenase signaling pathway, it is crucial for inflammatory processes in the vessel wall.[128]

2.1.3.11. Aneurysm rupture

Molecular studies in ruptured aneurysms must be interpreted with caution, since samples taken from the rupture site – if identified at all, vary in location and distance and reporting is not standardized.[129]

Wilson et al. reported a locally increased expression of MMPs1/8/9 in ruptured AAAs, hence speculating on a dysbalanced proteolysis.[130, 131] The same group demonstrated these findings to be independent of inflammatory activity in the aortic wall in general.[132]

In general, contradicting results have been reported for inflammatory cells, cytokines and pathways, which seem to vary on genetic, protein and cellular levels.[133] When comparing AAA histology to peak wall stress via finite element analysis, rupture is associated with higher "disintegration" of the wall represented by lower VSMC and elastic fibers number and increased plaque number with more calcification.[134] With

increasing calcification, the load bearing capacity of the aortic wall is reduced.[135] Also angiogenesis and hypoxia are speculated to be up-regulated at sites of rupture, eventually resulting in altered intracellular energy homeostasis affecting protein synthesis.[136, 137] Additionally, increased FDG-uptake upon PET-CT imaging at the rupture site might point towards increased cellular activity.[138] A study comparing ruptured and intact cerebral aneurysms identified a higher density of the M1 subtype of macrophages thought to be pro-inflammatory.[139] Our group however, also demonstrated this for intact AAA.[140]

In general, rupture seems to involve more than a mere physical aspect of a non-withstanding containment due to increased wall stress, but the exact factors remain unknown.[17, 141]

2.1.4. Current treatment

2.1.4.1. Open surgical aortic repair

The word "aneurysm" is derived from the ancient greek word for "widening". The first documented description of an aneurysmal pathology appears ca. 1550 BC in the Papyrus Ebers.[142] The term "aorta" was first applied by Aristotle in the 4th century BC. In the 3rd century, Antyllus introduced a method of aneurysm ligation.[143] However, only with the birth of modern surgery in general in the early 19th century, also vascular surgery advanced.

Sir Astley Cooper was the first to ligate the abdominal aorta for a ruptured iliac aneurysm in 1817 – however, the patient survived only four hours.[144] A major advance in the treatment of aneurysms came in 1923 with Rudolf Matas's concept of endoaneurysmorrhaphy after gaining proximal and distal bleeding control as a modern concept in vascular surgery. Henceforth, preservation of blood flow and an intact circulatory system were dogmas.[142] In 1944, Crafoord et al. published the first ever aorto-aortic anastomosis in a patient with aortic coarctation.[145] And in 1947 Rea et al. suggested a technique of external wrapping of aneurysms in cellophane.[146] This procedure was finally performed on Albert Einstein by Rudolf Nissen and he survived for 5 years.

Modern AAA surgery, still in large parts unchanged, started in 1951 when C. Dubost first resected the aneurysm and then made a graft interposition (**fig.5**).[147] After looking for the right graft material, this procedure soon became the standard of treatment and in 1953 Cooley and DeBakey published >200 procedures, shortly followed by Crawford et al., bringing the 30-day-mortality to under 5% narrowing in on our modern day standard.[143, 148] Attempts at full laparoscopic and laparoscopic assisted AAA repair have been made, but never reached clinical relevance.[149, 150]

Thus, open repair of AAA as performed today is a technique developed and evaluated for over almost 70 years (**table I**). Along with the improvement of anesthetics and complimentary care immediate, and long-term results are good and well accepted (**fig.6**).
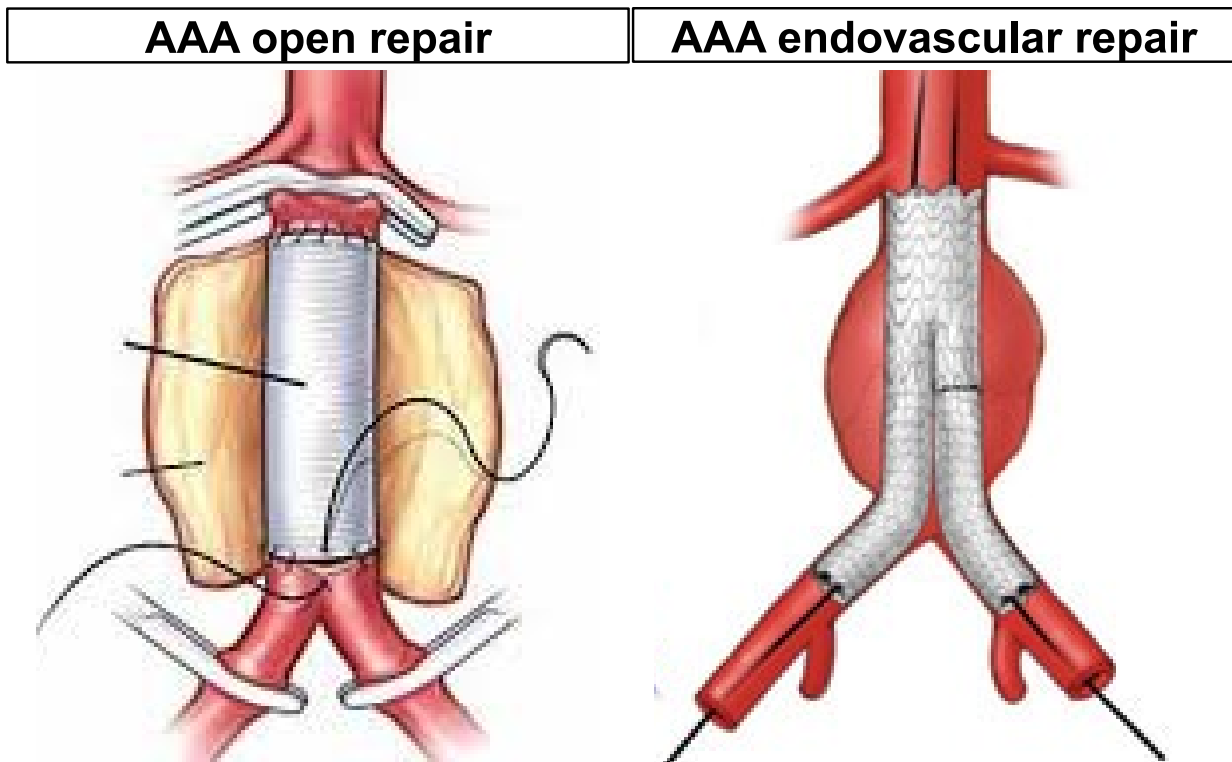
AAA open repair	AAA endovascular repair

Fig.5: Graphic depiction of the two AAA repair procedures: open repair (OR) and endovascular aortic repair (EVAR) (https://www.mayoclinic.org/ und http://www.uhs.nhs.uk/Media/**)**

2.1.4.2. Endovascular aortic repair

In 1964, C. Dotter performed the first endovascular balloon angioplasty of the superficial femoral artery as a vascular procedure from a remote access site.[151] After Werner Forßmann's 1929 first right heart catheter examination, this must be considered the beginning of the non-cardiac endovascular era.[152]

In 1984, unfortunately behind the iron curtain and thus not visible to the western world, Nikolay Volodos published his first implantation of a stentgraft into the thoracic aorta from a bilateral femoral access and in 1987 into an AAA.[142, 146] In 1991 finally, Julio Palmaz and Juan Parodi took the fame in the western world after implanting a primitive stentgraft consisting of a Dacron tube with a proximal fixation by a Palmaz stent.[153] Ever since, physicians and the medical device industry have driven and accelerated the development of this technique hand in hand: in 1994, the first bifurcated graft was implanted (**fig.5**). Rapid improvements including suprarenal fixation, fenestrations, branches, scallops, iliac branches and endo-anchors followed.[142, 154]

Today EVAR is a standard procedure that has long surpassed open repair in broad applicability in both intact and ruptured AAA (**fig.6**). Introducing total percutaneous access, preemptive AAA exclusion is not limited to vascular surgeons any more, but also performed by interventionalists.[155] However, since the AAA is not completely excluded from the circulation and the aortic branches (inferior mesenteric artery, lumbar arteries) remain open, specific complications, e.g. endoleaks have to be considered and patients have to undergo scheduled lifelong follow-up imaging.[6]

	Advantage	Disadvantage
EVAR	- in-hospital mortality 1% - reduced mortality in rupture - less invasive - discharge after 2-3 days - percutaneous access possible - no general anesthesia required	- longevity of material unclear - graft migration - endoleaks - secondary rupture - life-long follow-up: radiation/cost - cost-effectiveness unclear - high re-intervention rate - increased cancer risk?
OR	- longevity of material/results good - no radiation - no follow-up necessary - higher in-hospital complication rates	- proximal/distal anastomotic aneurysm - incisional hernia in 20% - possible impotence - in-hospital mortality 2-5% - longer hospital/ICU stay

Table I: Comparison of endovascular aortic repair (EVAR) and open repair (OR).

2.1.4.3. Clinical practice in Germany

In Germany, according to the Federal Bureau of Statistics, approx. 24.000 patients are admitted annually to a hospital with the diagnosis AAA (based on the ICD10 code I71.x). Thereof, 15.000 undergo AAA surgery, either open repair (OR) or endovascular aortic repair (EVAR), and approx. 2.000 patients are operated in the state of rupture (status quo 2014).[156] Since the effectiveness of AAA screening programs has been proven useful in many countries and is being offered with increasing density, AAA ruptures have declined, whereas surgery for intact AAA has increased (**fig.6A**).[6, 157]

While the overall prevalence since the 1970s due to improved diagnostics and changing disease awareness has risen, it has fallen back somewhat in recent years.[158] This could be due to the change in smoking behavior as the main associated risk factor.[159, 160] Worldwide, AAA is thus among the 20 leading causes of death, with prevalence in western countries slightly decreasing, whereas in many developing countries it is progressive.[161, 162]

In the last years, as mentioned above, the in-hospital mortality has gone down in both men and women receiving either OR or EVAR, even if corrected for the type of procedure applied (**fig.6B**).[156] However, the percentage of EVAR in both intact and ruptured AAA has significantly increased over the last years, with EVAR outperforming OR approx. 10 years ago (**fig.6C**).[163] In Germany, approx. 500 hospitals are performing aortic procedures, yet there is good evidence, that outcome is clearly associated with the number of procedures performed annually.[164] This is currently not reflected by legislative authority.

Despite the short- and midterm advantages and better survival of EVAR patients, adding to the ongoing debate of which procedure to be applied preferentially, we have learned in past years, that upon long-term follow-up, OR seems to outperform EVAR (**fig.6D**).[165] All major studies comparing both procedures that have reported 10 and 15 years follow-up see no advantage of EVAR, but a significantly higher re-intervention

rate and procedural or aneurysm-related death rate.[166, 167] Only in ruptured cases, after surviving the initial procedure, EVAR is clearly superior, however, only when EVAR is possible without too many compromises.[163, 168]
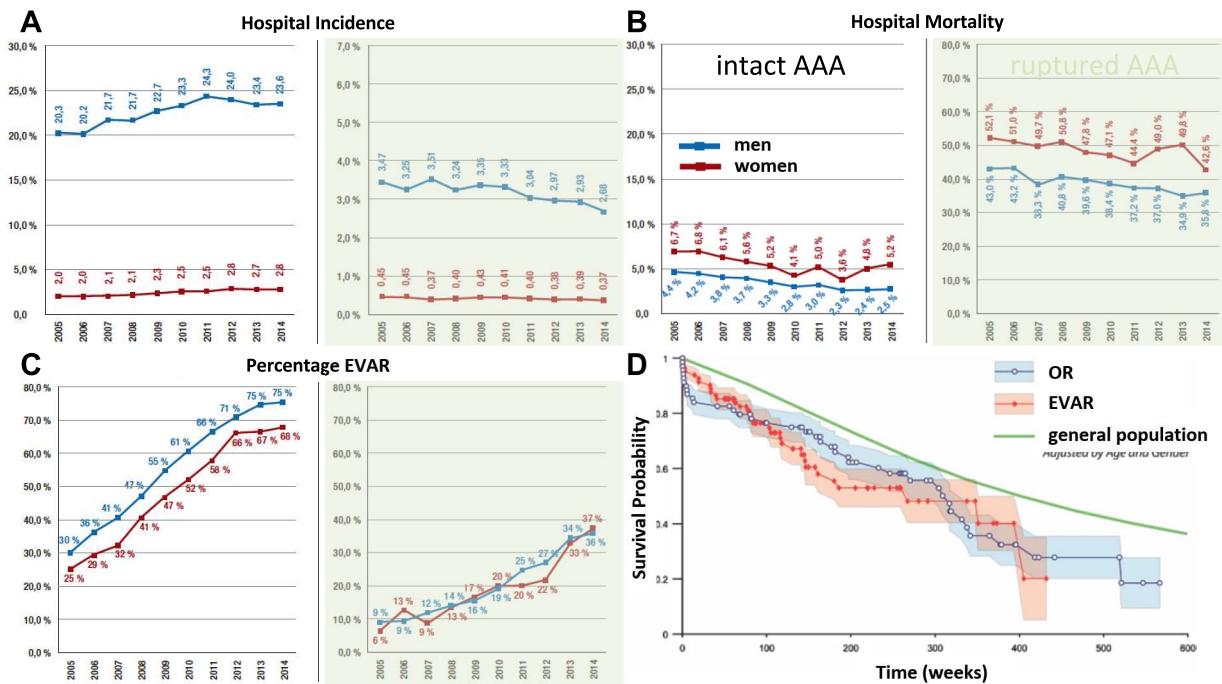
Fig.6: Comparison of OR and EVAR incidence and outcomes. Explanations in the text. Graphs are modified from Kuhnl et al. and Paolini et al.[156, 165]

2.1.5. Overview and shortcomings of previous non-surgical treatments

In the past 20 years, a variety of drugs have been tested for the treatment of AAA in human trials, mostly to abrogate growth. Some of them are based on experimental trials from animal models, some have been proposed by observations of associated concurrent treatments (e.g. hypertension). Recently, a timely and accurate review has been performed by Lindeman et al. in Circulation Research in 2019.[169] This provides the basis for the following overview and critical appraisal (**table II**).

Included here are only in-man studies that have reported outcomes on AAA growth rates or rates of rupture.

Most of the studies from **table II** report on AAA growth measured by either CT or ultrasound with an anticipated growth of approx. 2mm/year as a natural growth rate. However, both, CT and ultrasound have a threshold of 2-5mm false diameter measurement depending on the cardiac cycle and the observer, respectively.[6] Basically, none of the listed studies report on a core lab analysis of radiological data or similar to overcome this issue.

Another critical point is that most of the above-mentioned studies have their origin in studies in mouse models poorly taking into account the numerous limitations and specific time-dependent features of those models (s. 2.2.7.).[169-171]

drug of interest	type of study	major findings
Propanolol β-blocker	case-control studies 2 x RCT	- poor adherence to propranolol[172, 173] - underpowered for endpoint - no effect on AAA growth[172]
Ramipril, Perindopril ACE-inhibitor	case-control studies 1 RCT	- contradictory results in studies[174, 175] - no effect on AAA growth[176]
Simva-/Atorvastatin statin	retrospective studies case-control studies	- beneficial to cardiovascular risk - no effect on AAA growth[169, 177]
Aspirin NSAID/anti-platelet	cohort studies	- contradictory results in studies[178] - no effect on AAA growth[177, 179]
Metformin anti-diabetic	retrospective studies	**- decreased AAA growth**[110, 111]
Roxy/Azithromycin macrolide antibiotic	case-control studies	- underpowered for endpoint - no effect on AAA growth[169]
Doxycycline tetracycline antibiotic	case-control studies 1 RCT	- reduced MMP expression - contradictory results in studies[180, 181] - eventually dose dependent effect[169]
Pemirolast mast cell stabilizer	case-control study	- no effect on AAA growth[182]
Canakinumab IL-1β neutralization	case-control study	- no effect on AAA growth[169]

Table II: Completed studies on pharmacological treatment to abrogate AAA growth. Wherever RCTs are available, only those are included in the table. For further reference including non-RCT studies, please see reference.[169] (ACE = angiotensin converting enzyme; NSAID = non-steroid anti-inflammatory drug; MMP = matrix metalloproteinase)

Additionally, there are currently some trials recruiting for this very purpose of non-surgical aneurysm treatment (**table III**). Although some have been completed, no results have been reported yet.

drug of interest	name	status	type of study
Telmisartan AT$_1$ – R antagonist	TEDY	recruiting	case-control study (22 patients)
Doxycycline tetracycline antibiotic	N-TA(3)CT	completed	RCT (261 patients)
Metformin anti-diabetic	-	enrolling by invitation	single center RCT (170 patients)
Metformin anti-diabetic	MAAAGI	recruiting	RCT (500 patients)
Metformin anti-diabetic	-	not yet recruiting	two more studies currently planned
Eplerenone spirolactone	-	unknown	RCT (172 patients)
Ticagrelor anti-platelet	-	completed	case-control study (145 patients)
Cyclosporine A immune-supressive	-	unknown	RCT (360 patients)

Table III: Currently active studies on pharmacological treatment to abrogate AAA growth. This list is based on a thorough research on clinicaltrials.gov (January 2020).

2.2. Animal models in aortic aneurysm research

Over the last 15 years, a variety of animal models for the purpose of AAA research has been proposed. Those will be reviewed here in detail and their advantages and disadvantages are summarized in **table IV**.

2.2.1. Angiotensin II model

Although based on the initial description of aortic lesions in angiotensin II overloaded mice by Nishijo et al. in 1998, the model as we know it today is attributed to Daugherty et al., who published on "Unexpectedly, pronounced abdominal aortic aneurysms were present in *ApoE*$^{-/-}$ mice infused with Ang II" in 2000 while looking for a way to increase blood pressure in atherosclerotic mouse models (**fig.7D**).[183, 184]

The model is based on the subcutaneous infusion of angiotensin II via surgically implanted osmotic mini-pumps in a concentration of 1000ng/kg bodyweight/min into *ApoE*$^{-/-}$ mice. Mice can be either *ApoE*$^{-/-}$ or *LDLR*$^{-/-}$ best given a fat enriched diet. Although hypercholesterolemia is not specifically needed, it increases the incidence of the phenotype by 3-4x.[185] Development of AAA also occurs in C57BL/6 mice, the background of e.g. *ApoE*$^{-/-}$, but the frequency is much lower.[186] Antagonizing the angiotensin II receptor 2 (AT2) was demonstrated to augment the phenotype and knockout of AT1a was shown to inhibit aneurysm formation, especially with a endothelial-specific knockout.[187-189] Mechanistically, early medial disruption at the suprarenal aorta with subsequent dissection, lumen enlargement and secondary hemorrhage is seen by timely resolution.[185] After 10-14 days continuous remodeling with characteristic features of pronounced leukocyte infiltration of macrophages, T and B lymphocytes, collagen deposition and neovascularization occurs as a more chronic phase.[190] These observations seem to be independent from the animal's blood pressure.[191, 192] Additionally, the aneurysmatic formations were bigger in obese animals and decreased with weight loss.[193, 194]

Most notably, closer studies of the time course and the appearance of the aortic lesions have led to the conclusion that many of the aneurysms are indeed preceded by an aortic dissection with secondary hemorrhage.[190] Moreover, also the ascending aorta shows dilatation.[195] Unfortunately, all these observations are very heterogeneous from animal to animal, even within study groups under the same conditions. To overcome these issues and the inherent discrepancies of different groups reporting on their outcome using the model, the initial authors have even proposed a classification system to describe the variation among phenotypes:[185]

• Type I represents a small single dilation (1.5–2.0 times of a normal diameter)
• Type II denotes a large single dilation (> 2 times of a normal diameter)
• Type III is multiple dilations
• Type IV is aortic rupture that leads to death over bleeding into the peritoneal cavity

However, if more than one, most groups using the model report on three different experimental readouts in a heterogeneous way:

- rupture rate of the dissected aorta
- overall survival
- aneurysm/dissection diameter

With regards to treatment strategy evaluation, the model has been used in many different assays by many groups and shown good responses to e.g. doxycycline, oral vitamin E or amlodipine and many more, but only if given at the time of aneurysm induction and not when administered to an already established lesion (s. 2.1.5).[171, 196-199]
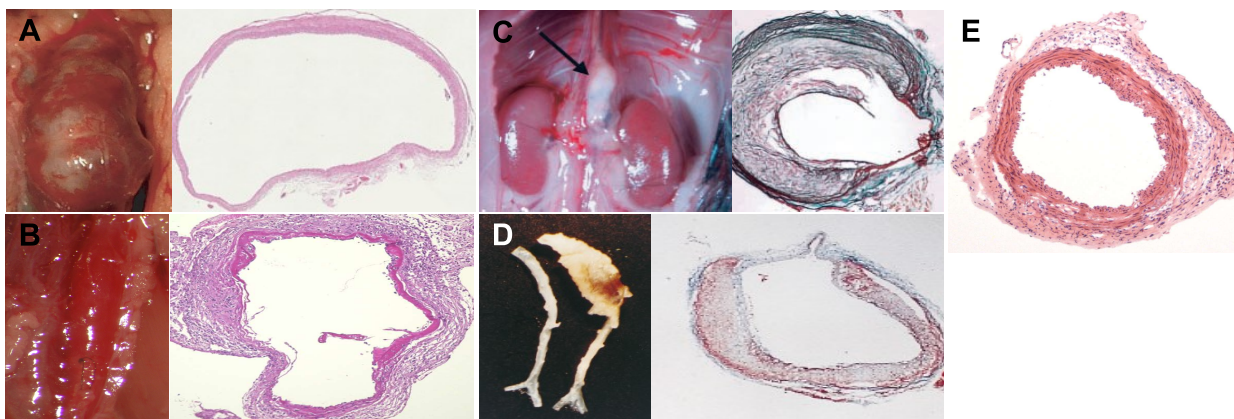
Fig.7: AAAs in different mouse models. The peri-adventitial topical elastase application leads to a large aneurysm at the treated position with a thinned aortic wall with vast inflammatory infiltration **(A)** (modified from[200]). The PPE aneurysm at the infrarenal position shows medial disruption with adventitial fibrosis, angiogenesis and chronic inflammation **(B)** (modified from[201]). Spontaneous development of a thoracic aneurysm in a *LDLR*^{-/-} mouse with semi-circumferential intramural thrombus after dissection **(C)** (modified from[202]). Note the apparent difference between dissection models C,D and matrix disruption in A,B. The angiontensin II induced aneurysm is typically seen at a suprarenal position, too, with a similar dissection morphology **(D)** (modified from[203]). The normal mouse aorta consists of 4 elastic layers with a fine endothelial lining and a homogeneous adventitia **(E)** (own unpublished work).

2.2.2. De-cellularized aortic xenograft

Transplantation of the infrarenal aorta from one species to another, for example guinea pig to rat, induces aneurysms. This model was first introduced by Allaire et al. in 1994.[204]

Prior to implantation of the aorta, the donor aorta is de-cellularized with a detergent, such as sodium dodecyl sulphate (SDS) to slow the immunological response and prevent an acute fatal rejection. Only the ECM collagen and elastin network is preserved. This, however, still triggers an immunity response ultimately causing aortic dilation.[205] Pre-immunization of recipient animals with donor aortic ECM accelerates xenograft destruction.[206]

The model has gained most attention for studying the role of VSMCs and endothelial cells on ECM remodeling in the context of aneurysms and the role of *Porphyromonas gingivalis*.[207, 208]

2.2.3. Topical chemical aneurysm induction

Calciumchloride CaCl₂: This model was also found by mistake by Gertz et al. in 1988.[209]

Looking to induce Prinzmetal angina-like vasospasm, they used $CaCl_2$ as an agent topically in the rabbit carotid artery. Signs of vasospasm including endothelial damage were observed in the short-term, however, after >3 days they did not find the anticipated stenosis, yet a diameter enlargement.[210] The model was then translated to the mouse aorta in 2001 by Chiou et al. (**fig.7A**).[211] Mechanistically, a $CaCl_2$-elastin complex with subsequent attraction of inflammatory leucocytes is described at a concentration of 0.25-0.5 M for 15 min.

The model was slightly modified by Yamanouchi et al. by applying additional PBS after the $CaCl_2$ procedure, hence adding phosphate to produce bigger aortic dilation along calcifications.[212]

Elastase: The topical application of elastase to the murine aorta was introduced by Bhamidipati et al. in 2012.[213]

Instead of calcium chloride, they applied porcine elastase to the ventral aorta and hence did not have to dissect and clamp the aorta. The changes observed include acute inflammation and macrophage infiltration meanwhile aortic dilation. The technique was later also applied to the descending aorta via a lateral thoracotomy.[214] Injecting elastase intrathecally can reproducibly induce cranial aneurysms and subarachnoidal hemorrhage. [215]

Despite there often being a misunderstanding of the common pathophysiology of intraluminal (s.2.2.4.) and topically administered elastase, our group was able to demonstrate distinct forms of inflammation in both models and a much higher concentration of elastase needed when applied from the outside.[201] In the latter we see severe ongoing acute inflammatory infiltrates resulting in excessive retroperitoneal inflammation in the animals.

2.2.4. Porcine pancreatic elastase perfusion

This surgically challenging model was first performed and described by Anidjar et al. in 1990 in rats and later translated to mice by Pyo et al. in 2000 (**fig.7B**).[216, 217]

Via a midline abdominal incision, the aorta is dissected and an atraumatic clamp or suture is positioned below the renal arteries and at the bifurcation. Via a catheter, the isolated part of the aorta is perfused with porcine pancreatic elastase. After the perfusion is finished, the catheter is removed and the blood flow is restored before the abdomen is closed. This results in degradation of the medial elastic lamellae with an inflammatory response followed by aneurysmal dilatation. Across publications, the concentration of elastase and the time of perfusion vary tremendously from 10min to 2h and 2U/ml to 15U/ml.[201, 217, 218] However, the exogenously infused PPE is undetectable 48 hours after infusion and heat inactivated elastase does not cause aneurysms.[219] Increased expression of various MMPs, cathepsins and other proteases was observed and chemical or genetic depletion of MMP activity was shown to halt

aneurysm induction, suggesting a macrophage-dependent increased elastolysis and extracellular matrix (ECM) turnover.[217, 220] Interestingly, the plasminogen-urokinase-plasmin axis seems to be critically involved in aneurysm formation, placing a certain emphasis on elastin breakdown products, like e.g. collagen XIII and endostatin.[108, 221] Upstream of increased MMP production, the leukotriene pathway is believed to enhance aneurysm formation and anti-asthmatic therapies have been successfully tested in the PPE model.[128, 222] Moreover, digoxin, cilostazol and doxycycline have been shown experimentally to protect from aneurysm formation.[223-225] The model can be performed on basically any mouse strain and the phenotype can be enhanced by additional external stimuli like e.g. nicotine.[226]

Finally, due to the surgical nature of the model, it can be modified by e.g. iliac ligation to trigger aneurysm bulging or even to juxta-/suprarenal aneurysm formation by careful dissection of the visceral segment of the aorta as shown by our group.[51, 170]

In many reviews, this model is accepted to have the most resemblance to features observed in human AAA disease.[227] The main limitation is of course the microsurgical challenge to manipulate the 500μm murine aorta and the fact that no intraluminal thrombus is seen in mice.

2.2.5. Spontaneous AAA in animals

All models described above have an artificial stimulus to induce aneurysm formation as a common denominator. Apart from that, a variety of (genetically modified) animals with spontaneous aneurysm formation are described throughout the literature. Here, only the ones that could be re-evaluated in mice are listed. Generally, most of these models have only been described once or cannot be considered a reliable model due to low penetrance of the phenotype and a very heterogeneous distribution of the described lesions (**fig.7C**).[228]

- The so-called blotchy or mottled mice, with an X-chromosome mutation resulting in abnormal copper absorption, developed spontaneous aortic aneurysms. Copper is an important co-factor of the lysyl oxidase (Lox) crosslinking elastin and collagen and the affected mice were shown to have less crosslinking.[229, 230] Hence, mice with a homo- or heterocygote Lox knockout were observed to die perinatally due to rupture of the thoracic aorta.[231]
- Apolipoprotein E (*ApoE*) and low-density lipoprotein (*LDLR*) receptor knockout mice fed a high-fat diet may also spontaneously develop aortic aneurysms as reported sparsely.[232] Reports are about aneurysms forming under mature atherosclerotic lesions with medial elastolysis, dilatation of the lumen, and the presence of necrotic cores with a predominant lipid component. To our current understanding, this would rather resemble a plaque-rupture, eventually also observed in humans and leading to aortic dissection or aortic ulcer.[233]
- The spontaneous development of an aortic aneurysm was shown to be more frequent in an *ApoE/TIMP-1* double knockout mouse on a high-fat diet.[234]

2.2.6. Large animal models

Over the years, modifications of the above-described models have been performed and reported in mice, rats, hamsters, guinea pigs, rabbits, turkeys, sheep, dogs and pigs.[227] In none of these species, an aortic dilation of clinical relevance of >50% was achieved.

For this thesis only the pig models will be introduced further since during the work performed, we have established such in our lab. Basically, two different types of pig models have to be considered.

AAA models with surgically created aneurysm-like formations:

- Initially introduced by Parodi et al. in 1991 in a dog, it was Whitbread et al. in 1996 who created a fusiform aneurysm by interpositioning a bovine jugular vein at the infrarenal position.[153, 235] Such models with artificial aneurysms at this very position were used in the early days of endovascular aortic repair to test newly developed deployment techniques and stentgrafts as such.

- In the "patch model" not the complete aorta is interpositioned, but a patch is sewn into a longitudinal aortotomy to increase the diameter at the operated area. This potects the animals from eventual paraplegia since the lumbar arteries remain patent. The model cannot be assigned to a specific group. A plethora of materials have been used including vein, prosthetic graft material, fascia, jejunum or peritoneum.[227] By using different shapes of patches, this model can even simulate juxta- and suprarenal aneurysms for deploying branched or fenestrated grafts.[236]

- In addition, Riber et al. have taken the de-cellularized aortix xenograft to the next level and created a pig model with a 90% diameter increase after orthotopic transplantation of a decellularized sheep aorta and followed up the animals over 47 days.[237]

AAA models with chemically induced aneurysms:

- Most models are a combination of chemically induced intraluminal perfusion with elastase and/or collagenase for 10-30minutes.[238] Additionally, most groups use at least a pre-, some also a post-perfusion angioplasty with a common, slightly oversized percutaneous transluminal angioplasty (PTA) balloon.[239] Variations are made by e.g. additional distal lumen narrowing by ligature of cuff for additional turbulent flow conditions resulting in a bigger diameter increase.[240, 241] An additional swab soaked with $CaCl_2$ and placed on the aorta after intraluminal angioplasty and perfusion has also been shown to increase diameter.[242]

- A purely endovascular approach did not cause sufficient damage to the healthy pig aorta since the diameter only changed by approx. 15% when applying perfusion between two balloons.[243]

- Gertz et al. have suggested a laparoscopy-based pig model using laparoscopic delivery of $CaCl_2$ to the periadventitial surface of the aorta combined with angiotensin-II infusion in the setting of a 1-month high fat diet.[210] They have observed variable degrees of luminal dilation, associated with disruption of the media, fragmented elastin, inflammatory infiltrates including giant cells and

depletion of smooth muscle cells with replacement by intercellular matrix and neovascularization.

- A different approach of intra-adventitial injection of elastase has been chosen by Tian et al. lately.[244] They operated on 6 pigs and saw a diameter increase of 60% over 3 weeks in the descending aorta.
- Most recently, Shannon et al. have suggested a perfusion model with a combination of balloon angioplasty, elastase and collagenase intra- and extraluminal, and, in addition, a lysyl oxidase inhibitor, called β-aminopropionitrile (BAPN), that is given orally in addition.[245]

2.2.7. A critical appraisal

Most models, and especially their modifications, have been restricted to singular groups.[227] Only the Angiotensin II model (2.2.1.), the PPE model (2.2.4.) and the topical application of $CaCl_2$ or elastase models (2.2.3.) have been reported by different groups. Considering the size of the murine aorta (approx. 500µm), the learning curve on both, surgical intervention, but also accurate diagnostics is steep, taking into account the average diameter increase across the different models of about 70%.

In terms of imaging, nowadays even mouse models are very accessible by ultrasound with high frequency probes allowing a resolution of up to 30µm.[203, 246] Therefore, size is not a restriction in terms of choice of animal. Even pulse wave velocity and ultrasound speckle tracking has become possible to map local wall distress.[247] Moreover CT, MRI and PET-CT studies are reported more frequently.[248, 249] Thus, other than murine models allowing for a plethora genetic strains and modifications do almost not deserve a role any more – except for endovascular treatment evaluation. Moreover, the incidence of aneurysms after induction varies between the models from ca. 50% (Angiotensin II in *ApoE*^{-/-} mice) to 100% (topical intra-/extraluminal elastase application).[228]

Mural thrombus, calcific deposits, intramural hemorrhage are features observed in human disease (**s.2.1.3.**) that are currently missing in most, if not all, animal models.[210] To exclude model specific effects, the aim of any in vivo experiment should always be to have two mechanistically different models involved (**table IV**).

In 2017, Ailawadi et al. suggested to increase the phenotype of their periadventitial elastase mouse model by feeding the animals additionally with β-aminopropionitrile (BAPN) in their drinking water.[250] BAPN is the toxic constituent of peas from Lathyrus plants and results in dissection and rupture of the abdominal aorta by interfering with lysyl oxidase activity necessary for cross-linking in collagen and elastin.[251] For the first time, they observed intraluminal thrombus formation in a mouse model.[252] Also, bigger aneurysms and a higher incidence of aneurysms were seen when orally fed to mice in the angiotensin II model.[253]

From a sex perspective it was demonstrated that orchidectomy, but not ovarectomy resulted in a less pronounced phenotype, hence androgens being involved in the pathomechanism in a yet to be elucidated way.[254, 255] For the PPE model, Ailawadi et al. reported a difference in the mean aortic diameter increase 14 days after elastase perfusion in male versus female mice and a 100% incidence of AAA in male but only

29% in female mice.[256] This apparent protection of female mice from AAA formation was further validated when estrogen treatment of male rats significantly decreased AAA formation indicating protection from AAA formation by estrogen.[257] Vice versa, exposure to testosterone in female mice led to increased AAA development.[258]

Considering the evaluation of a specific treatment or drug of interest, the natural course of the developmental steps after aneurysm induction in the different models has to be considered.[170]

In many reviews, the PPE model is accepted to have the most resemblance to features observed in human AAA disease.[227, 228, 259] The main limitation is of course the microsurgical challenge to manipulate on the 500µm murine aorta and the fact that no intraluminal thrombus is seen in mice.

Advantages	Disadvantages
Angiotensin II model	
angiotensin II receptor A mediated medial disruption at the suprarenal aorta with subsequent dissection, lumen enlargement and secondary hemorrhage followed by remodeling;	
- reproducible and reliable - good background in literature - little microsurgical skills needed - well investigated, yet complicated mechanism	- expensive compared to others - different readouts - heterogeneous outcome reports in literature - the location is rarely seen in humans - dissection, rather than aneurysm model - incidence of aneurysm 50-85%
Decellularized aortic xenograft	
auto-immunological transplant rejection with destruction of the graft;	
- 100% aneurysm incidence	- surgically challenging - based on immune system response
Topical chemical aneurysm induction	
$CaCl_2$-elastin complex with subsequent attraction of inflammatory leucocytes resulting in an ongoing acute inflammation;	
- surgically easy - 100% aneurysm incidence - aneurysm induction in designated locations	- limited features of human disease - uneven distribution of enlargement across aorta
Spontaneous AAA models	
supposed to result from ECM disruption with elastolysis;	
	- low incidence of AAA development - unclear mechanism
Porcine pancreatic elastase perfusion	
intraluminal elastase perfusion and pressure lead to macrophage dependent increased elastolysis and extracellular matrix (ECM) turnover;	
- best mimicry of human disease - good background in literature - well investigated mechanism - 100% aneurysm incidence - can be done on any mouse strain	- surgically challenging

Table IV: Summary of the mechanisms and characteristics of the most frequently used mouse models.

In their 2016 Review, Lysgaard Poulsen et al. have very nicely phrased it:

"The mechanisms triggering rupture may be very different from the mechanisms underlying aneurysmal progression, and the mechanisms behind progression may be very different from triggering factors. (…) Inflammation and proteolysis may be involved in both aneurysm formation and expansion, although with different contributions relative to other phenomena, such as angiogenesis and wall remodeling. Furthermore, the mechanisms behind terminal rupture are mostly unknown, although some similarities exist to the mechanisms of progression."[227]

2.3. New and alternative treatment strategies

2.3.1. Non-coding RNA

Non-coding RNA (ncRNA) represents a large segment of the human transcriptome and has been shown to play important roles in cellular physiology and disease pathogenesis.[260] Over the last few years, it has been established that only 3% of the human genome codes for protein. Approx. 80% of the genome is, however, transcribed regularly (**fig.8A**).[261] RNA and genomic deep sequencing have revealed that the ever growing number of non-coding transcripts by far exceeds protein-coding mRNA. This is believed to shape complexity in species, since the proportion of ncRNA increases with higher rank in evolutionary development (**fig.8B**).[262, 263] With the complexity of this regulatory machinery, defects in non-coding regions of genes and regulatory genomic regions are common in genetic disease and are also the most common site of variation conferring susceptibility to common, complex disease.[264, 265]

Based on their nucleotide (nt) lengths, a vast classification into small (<200nt) and long non-coding RNA (>200nt) is made.
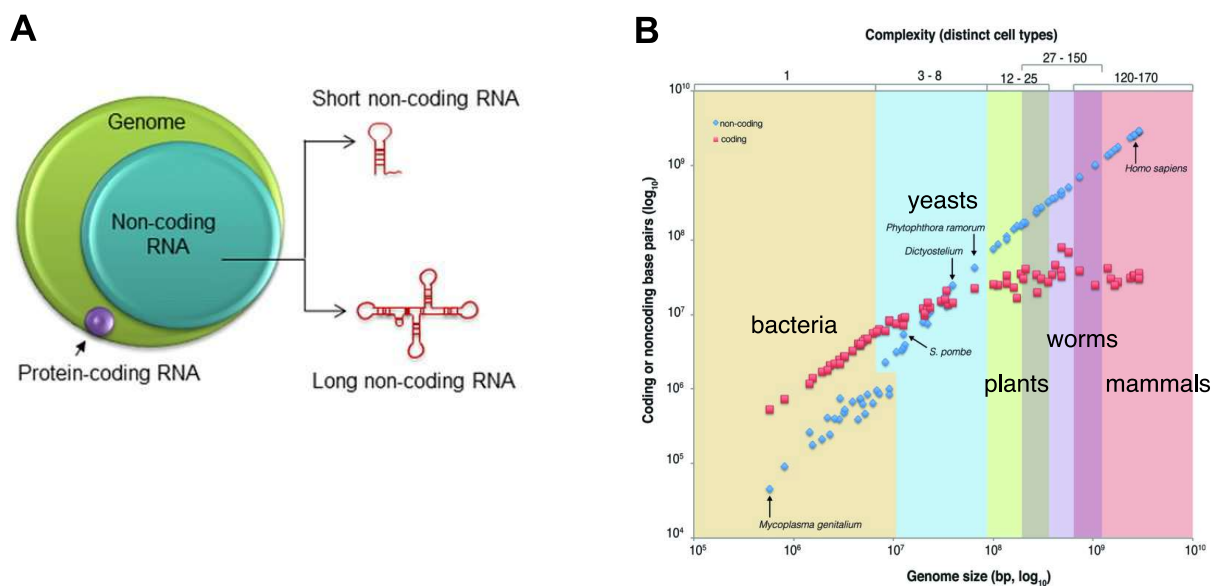
Fig.8: Overview of ncRNAs. Of the whole human genome **(A)**, only a small portion is protein coding RNA (pink). Almost 80% are transcribed regularly (pink+ turquoise). This ratio of coding (red) and non-coding (blue) transcripts increases with the complexity of species **(B)**. (Graphs modified from Parasramka et al. 2016 and Liu et al. 2013)[262, 266]

2.3.1.1. Small non-coding RNAs

The first microRNA (miRNA) was described in 1993 and since then, approximately 1800 of these 16-22 nucleotide (nt) long transcripts have been annotated, with great uncertainty about the final number.[267, 268] They are most often located in the promoter regions of distinct genes, either singly or in clusters. One molecule can have hundreds of (often functionally related) mRNA targets, thus miRNAs constitute dense regulatory networks.[269] Additionally, there is growing evidence suggesting numerous interactions

between the different classes of RNAs due to complementary binding sites.[270, 271] These closely interwoven relationships emphasize the likely involvement of a network, rather than a single gene, when investigating ncRNA changes in disease.[272]

In addition to miRNAs, short interfering RNAs (siRNA) have been identified with a length of 20-24nt. Both miRNAs and siRNAs bind to complementary sites in their target mRNA, regulating post-transcriptionally gene expression in both plants and animals.[273] While both act as relative mRNA silencers, their biogenesis is different, since miRNAs are built from stemloop-precursors and siRNAs from double stranded linear precursors.[274]

The biogenesis of different kinds of ncRNA, however, is not the actual matter of this thesis and thus not summarized in this introduction. Two nice and timely reviews on the subject are provided by e.g. Wang et al. in 2019 or Gangwar et al. in 2018.[275, 276]

2.3.1.2. Long non-coding RNAs

Long ncRNA (lncRNA) includes transcripts >200nt. This number is believed to be around 9000.[261] LncRNAs multiply the challenge to the central dogma of nuclear DNA-transcription and subsequent cytoplasmic mRNA-translation. They comprise multiple mechanisms including histone modification, transcript regulation, alternate splicing, mRNA fragmentation, endo-sponge activity and direct protein interaction. One molecule can have hundreds of (often functionally related) targets. LncRNAs have a more heterogeneous distribution in the genome, with nested and overlapping, sense and antisense transcripts.[277] Although their structure is not as evolutionary conserved as that of miRNAs, their function within the regulatory network is.[278, 279]

Recently, a novel type of ncRNA, circular RNA (circRNA) has been described.[280] A large portion of circRNAs is generated from exons of coding genes, and most do not express protein.[281] Most circRNAs are formed by a specific form of splicing from mRNA precursors with joining of 3'- and 5'-end at a certain step.[282] Due to this complex process there is only little conservation across species.[283] Circular RNAs are speculated to be stable because of their resistance to degradation and might thus have a special role in slowly dividing tissues.[284] Their regulatory role is a matter of ongoing research but includes regulation of transcription and splicing, miRNA sponge function, direct protein interaction and eventual protein translation.[280]

2.3.1.3. Non-coding RNA for therapeutic use

The best evidence for the possible therapeutic options for ncRNA stems from cancer research. Numerous ncRNAs have also shown potential as therapeutic targets because of their differential expression patterns between cancerous and normal tissues.[285, 286]

Due to their earlier discovery, miRNAs are the most extensively investigated, and are to function as either oncogenes or tumor suppressors, causing inhibition or degradation of their target mRNAs.[287] MiRNA mimics and anti-miRNAs are two major forms used to mimic these functions.[288] Ongoing clinical trials cover a broad variety of

cancer types including colorectal cancer, melanoma, breast, bladder and hepatocellular carcinoma (reviewed in detail by Wang et al.).[275]

The role of lncRNAs in this context is much more subject to basic research due to their heterogenic abilities to interfere with the tumor microenvironment, but also due to their pleiotropic effects of unknown significance.[285] Additionally, therapeutic induction or repression appears to be less straightforward compared to miRNAs.[286] Double-stranded RNA-mediated interference (RNAi) and single-stranded antisense oligonucleotides are two major approaches to target lncRNAs. They can reduce the levels of oncogenic isoforms by regulating alternative splicing, modulating RNA–protein interactions, or causing lncRNA degradation.[289] Despite some promising reports, a commercial human attempt for such is currently not possible.[275] Coherently, only two studies looking for lncRNA as biomarkers are currently listed on clinicaltrials.gov (NCT03057171; NCT03469544).

Similar to cancer, a variety of dysregulated ncRNA has been reported for cardiovascular disease (CVD) in general. A well-written and timely review on individual candidates, especially miRNAs, with experimental evidence of influencing atherosclerosis, hypertension and myocardial infarction is provided by Gangwar et al. 2018.[276] Noteworthy, the first publication reporting a lncRNA in CVD in 1996, identified H19 expression in human atherosclerosis (**s. 4.1.**).[290] To my best knowledge, no actual interventional studies using ncRNA in human cardiovascular disease are currently underway. However, various trials investigating the potential of miRNAs as biomarkers in cardiovascular disease (e.g. myocardial infraction) are being performed.[260]

Delivery of non-coding RNA for therapeutic purposes in humans remains challenging, especially avoiding possible side effects in other than the target tissues and low bioavailability limits systemic delivery. Due to the small size, exogenously delivered siRNAs providing RNA interference by mRNA decay seem to be the most promising candidate currently.[291] In 2018, Patisiran[©], a siRNA-based drug, has been approved by the Food and Drug Administration (FDA) under the orphan drug status (**s. 2.3.2.**).[292] It is designed to reduce the transthyretin protein levels by clearing its mRNA levels in the liver and thus providing a treatment for certain forms of amyloidosis. Similar is Custirsen[©], a second-generation phosphorothioate antisense oligonucleotide in clinical trials for various types of cancer.[293]

Recently, bio-conjugation is reported as a powerful delivery strategy to confer siRNA a variety of functionalities for efficient delivery by targeting ligands for cell type-specific delivery, lipids for better pharmacokinetics, cell-penetrating peptides and magnet nanoparticles for imaging and diagnosis.[291] Apart from this classic approach with single-stranded antisense oligonucleotides (miRNA and siRNA), stabilization of specific single-stranded oligonucleotides is achieved by flanking such sequences with locked nucleic acids (LNAs) leading to RNase-mediated degradation of the target sequence.[294] Similar mRNA decay can be induced by so called morpholinos, where a different non-DNA background is coupled with short DNA sequences.[295]

Nanoparticle-based oligonucleotide delivery including lipid, inorganic and polymeric nanoparticles as a strategy showed e.g. higher efficiency in delivering siRNA into hepatocellular carcinoma cells than into normal hepatocytes.[296] Similar effectiveness

can be achieved by conjugation of the RNA-molecule with cell-specific ligands.[297] However, cytotoxicity induced by delivery carriers such as cationic liposomes, which can trigger pulmonary inflammation and the production of reactive oxygen intermediates is described a major problem induced not by the RNA but the delivery system.[298] Stable RNA silencing via oncolytic adenovirus transfer is a different approach for a permanent, non-transient, sustaining effect of gene silencing.[299] Newly, stable delivery of ncRNA into the genome is provided using the CRISPR/CAS technique and thus allowing site-specific DNA-/RNA-editing.[300]

2.3.1.4. Non-coding RNA in experimental use for AAA

In experimental studies, usually a screening with heterogeneous "deepness" is performed in either human AAA samples vs. non-dilated samples or in tissue samples from animal models of AAA. In those approaches, a variety of non-coding RNA candidates has been identified and described in the literature. However, only few of those, especially miRNAs, have been validated by knockdown- or overexpression experiments in animal studies or in genetically modified animals. Only such are summarized in **table V**. However, a variety of additional candidate ncRNAs have been linked to disease mechanisms potentially relevant to AAA. Such have been reviewed by our group in the past extensively.[301-303]

So far, circRNA has only been reported in the context of VSMC fate and in patients with intracranial aneurysms.[304-306]

sncRNA	
miR-21	- overexpression decreases expression of PTEN, leading to increased phosphorylation and activation of AKT, a component of a pro-proliferative and antiapoptotic pathway[307]
miR-24	- regulates cytokine synthesis in macrophages and survival - promotes VSMC migration and cytokine production[308]
miR-29a/b/c	- reduce expression ECM proteins (elastin, collagen I/III)[309, 310]
miR-155	- promotes vascular inflammation[311]
miR-195	- regulates ECM (COL1A1/2, COL3A1, FBN1, ELN, MMP2/9)[312]
miR-205	- reduces biosynthesis of TIMP3[313]
lncRNA	
H19	- regulates VSMC apoptosis and aortic inflammation[77] - miR148b inhibition, regulating the Wnt/β-catenin pathway[314] - increase levels of macrophage chemoattractant protein-1 and IL-6[315]
PVT1	- promotes disease-triggering effects of Angiotensin-II and apoptosis, - elevates MMP-2/-9 and promotes VSMC phenotypic switch[316]

Table V: Overview of ncRNA well characterized in experimental use for AAA in human tissues and in vivo animal studies.

Due to this stability towards external and internal stimuli, non-coding RNAs from several classes have been suggested as potential biomarkers for cardiovascular disease including AAA. However, none of these have made it to clinical use so far. This has been extensively reviewed by our group in the past.[260]

2.3.1.5. Non-coding RNA in clinical use for AAA

Currently no interventional studies with non-coding RNA in AAA patients, or aneurysm patients in general, are registered at clinicaltrials.gov as of January 2020. In an extended bio banking approach, two studies are registered to analyze the diagnostic value of selected circulating miRNAs as a profile in degenerative aneurysmal aortic remodeling comparing AAA to PAOD patients (NCT03974958) or to the general population (NCT03090763).

2.3.2. Drug repurposing and orphan drug use

Drug repurposing is the re-usage of drugs already approved for clinical use in humans for other than the original purpose. This is to bypass the classical time- and money-consuming course of drug development supposed to easily exceed 1 billion USD per substance. However, of such drugs only about 10% successfully reach the clinical track.[317] This is what makes new medications cost-intensive for both the pharmaceutical industry, but especially the public and private healthcare systems.[318]

Orphan drug usage refers to the facilitated approval of medications for special indications.[319] It originates from the special clinical need of certain drugs in the treatment of otherwise untreatable rare diseases. These medications are of no interest to pharmaceutical companies due to the small market potential – the very nature of rare diseases.[318] Many countries, including the European Union (EU) and the USA have thus facilitated the approval process. For almost 20 years now, both governments have enacted a special agency and juridical act to speed up clinical approval in such cases:
EU: www.ema.europa.eu/en/committees/committee-orphan-medicinal-products-comp
USA: www.fda.gov/about-fda/office-special-medical-programs/office-orphan-products-development
Examples for such could be valproate, initially used as an anti-convulsive drug, in a phase-II-clinical trial for Wolfram Syndrome (approx. 300 cases worldwide), or the chemotherapeutic everolimus in the context of Tuberous Sclerosis (worldwide prevalence 1:8000).[320, 321]

Compassionate use finally, is the application of non-approved drugs in emergency cases with an imminent vital threat, where no other medication can usefully be applied or is available. In Germany for example, this is regulated in Art. 83, Absatz 2, Verordnung (EG) Nr. 726/2004 of the pharmaceutical law.[319]

All of these methods have been boosted by modern approaches of system biology. The use of multi-omics (protein, RNA, transcriptome, etc.) in combination with large

data sets on mechanisms, side effects, abandoned mechanisms and test lineages for a multitude of old and newly discovered drugs, helps to visualize and predict potential indications and effector mechanisms, previously not anticipated.[322, 323] This has been extensively reviewed by e.g. Jin et al. or Hodos et al.[317, 324] Additional benefit is to be expected from the combination of different medications, previously applied alone, in old or new contexts.[325, 326]

The modern endovascular therapies in vascular surgery finally harbor new and promising ways of administering such potential drugs of interest by e.g. drug coated balloons or stents(grafts).[327] This could even avoid systemic side effects "frequently" observed in basically every drug. Considering that for many vascular diseases like the aortic aneurysm or the popliteal aneurysm, prevalence and incidence are rather low and approaching the definition of a rare disease (<5:10.000 EU citizens affected), eventual clinical approval could thus be facilitated tremendously.[12, 156] The most prominent example currently is obviously Metformin, which is to be administered for AAA growth reduction in non-diabetic patients, with 3 different multicenter trials in planning.[328, 329]

Already known from previous experimental studies in the context of cancer, we aimed to apply the concept of *drug repurposing* to Lenvatinib® to study its anti-angiogenic capabilities in the context of aortic aneurysm.

2.3.2.1. Lenvatinib®

Lenvatinib® is a commercially available drug distributed by Eisai, Japan (www.eisai.com). It is also known by the name E7080. The drug is a multityrosin-kinase inhibitor inhibiting signaling via the vascular endothelial growth factor receptors (VEGFR) 1, 2, 3 and fibroblast growth factor receptors (FGF-R) 1-4 as well as the platelet derived growth factor receptor (PDGFR) alpha.[330] For experimental purposes it had been used in our lab before in a rodent model of colorectal cancer metastasis.[331]

It entered a phase I clinical trial in 2006 and was finally approved for its first clinical use in progressive, radioiodine refractory differentiated thyroid cancer by the U.S. Food and Drug Administration and the European Medicines Agency (EMA) in 2015.[332, 333] Before, it was granted an orphan drug status in 2012. In 2016, it was approved for the treatment of renal cell carcinoma and in 2018 for the treatment of hepatocellular carcinoma.[334,335] Common side effects include hypertension, proteinuria, fatigue, diarrhea and palmar-plantar erythrodysesthesia syndrome.[336-339] Additionally, from the Japanese adverse drug event report database, one case of aortic dissection under treatment with Lenvatinib is described compared to 59 cases in total treated with VEGF-inhibitors for malignant disease.[340] By December 2019, clinicaltrials.gov lists 111 clinical trials including Lenvatinib®, all of them for anti-cancerous treatments (**table VI**).

Indication of use	Lenvatinib	# trials
hepatobiliary cancers	alone + Pembrolizumab + Nivolumab + TACE + Sorafenib + PD1 antibody + Sintilimab + Toripalimab + CS1003	25
thyroid cancer	alone + Pembrolizumab + Denosumab + Everolimus	16
solid tumors	alone + Pembrolizumab + Eribulin + Everolimus + Etoposide	13
NSCLC non small cell lung carcinoma	alone + Pembolizumab + Docetaxel + Carboplatin/Cisplatin	6
renal cell carcinoma	+ Everolimus + Pembrolizumab	5
metastatic melanoma	alone + Pembrolizumab + Dacarbazine	5
endometrial and ovarial cancer	alone + Paclitaxel + Doxorubicin + Carboplatin	4
Lymphomas	alone	3
Osteosarcoma	+ Ifosamide and Etoposide	2
carcinoids/neuroendocrine npl.	alone + Everolimus	2
gastric cancer	+ Pembrolizumab	2
adenoid cystic carcinoma	alone	2
squamous cell carcinoma	+ Pembrolizumab + Cetuximab	2
breast cancer	alone	1
lung adeno carcinoma	alone	1
soft tissue sarcoma	+ Eribulin	1
pheochromocytoma/paraganglioma	alone	1
urothelial carcinoma	+ Pembrolizumab	1
rectal adenocarcinoma	+ Capecitabine/RTX	1
GIST	alone	1
glioma	+ Bevacizumab	1

Table VI: Overview of the number clinical trials including Lenvatinib alone or in combination sorted after the indication for use from clinicaltrials.gov (December 2019).

Other tyrosine kinase inhibitors, such as Pazopanib® have been suggested to reduce bleeding in hereditary hemorrhagic telangiectasia.[341] Imatinib and erlotinib were shown to halt aneurysm growth in *ApoE* $^{-/-}$ mice infused with Angiotensin II.[342, 343] However, no data or clinical trial applying Lenvatinib for other than anti-cancer treatments is available to my best knowledge.

2.4. Research aim

During my postdoctoral lecture qualification, I have identified angiogenesis as an important feature in aneurysm development. This is reflected in the currently available animal models, especially the PPE model.

The aim of this thesis was to study the modification of the angiogenic environment and its potential to influence aneurysm growth.

Therefore, two different approaches are chosen: On the one side, a candidate long non-coding RNA and its mechanistic role in the hypoxic microenvironment of the aneurysm wall is investigated. On the other side, applying the concept of drug repurposing, we investigate the translational value of the anti-angiogenic agent Lenvatinib® on aneurysm growth that is already in clinical use for a different indication.

3.   Material and Methods

3.1.   Mouse experiments

3.1.1. PPE model

Compliance and ethics:
All procedures involving were carried out in accordance with the protocols approved by the animal care committee of the Karolinska Institute (N119/15 and Amendment N229/15) and in compliance with the guidelines on animal welfare of the Committee for Animal Experiments.

Animals:
The PPE model has been described various times by us and others.[201, 218] Briefly, ten-week-old male C57BL/6J wild type mice (Charles River, Sulzfeld, Germany) on normal chow diet (R36; Lantmännen, Stockholm, Sweden) were kept under standard conditions (temperature 22 °C, humidity 56%).

Anesthaesia and PPE Procedure:
Anaesthesia was induced with isoflurane and analgesia was provided with Temgesic (4 mg/kg) before and after surgery. The aorta was isolated and a temporary proximal and distal suture were placed. Aneurysms were then induced with porcine pancreatic elastase (PPE) (SigmaAldrich, Stockholm, Sweden) at a final concentration of 2 U/mL for 10 min by inserting a microcatheter into the aortic lumen. The aorta was then flushed with warm saline, and a single knot suture (10-0) was placed to seal the catheter entry site. After layered closure of the abdomen, the animal was allowed to recover under infrared heat.

Murine ultrasound:
B-mode ultrasound was performed under general anaesthesia with isoflurane using a Vevo 770 system and a Vevo Imaging Station (both Visualsonics, San Antonio, TX, USA). Our protocol for diameter assessment has been described before.[170] (ultrasound data **s. 6.5.1.**).

3.1.2. Angiotensin II model

Compliance and ethics:
All procedures involving were carried out in accordance with the protocols approved by the animal care committee of the Karolinska Institute (N119/15) and in compliance with the guidelines on animal welfare of the Committee for Animal Experiments.

Animals:
Animals were purchased from The Jackson Laboratory (Bar Harbor, ME). All experiments were performed with ten-week-old male apolipoprotein E–deficient

43

(*ApoE−/−*) C57BL/6J mice with a bodyweight between 25-29 grams. Animals were kept under standard conditions (temperature 22 °C, humidity 56%).

Angiotensin II infusion model:
Osmotic mini-pumps (model 2004, Alzet) containing either AngII (1 µg/kg/min, A9525, Merck, Germany) or PBS were implanted in 10-week old *ApoE*$^{-/-}$ male mice. All pumps were put in 50ml tubes containing PBS overnight (at least 12h). The concentration of AngII was adopted according to bodyweight, range from 25to 29g (1.1mg/g bodyweight). The pumps were injected with 230µl AngII solution, spun down for 5s and then put in PBS overnight. Anesthesia was induced as described before (**s. 3.1.1.**). A small incision on the back of the mice was performed and a subcutaneous pocket was created to insert the pump. The skin was closed free of tension with a single layer suture. The animal was allowed to recover under infrared light. 0.1mg/kg bodyweight of buprenorphine was provided subcutaneously.
Ultrasound was performed on days 0, 7, 14 and 28 after surgery. Aneurysmal (proximal to the renal arteries) and control segments (distal to the renal arteries) of the aorta were harvested after 28 days.

3.1.3. Lenvatinib experiment

Oral Lenvatinib treatment:
Anesthesia was induced with isoflurane. Subsequently, each animal was fed an individual bodyweight dependent dose (5mg/kg) of 2.5mg/ml E7080 (Catalog No S1164, Selleckchem, Germany, **s.6.5.1.**) solution dissolved in DMSO (SigmaAldrich, Sweden).[331] Intraoral administration was secured by placing a pipet tip in glucose and then down the animals throat. This procedure was repeated on a daily basis from day 7 until day 24 after PPE induction. The procedure was performed on 7 animals, no animal died (procedure time approx. 4min).

Local Lenvatinib treatment:
Anesthesia was induced with isoflurane and analgesia was provided with Temgesic (4 mg/kg) before and after surgery on day 7 after PPE AAA induction. The retroperitoneum was re-exposed and the established AAA was carefully dissected from adherent soft tissue. Temporary proximal and distal silk ligatures were placed. Proximally to the initial aortic incision a second incision was made using a 30G needle. Aneurysms were then perfused with a 2.5mg/ml E7080 solution in DMSO for 10 min by inserting a microcatheter. The aorta was then flushed with warm saline, and a single knot suture (10-0) was placed to seal the catheter entry site. After layered closure of the abdomen, the animal was allowed to recover under infrared heat. The procedure was performed on 6 animals, one animal died due to surgical bleeding during dissection (procedure time approx. 55min).

3.1.4. LNA–Anti-H19 GapmeR Injection

Either an LNA–anti-H19 GapmeR or scr-GapmeR (LNA negative control GapmeR from Exiqon) was injected intra-peritoneally (in 0.2 mL of PBS over 3–6 seconds). The concentration of anti-GapmeR or scrambled GapmeR was 20 mg/kg. Injections were carried out at 0, 7, and 14 days after AAA induction in the PPE or the AngII AAA models. The custom-made LNA–anti-H19 GapmeR sequence was 5'-GACGGAGATGGACGAC-3'. The LNA scrambled GapmeR control sequence was 5'-GTGTAACACGTCTATACGCCCA-3'.

The procedure time was approx. 4min per mouse. Procedures were carried out in combination with the routine ultrasound measurement under general anesthesia (**s. 3.1.1.**). No animal died from i.p. injections (data not shown).

3.1.5. H19 knockout mouse experiment

H19 deficient mice were obtained from Professor Karl Pfeifer (Division of Intramural Research, Eunice Kennedy Shriver National Institute of Child Health and Human Development, National Institutes of Health, Bethesda, MD, USA) and were backcrossed to C57BL/6J background at the Karolinska Institute (Dr. A. Baecklund).[344] After successful genotype quality control 10 homozygote knockout animals and 7 wildtype littermates underwent the PPE procedure as described above (**s. 3.1.1.**). Two animals died during the PPE procedure. The phenotype and gross appearance of the H19 deficient mice was not different from the wildtype animals upon surgery (data not shown).

Ultrasound was performed on days 0, 7, 14 and 28 after the PPE procedure under general anesthesia. The infrarenal part of the aorta (AAA) was harvested at day 28 after sacrifice.

3.1.6. Tissue processing

In all experiments presented in this study, animals were sacrificed 4 weeks after aneurysm induction by CO_2 based method. Operations and images were performed using the operating microscope LEICA EZ4HD with a built-in camera and the Leica Acquire Version 3.1 software (both Leica Microsystems, Buffalo Grove, IL, USA). Tissue samples were collected at the time of animal sacrifice. The dilated part of the aorta was carefully dissected and then cut in half. One part was kept for formalin fixation for histochemistry and the second part was placed in RNAlater (SigmaAldrich) and stored at -80°C until further use. Control tissue was non-dilated infrarenal aorta from an additional six animals (also ten-week-old male C57BL/6J wild type mice [Charles River]) sacrificed explicitly for this purpose.

Mouse RNA extraction:
Approximately 1 mm long pieces of mouse aortic tissue were homogenized in Qiazol using Multi-Gen probes (Pro-Scientific, Stockholm, Sweden) and RNA extraction was performed using the Qiagen miRNeasy Micro Kit (Qiagen, Sollentuna, Sweden)

following the manufacturer's protocol. Total RNA concentration was assessed using a NanoDrop 2000 spectrophotometer (Thermo Fisher Scientific, Waltham, MA, USA).

In the MTA analysis (Affymetrix, Sweden), samples from N=6 PPE, N=7 PPE+Lenvatinib and N=5 control aortae were included with RIN numbers 5.7-9.8 (data not shown). The MTA procedure was performed by the CMM (Affiliation 2) core facility according to the manufacturer's protocol.

Mouse transcriptomic array (MTA) analysis:

RNA profiling was performed using the Mouse Transcriptome Assay 1.0 (Affymetrix, Santa Clara, CA, USA). Differential expression analysis was performed using Transcriptome Analysis Console v4.0.1.36 (Affymetrix) using the manufacturers default settings and SST-RMA summarization method. Three separate groups (as described above) of mouse aortic tissues were analyzed for differential expression. The results were exported and further processed using RStudio v1.1.463/Rv3.5.3. Raw exported data and R Script files used can be found in the Supplement section. Standard filtering was performed ($p>0.05$, absolute fold change > 2). Only annotated genes that were not immunoglobulins were included in further analysis. Plotting was performed using the ggplot2 v3.2.1 library.[345]

Mouse Immunohistochemistry:

5 µm sections were stained for different targets with an overnight protocol with primary antibodies (**Table VII**). Endogenous peroxidase activity was quenched with hydrogen peroxide for 10 min (Merck, Darmstadt, Germany). Target staining was done with the Vectastain ABC and the Peroxidase Substrate kit (both Vector Laboratories, Burlingame, CA, USA) after species-specific secondary antibody incubation. Counterstaining was done with Mayer's hematoxylin (both Carl Roth, Karlsruhe, Germany). Negative control, including incubation with phosphate buffered saline instead of primary antibody, was done for each antibody. Slides were then photographed with a Keyence BZ9000 microscope (Keyence, Kyoto, Japan) or scanned with a NanoZoomer 2.0-HT Digital slide scanner C9600 and pictures were taken with the NDP.view2 software (both Meyer Instruments, Hamamatsu, Japan). Image analysis was performed with AZ AnalyserII software (Keyence).

Mouse OCT frozen sections were fixed in 4% paraformaldehyde PBS buffered solution and incubated with primary Ki-67 antibodies (Abcam, ab16667) 1:200 overnight. To visualize staining TSA Plus Cyanine 5 Evaluation Kit (PerkinElmer, NEL745E001KT) was applied in 1:50 dilution. Sections were mounted with ProLong Gold (Thermofisher) and pictures were taken using confocal microscope Leica SP5.

target	used in	antibody	manufacturer	dilution
mouse mouse mouse mouse mouse mouse mouse mouse mouse mouse				
KI67	IHC	ab16667	Abcam	1:50
MYH11	IHC	ab224804	Abcam	1:100
α smooth muscle actin	IHC	ab119952	Abcam	1:200
CD31	IHC	ab28364	Abcam	1:200

SMA	IHC prim IF	ab7817	Abcam	1:200
CD31	IHC	ab28364	Abcam	1:500
MYH11	IHC prim IF WB	ab53219	Abcam	1:300 1:200 1:500
Alexa Fluor 488	sec IF human/pig	A11034	Invitrogen	1:300 (human) 1:500 (pig)
Alexa Fluor 594	sec IF pig	A11032	Invitrogen	1:500
Alexa Fluor 647	sec IF human	A21236	Invitrogen	1:300
β-actin	WB	A1978	Sigma-Aldrich	1:5000
Phospho-p44/42 MAPK (Erk1/2)	WB	4370	Cell Signaling	1:2000
p44/42 MAPK (Erk1/2)	WB	4695	Cell Signaling	1:1000
SAPK/JNK	WB	9252	Cell Signaling	1:1000
Phospho-SAPK/JNK	WB	9255	Cell Signaling	1:2000
Phospho-Akt	WB	9271	Cell Signaling	1:1000
Akt	WB	9272	Cell Signaling	1:1000

Table VII: Antibody list. The table shows the list of antibodies used in the study for immunohistochemistry (IHC), double immunofluorescence (IF; prim = primary; sec = secondary) and Western Blot (WB). Additionally, the final dilution for the primary antibody is shown.

In Situ Hybridization (ISH):

ISH for H19 and the HIF1α promoter region was performed using the miRCURY LNA microRNA ISH Optimization Kit (Exiqon), according to the manufacturer's protocol. The sequence of the H19 probe was 5'-DIG/ ATACAGCGTCACCAAGTCCA/DIG-3' and 5'-Biotin/ATACAGCGTCACCAAGTCCA/-3'. The sequence of the HIFA promoter region probe was 5'-Biotin/TGAGGAGCTGAGGCAGCGTCAGGGGGCGGGCAAGGGCGGA GGCG/-3'. The signal was captured and analyzed using a Leica Confocal Microscope (CMM, Karolinska Institute).

3.2. Pig experiments

3.2.1. Pig PPE experiments

Compliance and ethics:
The study was performed in compliance with the EU Directive 2010/62/EU for animal experiments and the German Animal Welfare Act (2018). All procedures and animal handling were approved by the Animal Research Ethical Committee of the Government of Upper Bavaria (Munich, Germany; protocol No. ROB-55.2-2532.Vet_02-18-53).

Animals:
13-month-old female and castrated male LDLR$^{-/-}$ Yucatan Miniature Pigs from Exemplar Genetics (Coralville, IA, United States) with 77.8±5.1kg body weight were used. They were housed in groups of 2-4 under conventional hygienic conditions and acclimatized to the new environment for a period of at least 9 days prior to surgery

(temperature 19±2°C; humidity 50–60%; 12h/12h light–dark cycle; Environmental enrichment provided). Animals were fed with a pelleted high-fat diet (Altromin, Lage, Germany) twice a day and received water ad libitum. Prior to anesthesia, animals were starved for 12 hours with free access to water.

Anesthesia:
The basic anesthesia regime included: Sedation by combination of ketamine 15mg/kg, azaperone 2mg/kg and atropine 0.1mg/kg intramuscularly. An intravenous catheter was placed in the lateral auricular vein. Induction of anesthesia by Propofol (4-8 mg/kg) and oral intubation with a 7.0-8.5 mm cuffed endotracheal tube. Anesthesia was maintained by continuous infusion of propofol (2.5-7mg/kg/h). Pigs were mechanically ventilated in volume-controlled mode (6-10ml/kg) with 40-50% oxygen (1-2l/min) and breathing rate 11-13x/minute. Parameters were adjusted to maintain normocapnia (end-tidal CO2: 35-45mmHg). Saline was infused at a maintenance rate of ~10 ml/kg/h. Intraoperative monitoring included reflex status, heart rate and peripheral arterial oxygen saturation. External warm-air supply was provided. A single-shot Cefuroxim (750mg) was administered before skin incision. For multimodal analgesia during the surgery, metamizole (50mg/kg), carprofen (4mg/kg) and fentanyl (0.001–0.01mg/kg) were administered.

Ultrasound:
Ultrasound was performed immediately after anesthesia before any further procedure by 2 independent examiners using a GE Logiq S7 system equipped with a 4-5MhZ abdominal ultrasound probe (GE, Frankfurt). The aortic trifurcation and the renal arteries were identified and aortic diameter was acquired using the leading edge method in transverse and longitudinal sections at the point of maximum diameter (**s. 6.5.1.**).[6]

PPE procedure:
Via a left lateral flank access, retroperitoneal exposure of the aorta was achieved. Preparation included anteflexio of the left kidney and complete dissection of the aorta from the left renal artery to the aortic trifurcation. 2-3 pairs of lumbar arteries were clipped and cut off. 3000IE heparin were administered before clamping of the aorta over a distance of 3-4cm. A 9-11x20mm PTA balloon (Medtronic Admiral Xtreme) depending on the previous ultrasound measurement (diameter+2mm) was inserted via a puncture incision and inflated to 10atm for 1min for pre-dilation of the aorta in order to allow better elastase perfusion. Afterwards, a blunt 5G needle was inserted and perfusion with 10IU/ml elastase (porcine pancreatic elastase, SigmaAldrich, Germany) was started after a tourniquet secured the needle at the puncture site. The aorta was perfused to maximum diameter before effusion of elastase through the vessel for 10min. Afterwards, the aorta was flushed with heparinized saline (1000IE/L) and the incision closed with 5-0 suture before opening the clamps. Layer-by-layer closure including 2xmuscle, fat and skin were done and the wound was coated with spray on dressing (Aqueos, UK).

3.2.2. Local Lenvatinib experiment

Experimental design:
In general, the experiment consists of three distinct procedures: day 0 (ultrasound and AAA induction by PPE procedure), day 8±2 (ultrasound and endovascular coated balloon treatment via femoral access) and day 28±3 (ultrasound, euthanasia and tissue collection). Detailed protocols for anesthesia and ultrasound measurements can be found in the Supplement.

Endovascular coated balloon treatment:
The animal was put in a supine position. A 4cm incision in the right groin was made and the common femoral artery was surgically exposed. 3000IE heparin were administered. The vessel was then ligated distally and with Seldinger technique a 5F introducer sheath (TerumoAortic, Germany) was placed in retrograde direction. Using a Terumo$^©$ guide wire and a mobile C-arm a 4F pig tail catheter (Aimecs, Germany) was advanced into the aorta. An angiography was made using 6ml contrast agent (Imeron, Bracco, Germany) to identify aortic landmarks and the aneurysm lesion. A 10-12x20mm PTA balloon (Medtronic Admiral Xtreme) was then spray coated with 50mM E7080 solution. Using a special introducer sheath to protect the coated area, the balloon was advanced to the identified aneurysm site and inflated to 10atm for 3min. Afterwards, the balloon was retrieved, and a control angiography was done to exclude aortic occlusion or dissection. The introducer sheath was retrieved and the common femoral artery ligated proximally to the puncture site. Layer-by-layer closure was performed and coated with spray on dressing. Postoperative analgesia, blood sampling, and euthanasia protocols can be found in the Supplement.

Postoperative analgesia:
After each surgery, carprofen (4mg/kg) orally for at least 5 days and a single dose of buprenorphine (0.005–0.1mg/kg) shortly before the end of anesthesia. After the first surgery (induction of aneurysm), the administration of buprenorphine was continued for at least 2 days.

Blood sampling:
Blood sampling (10ml) under anesthesia was performed at day 0, day 8±2 (catheterization) and day 28±3 (euthanasia) via lateral auricular vein or femoral arteria. Parameters: Blood cell count, alkaline phosphatase, AST, ALT, γ-GT, GLDH, bilirubin total, creatinine, urea, albumin, total protein, glucose.

Euthanasia:
After a final ultrasound examination, the animals were sacrificed under general anesthesia with pentobarbital (>50mg/kg) and 40ml of 1M KCl solution.

3.2.3. Tissue processing

<u>Pig Tissue collection and processing:</u>
Directly after euthanasia, the incisional wounds were reopened and access to the infrarenal aorta was gained in order to identify the area of the aneurysmatic lesion. Samples were collected from the AAA, the surgically untouched pararenal aorta (no additional animals were sacrificed for control tissue sampling), the common carotid, the iliac and the coronary arteries, the aortic valve, the left ventricle myocardium, a jugular lymph node, liver, kidney, spleen and lung parenchyma as well as whole blood in EDTA and serum. All samples were divided for RNA isolation and snap frozen in liquid nitrogen and formalin fixation.

<u>Pig RNA extraction and qPCR experiments:</u>
Approx. 3mm sections of aortic tissue were homogenized with the Bio-Gen PRO200 Homogenizer and Multi-Gen 7XL Probes (PRO Scientific, Oxford, CT, USA) after adding Qiazol. RNA extraction was performed using the miRNeasy Mini Kit (Qiagen, Hilden, Germany) according to the manufacturer's protocol and total RNA concentration was determined with the NanoDrop2000c (Thermo Fisher Scientific, Waltham, MA, USA).
300ng RNA were reverse-transcribed using the High-Capacity RNA-to-cDNA Kit (Thermo Fisher Scientific, Waltham, MA, USA). mRNA expression was measured based on quantitative polymerase chain reaction using TaqMan FAM labelled assays. Amplification was performed on a QuantStudio 3 PCR System (Thermo Fisher Scientific, Waltham, MA, USA) and all samples were normalized to RPLP0 (Ribosomal Protein Lateral Stalk Subunit P0). RNA expression was calculated by the $\Delta\Delta Ct$ method and displayed as fold change compared to untreated pig aortas from above the surgically treated segment with a relevant distance.

<u>Pig Immunohistochemistry:</u>
2µm sections of paraffin-embedded tissue were mounted on SuperFrost slides (Thermo Fisher Scientific, Waltham, MA, USA) and standard hematoxylin-eosin (HE) and Elastica van Gieson (EVG) stainings were performed.
For immunohistochemistry (IHC), sections were mounted on 0.1% poly-L-lysine (Sigma-Aldrich, St. Louis, MO, USA) pre-coated SuperFrost Plus slides (Thermo Fisher Scientific, Waltham, MA, USA). For antigen retrieval the slides boiled in a pressure cooker with 10nM citrate buffer (distilled water with citric acid monohydrate, pH 6.0) and endogenous peroxidase activity was blocked with 3% hydrogen peroxide. Samples were incubated with primary antibodies (**Table VII**) diluted in Dako REAL Antibody Diluent (Dako, Glostrup, Denmark). Slides were then treated with biotinylated secondary antibodies and target staining was performed with peroxidase conjugated streptavidin and DAB chromogen (Dako REAL Detection System Peroxidase/DAB+, Rabbit/Mouse Kit; Dako, Glostrup, Denmark). Mayer's hematoxylin (Carl Roth, Karlsruhe, Germany) was used for counterstaining and appropriate positive and negative controls were done for every target antibody. All slides were scanned with

Aperio AT2 (Leica, Wetzlar, Germany) and images were taken with the Aperio ImageScope software (Leica, Wetzlar, Germany).

Pig double immunofluorescence staining:
4µm sections of paraffin-embedded samples were mounted on pre-coated SuperFrost Plus slides (Thermo Fisher Scientific, Waltham, MA, USA). Antigen retrieval and blocking of peroxidase activity was performed as described for IHC. Additional blocking with 1%BSA and 2%FBS was applied for 1h. Primary and secondary antibodies (**Table VII**) were diluted in 1%BSA and 2%FBS. Both primary antibodies were incubated together for 1h at room temperature, followed by both secondary antibodies for 1h. TrueBlack® Lipofuscin Autofluorescence Quencher (Biotium, Fremont, CA, USA) was used to reduce background fluorescence. Sections were counterstained with 4,6-diamidino-2-phenylindole (DAPI, Thermo Fisher Scientific, Waltham, MA, USA) and images were taken under a confocal microscope (TCS SP5 II, Leica, Wetzlar, Germany).

Proteinisolation, Concentration Measurement and WB:
AAA tissue of 25mM Lenvatinib-treated (n=4) and control-treated pigs (n=3) was cut in ~50mg pieces on dry ice. Tissue was homogenized in 200µl Tissue Extraction Reagent I (Thermo Fisher, USA). After homogenization with the Bio-Gen PRO200 Homogenizer and Multi-Gen 7XL Probes (Pro Scientific, USA), samples were centrifuged for 20 min, 14.000 rpm at 4°C and the supernatant was frozen down at -80°C in aliquots of total protein lysate. Total protein concentration was measured using the Pierce™ BCA Protein Assay Kit (Thermo Fisher, USA) following the manufacturer´s instruction.

7.5µg of protein of each sample was denatured and reduced at 70°C for 10 minutes, then separated in a NuPage™ 3-8% Tris Acetate-Gel and transferred onto Trans-Blot® Turbo™ Mini-Size LF-PVDF Membranes (BioRad, USA). The blots were blocked with 5% BSA in Tris-buffered saline+0.1% Tween-20 for 1h, followed by overnight incubation with the primary Rabbit Anti-smooth muscle Myosin heavy chain 11 antibody (ab53219, Abcam, United Kingdom) in TBS-T+5%BSA. After washing with TBS-T, blots were incubated with anti-mouse and rabbit HRP (horseradish peroxidase)-conjugated secondary antibody and visualized using Enhanced Chemiluminescence (Pierce® Fast Western Blot Kit ECL Substrate, Thermo Fisher, USA) in the Intas ECL Chemocam Imager (Intas, Germany) using the Intas ChemoStar Imager Software (Intas, Germany). Blots were stripped using Restore™ Plus Western Blot Stripping Buffer (Thermo Fisher, USA) and incubated with the loading control primary antibody in TBS-T+5%BSA for 1h. After washing with TBS-T, blots were again incubated with anti-mouse and rabbit HRP (horseradish peroxidase)-conjugated secondary antibody and visualized using Enhanced Chemiluminescence (Pierce® Fast Western Blot Kit ECL Substrate, Thermo Fisher, USA) in the Intas ECL Chemocam Imager (Intas, Germany) using the Intas ChemoStar Imager Software (Intas, Germany).

3.3. Human sample experiments

3.3.1. Primary cell culture

<u>Establishing a primary human cell culture:</u>
Human AAA material was harvested during open surgery repair of the abdominal aorta, and transported to the laboratory in complete DMEM/F12 Medium (Sigma Aldrich, USA, containing 5%FBS and 1%PS). Written and informed consent was obtained from the patients and approved by the local ethics committee.[346] Tissue was placed in a sterile petri dish and washed with PBS. Adventitia, neo-Intima and calcifications were removed and the remaining media was cut into small pieces using a sterile scalpel. These were placed in digestion medium (1.4mg/ml Collagenase A, Roche, Germany, in complete DMEM/F12 Medium) in a humidified incubator at 37°C and 5%CO2 for 4-6h. Cells were strained using a 100µm cell strainer to remove debris. After 2 washing steps (centrifuge 400g, 5min; discard supernatant, re-suspended in 15ml complete DMEM/F12 Medium) cells were re-suspended in 7ml complete DMEM/F12 Medium and placed in a small cell culture flask of 25cm^2 in a humidified incubator at 37°C and 5%CO2. Medium was changed every other day. After 1 week, when cells started to grow, the medium was replaced by SMC Growth Medium (PeloBiotech, Germany). Medium was changed every other day until confluence. Cells were subsequently transferred into bigger flasks (75cm^2) and stored in liquid nitrogen if not processed immediately. In this study, primary cells (strains #1-3) from 3 different patients with AAAs (diameter 6.7±0.4cm) were obtained.
Primary patient-derived SMCs were used between passages 3-7 in all experiments. Primary SMCs from healthy donors (control SMCs) were purchased at Cell Applications (USA, 354-05a) and used between passages 5-7 in all experiments.

<u>Primary human AAA cells RNA isolation and qPCR:</u>
Cells were placed in 6well plates (triplicates each) and treated with 0.1µM Lenvatinib in OptiMEM (Thermo Fisher, USA, Lenvatinib-treatment) or 0.1% DMSO in OptiMEM (control-treatment) for 6, 24 and 48h. Cells were washed with PBS and harvested with 350µl RLT Lysis Buffer (Qiagen, Netherlands). Total RNA was isolated using the RNeasy Mini Kit (Qiagen, Netherlands) according to manufacturer´s instruction. RNA concentration and purity were assessed using the NanoDrop. Next, first strand cDNA synthesis was performed using the High-Capacity-RNA-to-cDNA Kit (Applied Biosystems, USA), following the manufacturer's instruction.
Quantitative real-time TaqMan PCR was then performed using primers for the following genes: Tagln, Cnn1, Myocd, Itga8, Col3A1, Cald1, S100A1, Kdr, Vcan, Hif1a, Acta2, Smtn and Mmp2 (**Suppl.TableIV**). PCR was run on a QuantStudio5 Cycler (Applied Biosystems, USA) using 384 well plates. Gene expression was normalized to Rplp0 and Gapdh and quantified with the $2^{\Delta\Delta Ct}$ method.
For Myh11 SYBR Green based quantitative real-time PCR was performed. PCR was run on a QuantStudio5 Cycler using 384 well plates. Gene expression was normalized to Rplp0 and Gapdh and quantified with the $2^{\Delta\Delta Ct}$ method.

<u>Kinetic live-cell culture experiments:</u>

All dynamic live-cell imaging experiments were performed following the instructions provided by Essen Bioscience using the IncuCyte ZOOM system.

Dose finding experiment: Cells were plated in 24well plates (Corning/Falcon). The next day medium was changed to Optimem 10%FBS+1%PEST. Lenvatinib was dissolved in 2.3ml DMSO (according to commercial protocol). Stock - 10mM. This stock was diluted for working concentrations 10μM, 1μM and 0.1μM. 1μl DMSO was added to control wells. Cell confluence was checked on Incucyte over 72h.

Proliferation and Apoptosis: Cells were placed with 30% confluence in a 96-well plate and treated with 0.1μM Lenvatinib in OptiMEM (Thermo Fisher, USA, Lenvatinib-treatment) or 0.1% DMSO in OptiMEM (control-treatment) for 72h. The IncuCyte® Caspase-3/7 Apoptosis Reagent (Essen Bioscience, USA) was added at a final concentration of 5μM. The plate was monitored in the IncuCyte ZOOM System (Essen Bioscience, USA) with phase/fluorescence and a 2h imaging pattern. Images were auto-collected and analyzed using the IncuCyte ZOOM software (Essen Bioscience, USA)

Migration: Cells were placed with 100% confluence in a 96-well ImageLock plate (Essen Bioscience, USA) and homogeneous, 700-800μm wide wounds were created using the WoundMaker (Essen Bioscience, USA). Cells were treated with 0.1μM Lenvatinib in OptiMEM (Thermo Fisher, USA, Lenvatinib-treatment) or 0.1% DMSO in OptiMEM (control-treatment) for 72h and the plate was monitored in the IncuCyte ZOOM System (Essen Bioscience, USA) with phase and a 2h imaging pattern. Images were auto-collected and analyzed using the IncuCyte ZOOM software (Essen Bioscience, USA)

<u>Protein isolation and WesternBlot:</u>

Cells: Cells were placed in 75cm^2 flasks and treated with 0.1μM Lenvatinib in OptiMEM (Thermo Fisher, USA, Lenvatinib-treatment) or 0.1% DMSO in OptiMEM (control-treatment) for 6 and 48h. Cells were washed with ice-cold PBS and harvested with 750μl freshly prepared complete RIPA Buffer (RIPA Lysis and Extraction Buffer, Thermo Fisher, USA) containing Phosphatase Inhibitor Cocktail 2 and 3 (Sigma Aldrich, USA) and Halt™ Protease Inhibitor Cocktail (Thermo Fisher, USA). After homogenization with a pistil, and centrifugation for 20 min, 14.000rpm at 4°C the supernatant was frozen down at -80°C in aliquots of total protein lysate. Total protein concentration was measured using the Pierce™ BCA Protein Assay Kit (Thermo Fisher, USA) following the manufacturer´s instruction.

Western Blot for signaling cascade: 10μg of protein from each sample was denatured and reduced at 70°C for 10min, then separated in a Bolt™ 4-12% Bis-Tris Plus Gel (Thermo Fisher, USA) and transferred onto Trans-Blot® Turbo™ Mini-Size LF-PVDF Membranes (BioRad, USA). The blots were blocked with 5% BSA in Tris-buffered saline+0.1% Tween-20 for 1h, followed by overnight incubation with the primary antibody against the un-phosphorylated Kinase in TBS-T+5%BSA. After washing with TBS-T, blots were incubated with anti-mouse and rabbit HRP (horseradish peroxidase)-conjugated secondary antibody and visualized using Enhanced Chemiluminescence (Pierce® Fast Western Blot Kit ECL Substrate, Thermo Fisher,

USA) in the Intas ECL Chemocam Imager (Intas, Germany) using the Intas ChemoStar Imager Software (Intas, Germany). Blots were stripped using Restore™ Plus Western Blot Stripping Buffer (Thermo Fisher, USA) and incubated overnight with the primary antibody against the phosphorylated Kinase in TBS-T+5%BSA. After washing with TBS-T, blots were again incubated with anti-mouse and rabbit HRP (horseradish peroxidase)-conjugated secondary antibody and visualized using Enhanced Chemiluminescence (Pierce® Fast Western Blot Kit ECL Substrate, Thermo Fisher, USA) in the Intas ECL Chemocam Imager (Intas, Germany) using the Intas ChemoStar Imager Software (Intas, Germany).
The blots were quantitated by using Fiji ImageJ Software.

Western Blot for MYH11: 10μg of protein of each sample was denatured and reduced at 70°C for 10min, then separated in a NuPage™ 3-8% Tris Acetate-Gel and transferred onto Trans-Blot® Turbo™ Mini-Size LF-PVDF Membranes (BioRad, USA). The blots were blocked with 5%BSA in Tris-buffered saline+0.1%Tween-20 for 1h, followed by overnight incubation with the primary Rabbit Anti-smooth muscle Myosin heavy chain 11 antibody (ab53219, Abcam, United Kingdom) in TBS-T + 5% BSA. After washing with TBS-T, blots were incubated with anti-mouse and rabbit HRP (horseradish peroxidase)-conjugated secondary antibody and visualized using Enhanced Chemiluminescence (Pierce® Fast Western Blot Kit ECL Substrate, Thermo Fisher, USA) in the Intas ECL Chemocam Imager (Intas, Germany) using the Intas ChemoStar Imager Software (Intas, Germany). Blots were stripped using Restore™ Plus Western Blot Stripping Buffer (Thermo Fisher, USA) and incubated with the loading control primary antibody against β-Actin (A1978-200μl, Sigma Aldrich, USA) in TBS-T+5% BSA for 1h. After washing with TBS-T, blots were again incubated with anti-mouse and rabbit HRP (horseradish peroxidase)-conjugated secondary antibody and visualized using Enhanced Chemiluminescence (Pierce® Fast Western Blot Kit ECL Substrate, Thermo Fisher, USA) in the Intas ECL Chemocam Imager (Intas, Germany) using the Intas ChemoStar Imager Software (Intas, Germany).

3.3.2. Human tissue biobank

Ethics:
Human aortic aneurysm samples and control aortic wall samples (non-aneurysmatic) were taken from our Munich biobank described previously with patients' informed consent.[346] The Biobank is approved by the local Hospital Ethics Committee (2799/10, Ethikkommission der Fakultät für Medizin der Technischen Universität München, Munich, Germany) and in accordance with the Declaration of Helsinki.

Sample Acquistion:
Briefly, AAA samples were acquired during open repair from the left anterior wall of the aneurysm, control, non-aneurysmatic samples included donor patients from kidney transplants and samples from PAOD procedures. Samples were divided for both formalin-fixation and paraffin embedding, and snap frozen in liquid nitrogen until further use.

Immunohistochemistry human tissue:

2μm sections of paraffin-embedded human aortic samples were mounted on SuperFrost slides (Thermo Fisher Scientific, Waltham, MA, USA) for HE and EvG stainings. For IHC, sections were stained with different target antibodies (**Table VII**) following the protocol described previously for pig sections.

Slides (including immunohistochemistry) were scanned with Aperio AT2 (Leica, Wetzlar, Germany), and pictures were taken with the Aperio ImageScope software (Leica).

Human immunofluorescence (IF) double staining:

4μm sections of paraffin-embedded human aortic samples were mounted on pre-coated SuperFrost Plus slides. Antigen retrieval and blocking of peroxidase activity was performed as described previously for IHC. In addition, slides were blocked with 5% horse serum for 30 min and all antibodies were diluted in 5% horse serum. Two primary and appropriate secondary antibodies (**Table VII**) were added subsequently to the slides, with the primary antibody of interest (MYH11) being incubated overnight at 4°C and the following primary antibody for co-staining (SMA) for 1h at room temperature. Secondary antibodies were incubated for 1h each. Autofluorescence quenching, counterstaining and imaging were performed as described in the pig double IF section.

Human tissue RNA extraction and qPCR:

Tissues were cut in ~50mg pieces on dry ice. Tissue was homogenized in 700μl Qiazol lysis reagent and total RNA was isolated using the miRNeasy Mini Kit (Qiagen, Netherlands) according to manufacturer´s instruction. RNA concentration and purity were assessed using the NanoDrop. RIN number was assessed using the RNA Screen Tape (Agilent, USA) in the Agilent TapeStation 4200. Next, first strand cDNA synthesis was performed using the High-Capacity-RNA-to-cDNA Kit (Applied Biosystems, USA), following the manufacturer's instruction.

Quantitative real-time TaqMan PCR was then performed using primers for the following genes: *TAGLN, CNN1, MYOCD, ITGA8, COL3A1, CALD1, S100A1, KDR, VCAN, HIF1a, ACTA2, SMTN* and *MMP2* (**Table VIII**). PCR was run on a QuantStudio5 Cycler (Applied Biosystems, USA) using 384 well plates. Gene expression was normalized to Rplp0 and Gapdh and quantified with the $2^{\Delta\Delta Ct}$ method.

For Myh11 SYBR Green based quantitative real-time PCR was performed. PCR was run on a QuantStudio5 Cycler using 384 well plates. Gene expression was normalized to Rplp0 and Gapdh and quantified with the $2^{\Delta\Delta Ct}$ method.

target	name	sequence/name	supplier
TAGLN	transgelin	Hs01038777_g1	Thermo Fisher
change and transformation sensitive actin-binding protein; belongs to calponin family; ubiquitously expressed in vascular smooth muscle; early marker of smooth muscle differentiation			
CNN1	calponin 1	Hs00959434_m1	Thermo Fisher
an actin filament-associated regulatory protein; role in contractile functions;			

MYOCD	myocardin	Hs00538076_m1	Thermo Fisher

nuclear protein, expressed in heart, aorta, and smooth muscle cell-containing tissues; modulates expression of smooth muscle-specific SRF-target genes; crucial role in differentiation of the smooth muscle cell lineage

ITGA8	integrin subunit alpa 8	Hs00233321_m1	Thermo Fisher

Integrins are heterodimeric transmembrane receptor proteins that mediate numerous cellular processes; the integrin alpha8beta1 protein thus plays an important role in wound-healing and organogenesis;

COL3A1	collagen type III alpha 1 chain	Hs00943809_m1	Thermo Fisher

fibrillar collagen extensible in connective tissues such as the vascular system; Mutations are associated with Ehlers-Danlos syndrome types IV and with aortic and arterial aneurysms

CALD1	caldesmon 1	Hs00921987_m1	Thermo Fisher

calmodulin- and actin-binding protein that plays an essential role in the regulation of smooth muscle and nonmuscle contraction

S100A1	S100 calcium binding protein A1	Hs00984741_m1	Thermo Fisher

S100 proteins are localized in the cytoplasm and/or nucleus of a wide range of cells and involved in the regulation of a number of cellular processes such as cell cycle progression and differentiation

KDR	kinase insert domain receptor	Hs00911700_m1	Thermo Fisher

VEGF receptor 2 functions as the main mediator of VEGF-induced endothelial proliferation, survival, migration, tubular morphogenesis and sprouting

RPLP0	ribosomal protein lateral stalk subunit P0	HS00420895_gH	Thermo Fisher

housekeeping gene for PCR

VCAN	versican	HS00171642_M1	Thermo Fisher

aggrecan/versican proteoglycan family; major component of the extracellular matrix; nvolved in cell adhesion, proliferation, proliferation, migration and angiogenesis;

HIF1a	hypoxia inducible factor 1 subunit alpha	Hs_00153153_m1	Thermo Fisher

HIF-1 functions as a master regulator of cellular and systemic homeostatic response to hypoxia; essential role in embryonic vascularization, tumor angiogenesis and ischemic disease;

ACTA2	actin alpha 2	HS00426835_G1	Thermo Fisher

smooth muscle actin that is involved in vascular contractility;

GAPDH	glyceraldehyde-3-phosphate dehydrogenase	HS03929097_G1	Thermo Fisher

housekeeping gene for PCR

SMTN	smoothelin	Hs01022255_g1	Thermo Fisher

structural protein that is found exclusively in contractile smooth muscle cells;

MMP2	matrix metallopeptidase 2	Hs_01548727	Thermo Fisher

zinc-dependent enzymes capable of cleaving components of the extracellular matrix; type IV collagenase;

GAPDH	s. above	Hs_GAPDH_1_SG	Qiagen

housekeeping gene for PCR in pig tissues

MYH11_human_fwd	myosin heavy chain 11	TCGAAGAAGAAGCTGCAGGA	Thermo Fisher
MYH11_human_rev		GTACTGCTGGGTGAGGTTCT	Thermo Fisher

smooth muscle myosin; major contractile protein

RPLP0_human_fwd	s. above	ATGGCAGCATCTACAACCCT	Thermo Fisher
RPLP0_human_rev		TTGGGTAGCCAATCTGCAGA	Thermo Fisher

housekeeping gene for PCR in pig tissues

Table VIII: Primer list and target gene description The table shows all primers used for target analysis. The target gene function is briefly described with data available from NCBI's gene identifier: https://www.ncbi.nlm.nih.gov/gene

3.4. Statistics and figure composition

Ultrasound data from animals is shown normalized to the individual baseline diameter of the aorta. QPCR gene expression data is shown using the ΔΔCt-method normalized to housekeeping genes and individual control vessel (fold change=$2^{-\Delta\Delta Ct}$).[347] A Welch t-test for unpaired samples of small numbers (parametric) was used with a level of <.05 considered significant on gene expression data.

GraphPad Prism or Excel© was used to prepare graphs. Composite figures were assembled using PowerPoint©.

4.   Results

4.1.   Part I: Repurposing Lenvatinib®

4.1.1. Systemic oral Lenvatinib halts aneurysm growth in murine AAA

In a first attempt, mice with PPE induced AAA were orally given Lenvatinib (adjusted to their bodyweight) daily, starting at day 7 after aneurysm induction when an aneurysm was already established. This resulted in a significant reduction of aneurysm growth and a stable aortic diameter over the next 3 weeks until sacrifice (week 2: 1.54x vs. 1.35x; p=0.01; week 4: 1.63x vs. 1.38x; p=0.004) (**fig.9A**).
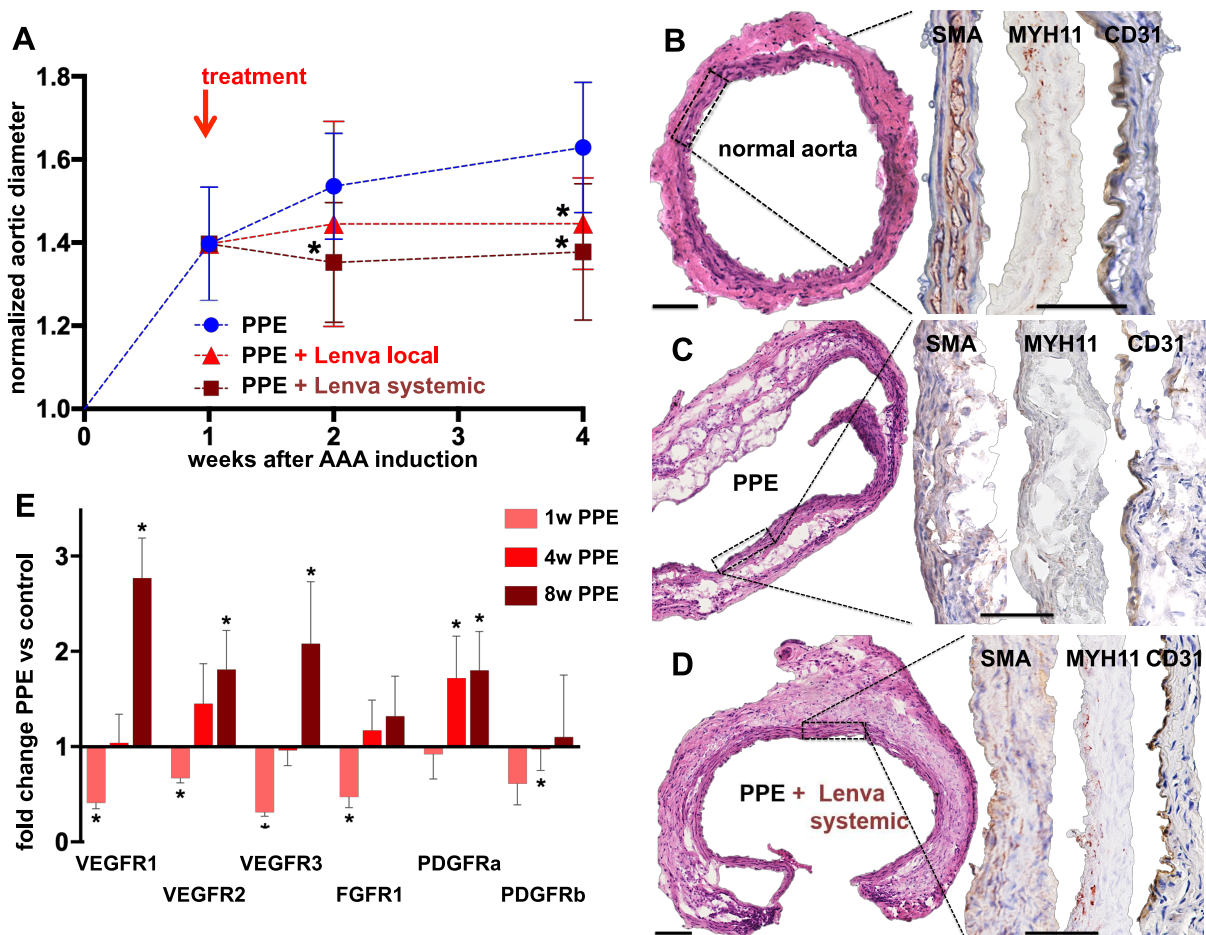
Fig.9: Both, systemic oral and local endovascular Lenvatinib treatment, starting day 7 after PPE aneurysm induction block aortic diameter enlargement (local: red; N=5; systemic: dark red; N=7) based on ultrasound measurement compared to non-treated PPE mice (blue; N=22). **(A)** HE staining revealed a disrupted media with pronounced cellular infiltrates in PPE-AAA compared to control aortae **(B,C)**. After systemic Lenvatinib treatment, cellular infiltrates were reduced and the media was more compact with, however, a thickened adventitia with marked fibrosis **(D)**. SMA stained positive in all three groups, emphasizing a more linear organized media in control aortae and importantly upon Lenvatinib treatment. MYH11 (red target staining) in contrast was absent in PPE, and positive in the media of Lenvatinib-treated mice. CD31 staining indicates intact endothelial lining in all three groups, but only in PPE-AAA few positive cells are also present in the media and adventitia **(B-D)**. (MYH11: red target staining; CD31/SMA: brown target staining; magnification 10x/40x; scale bar 1mm) The Lenvatinib target receptors as taken from the datasheet show a time-dependent up-regulation after initial suppression in normal PPE mice compared to non-treated control animals over 8 weeks (N=5 control animals, PPE 1 week, PPE 4 weeks and N=4 PPE 8weeks; *=p<0.05) **(E)**.

Based on previous experiments by others and us, we knew that VEGF and its receptors (VEGFR1/2/3) are dysregulated in a time-dependent manner in mice with PPE-induced aortic aneurysms.[170] The same could be demonstrated for the other Lenvatinib target receptors (**s.6.5.1.**) (**fig.9E**). All mice gained weight over the course of the experiment, and no alterations in basic blood laboratory assessment could be detected (**s. 6.5.1.**).

4.1.2. Array analysis identifies MYH11 as altered transcript

Mouse transcriptome array (MTA, 2.0) gene expression analysis comparing control animals (no aneurysm), normal PPE animals (aneurysm) and Lenvatinib treated animals (aneurysm+treatment) revealed Myh11 as the most significantly changed transcript (downregulated in controls vs PPE aneurysms, then upregulated in PPE aneurysm + Lenva vs PPE aneurysm) (**fig.10**). MYH11 is an established marker with importance in contractile VSMCs and known to be decreased in AAA compared to non-aneurysmal controls.[348]
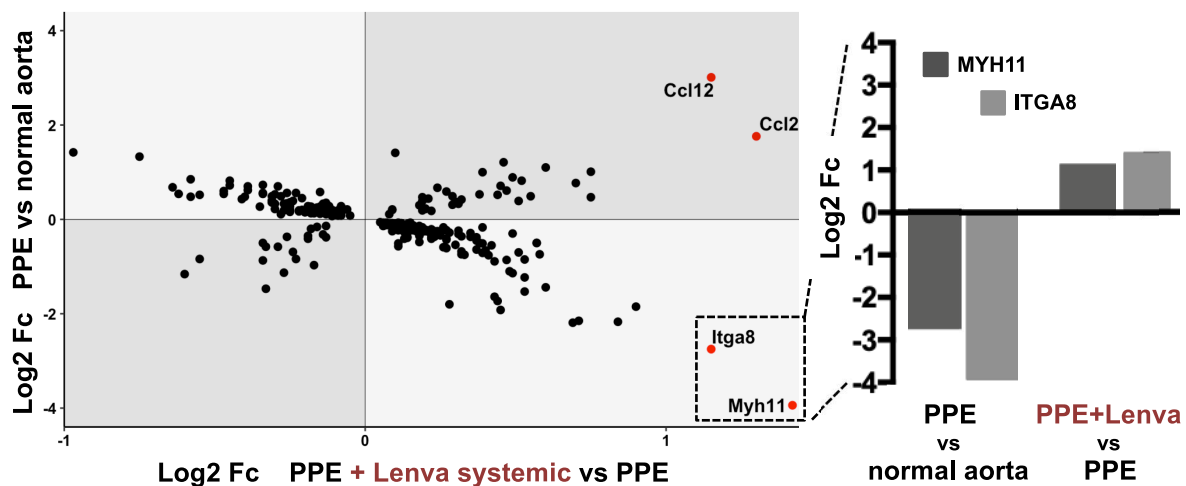
Fig.10: Double Fc plot depicts results of a mouse transcriptomic array (MTA). Areas with light-grey background represent genes that were regulated in opposite directions (e.g. rescue effect) upon Lenvatinib treatment. *Myh11* was seen with the most pronounced changes comparing log2 fold changes (Fc) of gene expression in PPE vs control and PPE+Lenva vs PPE. The bar chart highlights and indicates direction (up or down) of the most prominent changes in gene expression from the Fc plot (MTA analysis: N=6 PPE; N=7 PPE+Lenvatinib; N=5 untreated control aortae).

Immunohistochemical analysis revealed that MYH11 was present in the media of control aortae as well as in PPE+Lenvatinib, however, completely absent in regular PPE-induced aneurysms (**fig.9B-D**). CD31 staining showed signs of angiogenetic activity in the PPE aneurysms' media and endothelium, whereas only the endothelium stained positive in control and Lenvatinib treated animals with AAA. Thus, gene expression and protein analysis based on immunohistochemistry, along with basic morphologic analysis upon HE staining suggested a phenotypic aortic wall restoration upon Lenvatinib treatment with reduced angiogenesis, re-established MYH11 levels and signs of increased fibrosis (**fig.9B-D**).

4.1.3. Mimicking local Lenvatinib delivery in mice

Secondly, unable to locally deliver Lenvatinib by a drug-coated balloon due to size restriction of the model, we performed a re-operation and local perfusion of the established AAA on day 7 after PPE induction in mice (**fig11A**). This also resulted in a significant diameter reduction compared to normal sham-intervened PPE mice at the time of sacrifice at week 4 (week 2: 1.54x vs. 1.44x; p=0.3; week 4: 1.63x vs. 1.45x; p=0.03) (**fig.11B**). Similar characteristics as described above for a phenotypic salvage with a more contained aortic structure and MYH11 positivity after local Lenvatinib treatment could be observed (**fig.11C/D**). These effects were not seen after local reperfusion with PBS as a surgical (sham) control experiment.
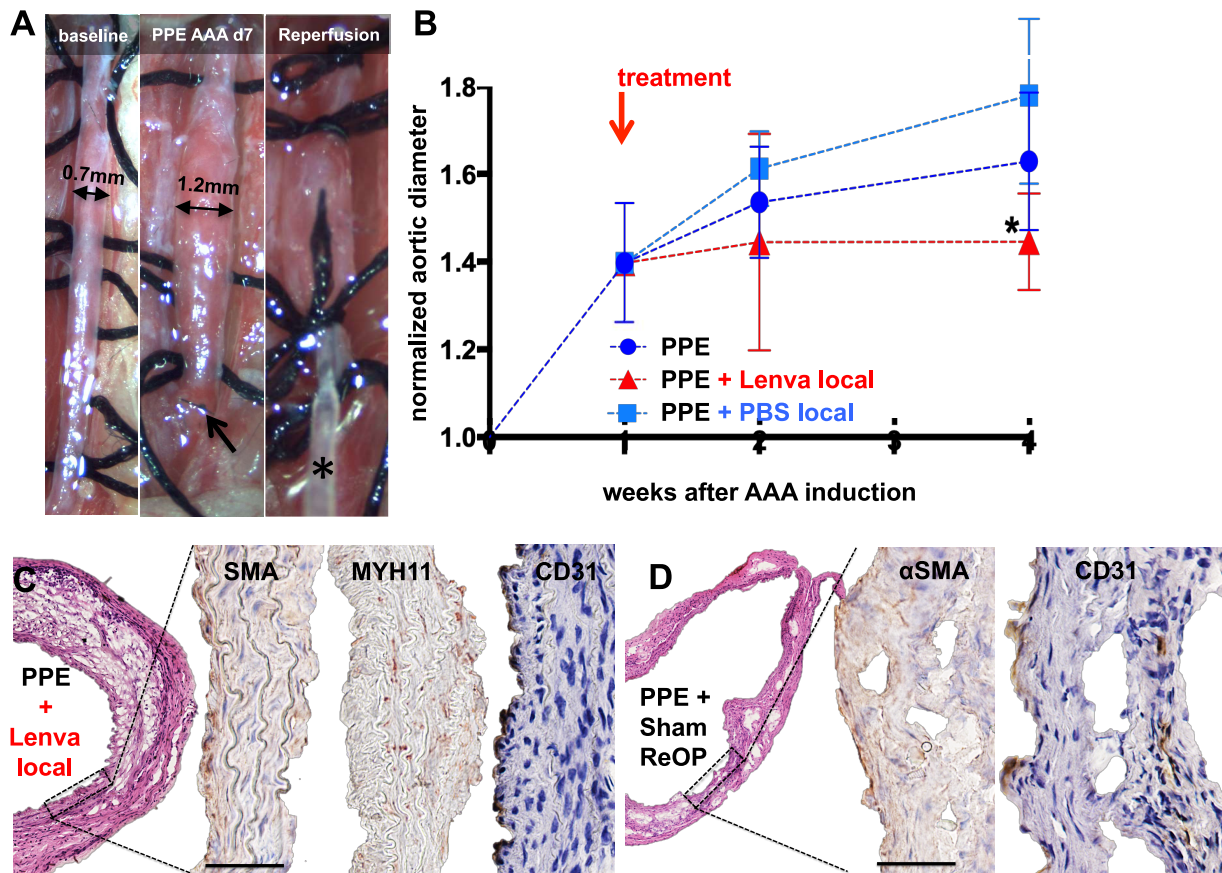
Fig.11: To simulate local endovascular Lenvatinib treatment, mice are re-operated on day 7 after aneurysm induction **(A)**. The established AAA (arrow indicates the previous aortic suture from the initial procedure) is prepared from the retroperitoneum, and a local perfusion with Lenvatinib is performed (asterisk indicates the perfusion catheter). This procedure (red; N=5) significantly reduced aortic diameter growth compared to regular PPE (blue; N=22) **(B)**. In contrast, re-operation with sham re-perfusion (PBS; light blue; N=3) did not show any significant effect. Comparable to **Fig.9**, histologic and IHC analysis showed a more condensed aorta with MYH11 positive cells in the media **(C)**. PPE+Sham re-operation showed a disrupted media with remaining CD31 and αSMA positivity 4 weeks after the initial aneurysm induction **(D)**. (MYH11: red target staining; CD31/αSMA: brown target staining; magnification 10x/40x; scale bar 1mm)

4.1.4. MYH11 is similarly involved in human AAA pathogenesis

The phenotype switch in VSMCs in AAAs has been demonstrated several times before.[348-350] We analyzed human AAA samples from an advanced disease state (6-7cm diameter) from patients undergoing open aortic repair in our department.

The morphology of AAA compared to non-dilated aorta is completely altered in terms of degradation of the elastic fibers, disruption of the media and adventitia, angiogenesis in the aortic media and inflammatory infiltrates (**fig.12A,B**). CD34 positive cells and neo-angiogenesis were found abundantly in diseased aortic media layers (data not shown). Further, different vascular endothelial growth factors as well as their receptors (VEGF/VEGFR1/2) were identified for being increased in human AAA.[24] A gene expression analysis of characteristic SMC markers showed a definite loss of contractile features in AAA compared to non-dilated control aorta (**fig.12C; Table VIII**).
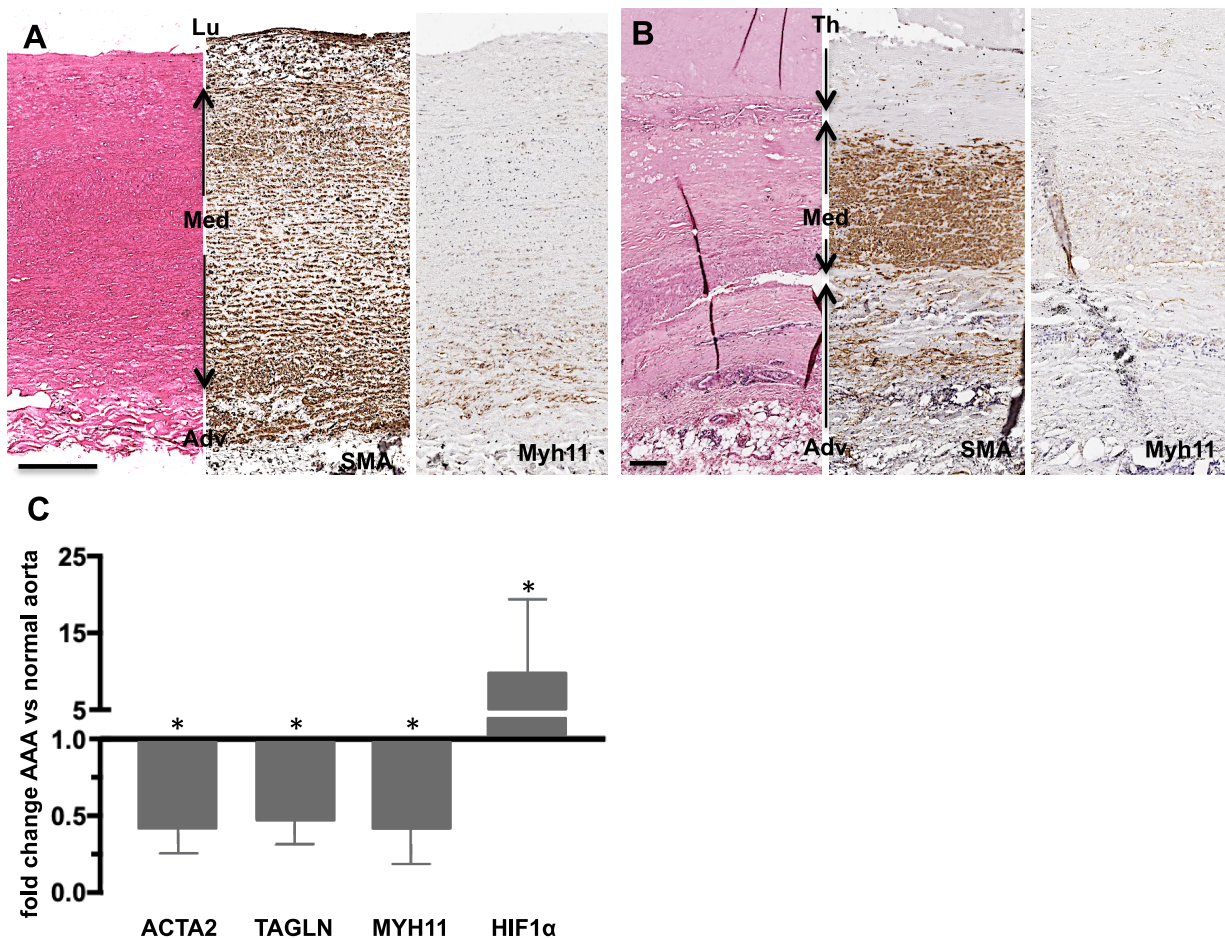
Fig.12: The non-aneurysmatic human aorta has a densely organized media with approx. 30 layers of elastic fibers organized in parallel with the SMA- and MYH11-positive VSMCs **(A)**. This morphology is completely altered in AAA, with the media and the elastic fibers being disrupted **(B)**. SMA positivity remains, whereas MYH11 positivity is lost in the media. New small vessels are found in the media with CD34 positivity and marked expression of VEGFR2. The contractile VSMC phenotype genes *ACTA2, TAGLN* and *MYH11* are significantly reduced, whereas *HIF1α* is highly overexpressed **(C)**. (Lu=Lumen; Adv=Adventitia; Med=Media; Th=Thrombus; magnification 2.5x/40x in IHC; scale bar 200µm; *=p<0.05)

Smooth muscle cell α-actin (SMA), a major component of the contractile apparatus is highly prevalent in the media and adventitia of dilated and control aorta with, however, a more organized structure in non-aneurysmatic vessels (**fig.13**). Double immunofluorescent staining confirmed MYH11 being co-localized with SMA in non-dilated aortas, but interestingly completely absent in AAA (**fig.13**).
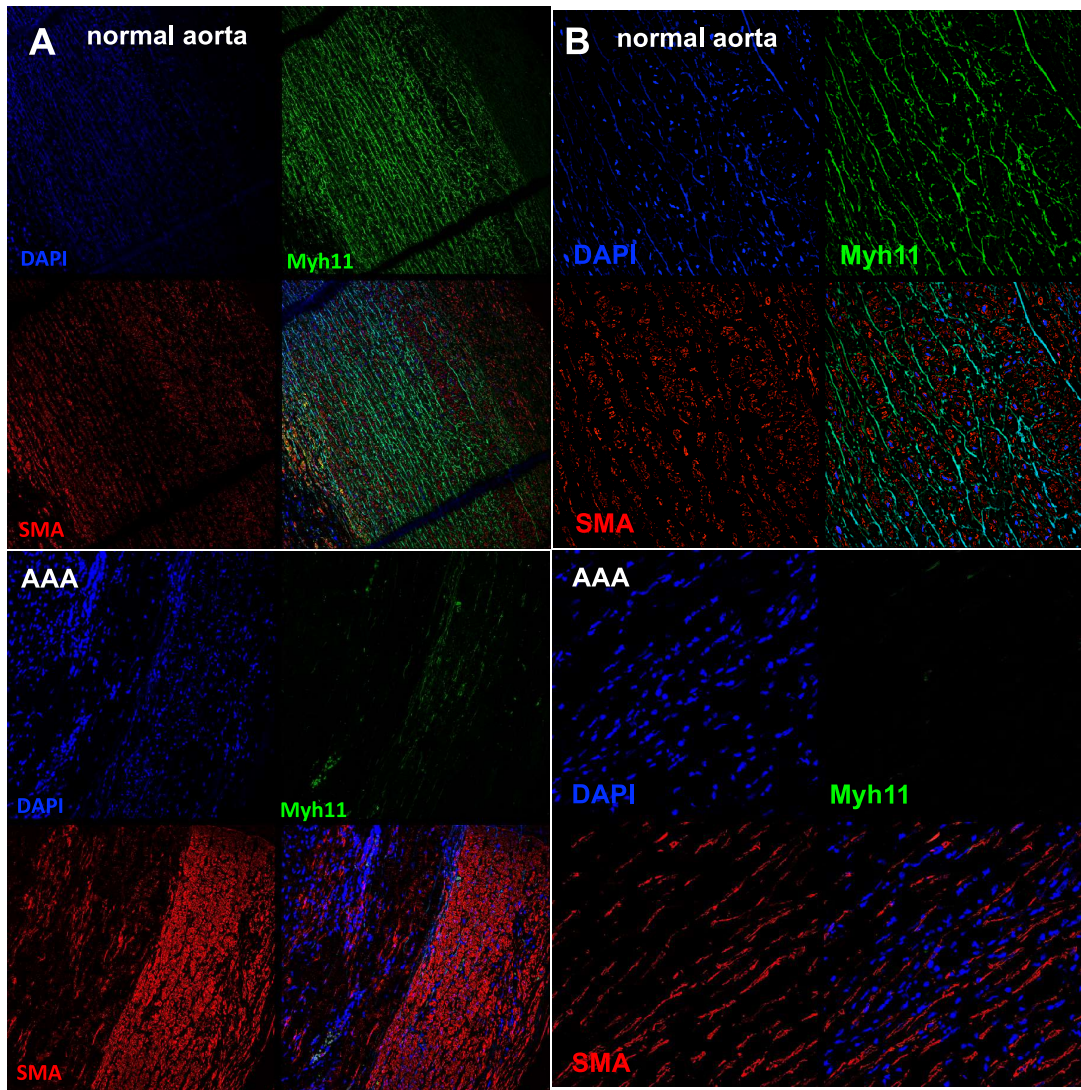

Fig.13: Double immunofluorescence reveals the distribution pattern of the two filaments SMA and MYH11 in the aortic media and the disruption of this co-localization in AAA in comparison in low **(A)** and high magnification **(B)**. (Lu=Lumen; Adv=Adventitia; Med=Media; Th=Thrombus; magnification 2.5x/40x in IHC; 63x in IF; scale bar 200µm; *=$p < 0.05$)

4.1.5. Primary human AAA cell culture experiments

We found a dose dependent anti-proliferative effect of Lenvatinib in cell culture on human aortic smooth muscle cells using the Incucyte live-cell imaging system (**fig.14**). Since already for **0.1µM Lenvatinib** a markedly reduced mobility was seen, this was further used for cell-based assays.
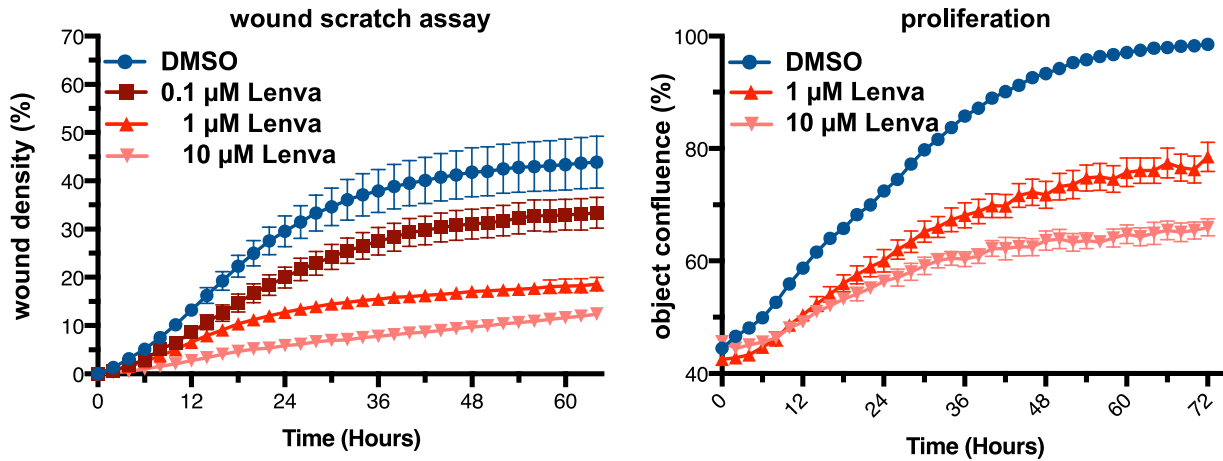
Fig.14: To estimate the least harmful concentration of Lenvatinib with a distinct effect on cell proliferation, a dose-response wound scratch assay and proliferation assay was performed. (AAA control=treatment with 0.1% DMSO; *=p<0.05; ****=p<0.001; for list of genes and explanation s. **Table VII**)

For better validation, additionally to this commercially available cell culture **(fig.15)**, a primary VSMC culture derived from three different AAA patients, was obtained (age: 71±3y; diameter: 65±5mm; only two cell strains shown) (**fig.16/17**).
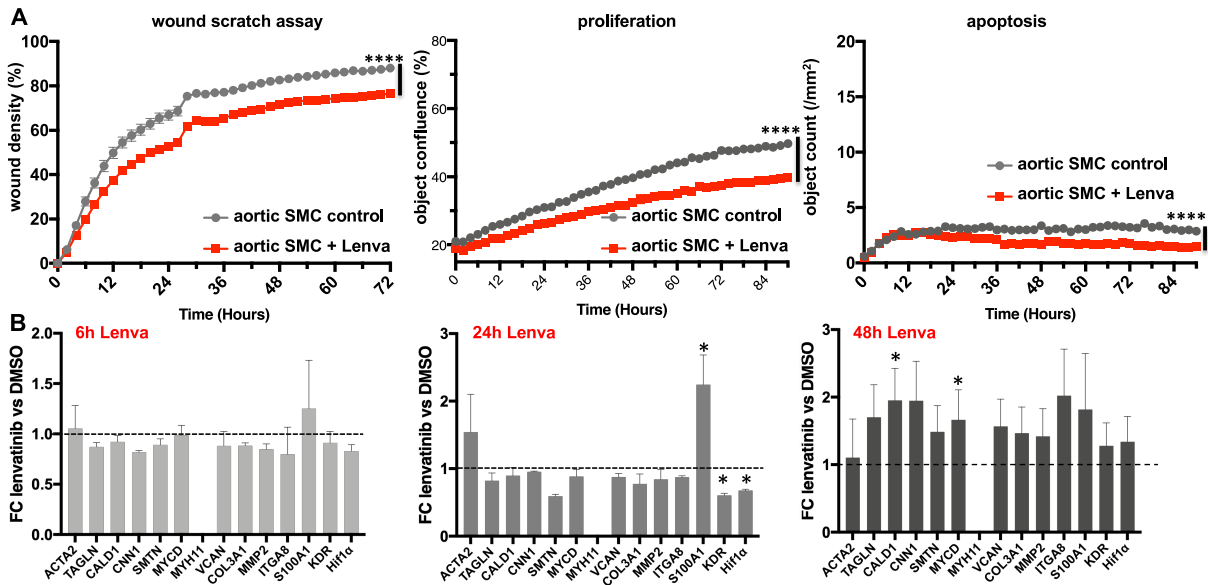
Fig.15: Commercial aortic smooth muscle cells: Live-cell imaging with automated cell counting comparing cells treated with 0.1%DMSO (control) vs. 0.1μM Lenvatinib showed impaired VSMC mobility upon wound scratch assay over 3 days **(A)**. Lenvatinib decreases proliferation, whereas the number of apoptotic cells does not differ. At 48h after Lenvatinib treatment, e.g. *CALD1* any *MYCD* are significantly up regulated **(B)**. (* = p<0.05, *** = p<0.01)

Cell mobility in a wound scratch assay and cell proliferation were markedly reduced after Lenvatinib treatment compared to controls treated with vehicle (DMSO) only **(fig.15-17)**. Apoptosis was low in general, and not overly affected by Lenvatinib in all four cell strains. Of the investigated genes, a subset typically involved in the contractile function of VSMCs was up regulated upon Lenvatinib treatment in a time-dependent

manner. *VEGFR2 (KDR)*, a direct and established target of Lenvatinib was significantly down-regulated in all three cell strains after 48h treatment. Primary cells showed a better reactivity to Lenvatinib in all live-cell assays, with more significant effects based on altered gene expression (**fig.15-17).**
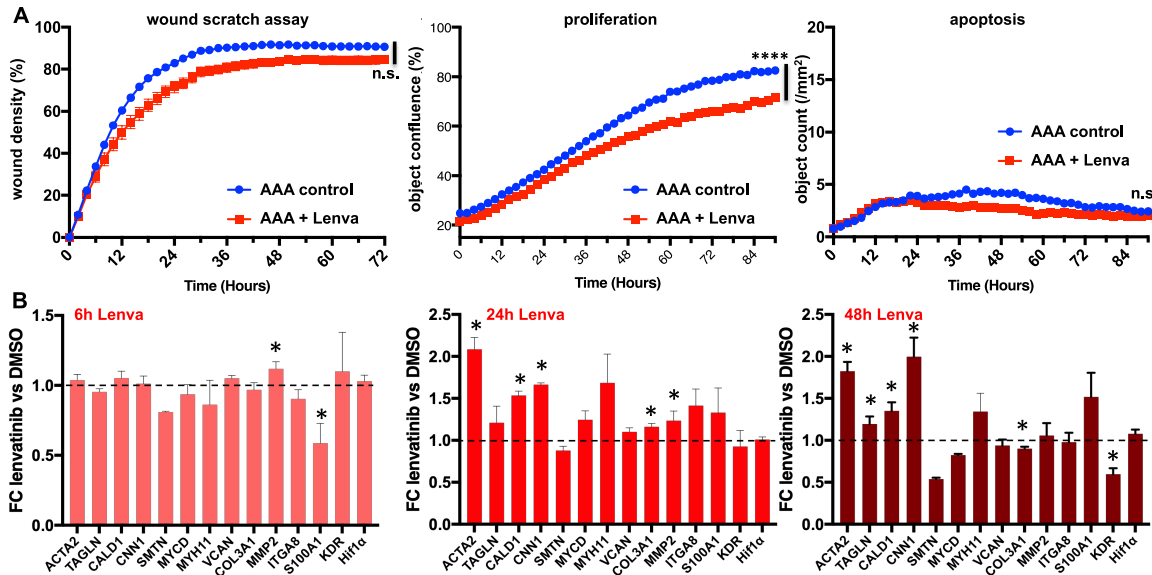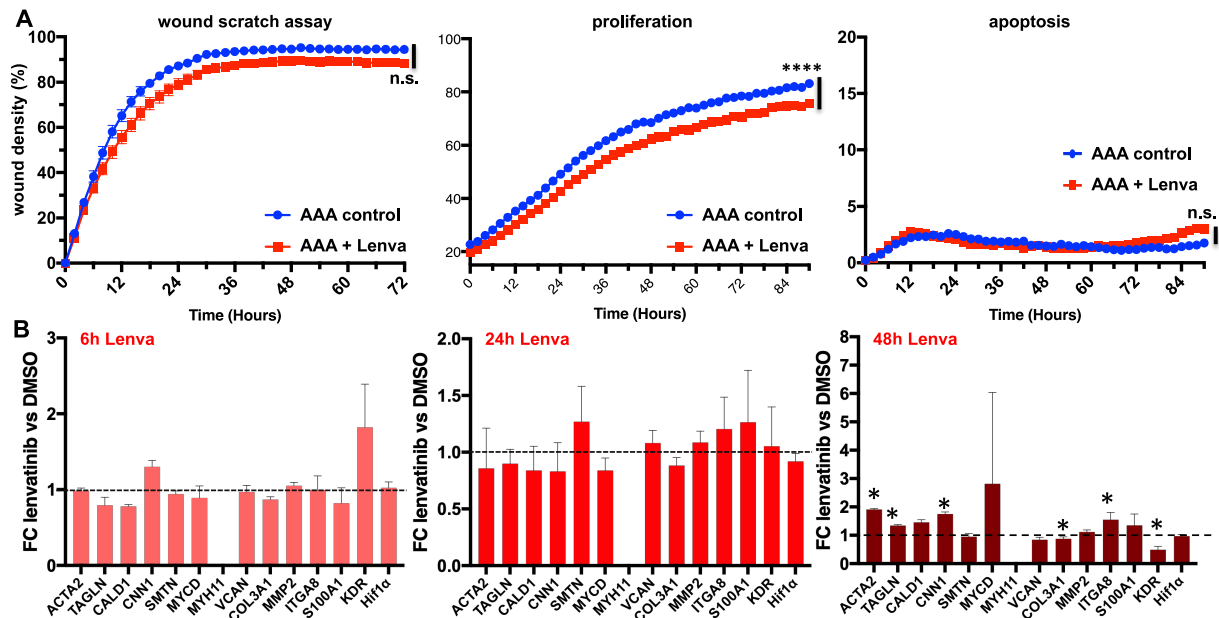

Fig.16: Lenvatinib treatment in primary human AAA cells strain #1: Live-cell imaging with automated cell counting comparing cells treated with 0.1%DMSO (control) vs. 0.1μM Lenvatinib showed impaired VSMC mobility upon wound scratch assay over 3 days **(A)**. Lenvatinib decreases proliferation, whereas the number of apoptotic cells does not differ. At 48h after Lenvatinib treatment, e.g. *ACTA2, CNN1* and *CALD1* are significantly up regulated, whereas e.g. *KDR* is significantly down regulated **(B)**. (* = p<0.05, *** = p<0.01)

Fig.17: Lenvatinib treatment in primary human AAA cells strain #2: Live-cell imaging with automated cell counting comparing cells treated with 0.1%DMSO (control) vs. 0.1μM Lenvatinib showed impaired VSMC mobility upon wound scratch assay over 3 days **(A)**. Lenvatinib decreases proliferation, whereas the number of apoptotic cells does not differ. At 48h after Lenvatinib treatment, e.g. *ACTA2*, and *CNN1* are significantly up regulated, whereas e.g. *KDR* is significantly down regulated **(B)**. (* = p<0.05, *** = p<0.01)

65

In accordance with immunohistochemistry and gene expression, Western Blot analysis also detected MYH11 being substantially more abundant upon Lenvatinib stimulation (**fig.18/19/20**). Exploring possible downstream signaling pathways affected by Lenvatinib, we discovered phospho-ERK1-2 significantly decreased compared to total-ERK1-2 in all 4 cell strains, 6h and 48h after cells were exposed to treatment (**fig.18/19/20**).
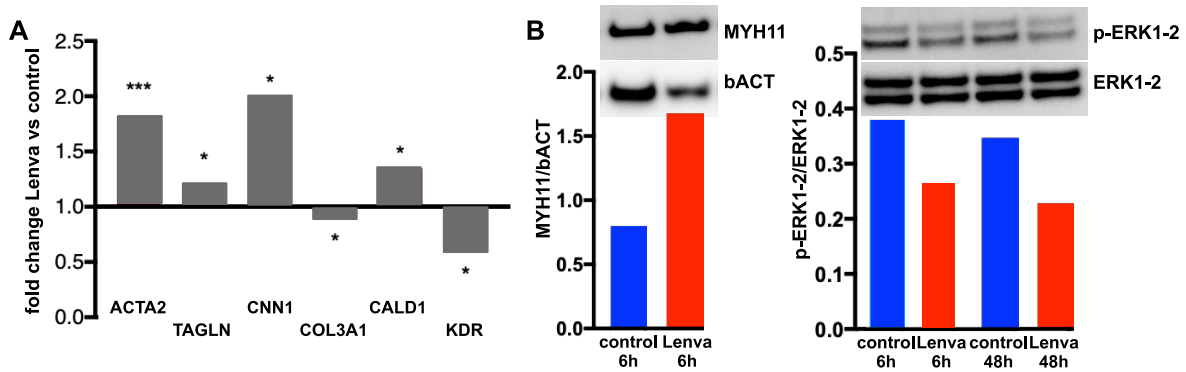

Fig.18: Summary of gene expression and WB data for cell strain #1: At 48h after Lenvatinib treatment, e.g. *ACTA2, CNN1* and *CALD1* are significantly up regulated, whereas e.g. *KDR* is significantly down regulated **(A)**. On protein level, MYH11 is found in higher abundance normalized to β-actin at 6h after Lenvatinib. Markedly less phosphorylated ERK1-2 is seen after Lenvatinib treatment at 6h and 48h **(B)**. (* = p<0.05)
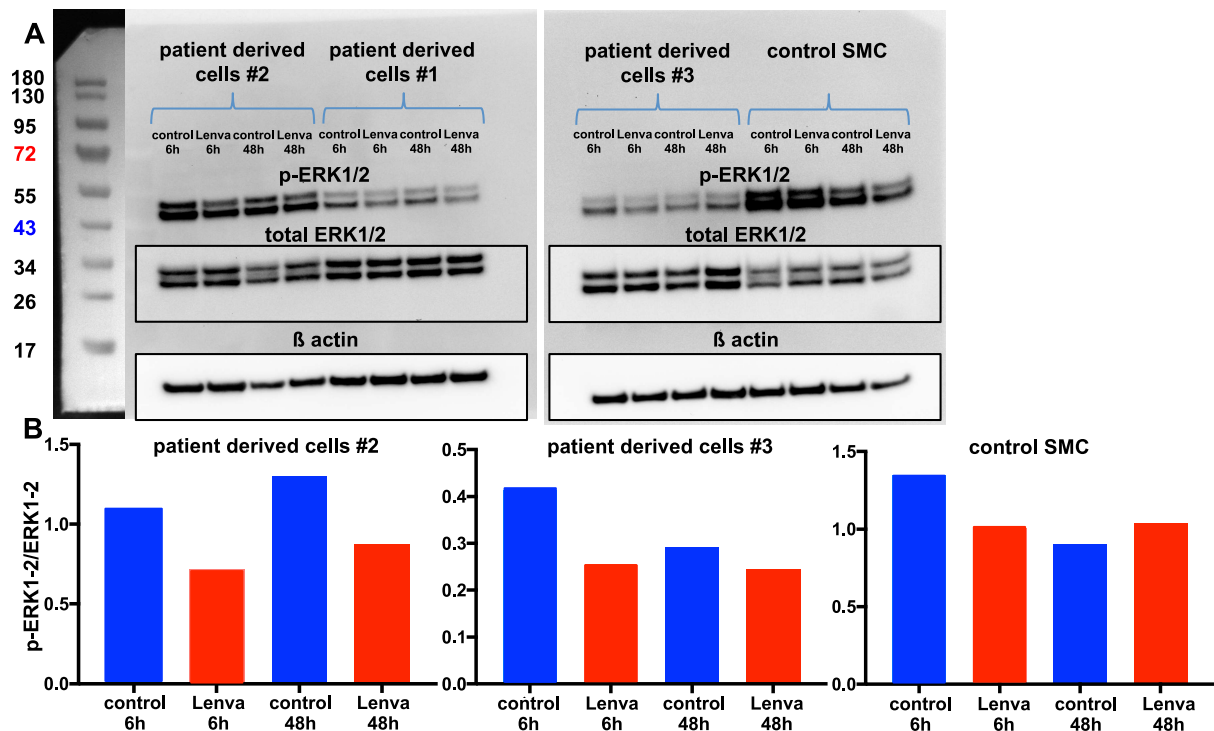

Fig.19: The two membranes show the WB experiment for ERK1-2/pERK1-2 for the 3 primary human AAA cell lines (#1-3) and the commercial non-aneurysmatic aortic SMCs **(A)**. Total ERK1-2 and β-actin for loading control are shown as inlay. A cell strain #1 blow-up is shown in **fig.4**. Additionally, the quantification of the staining intensity comparing pERK1-2/ERK1-2 is shown for all conditions DMSO 6h/48h and Lenvatinib 6h/48h **(B)**.
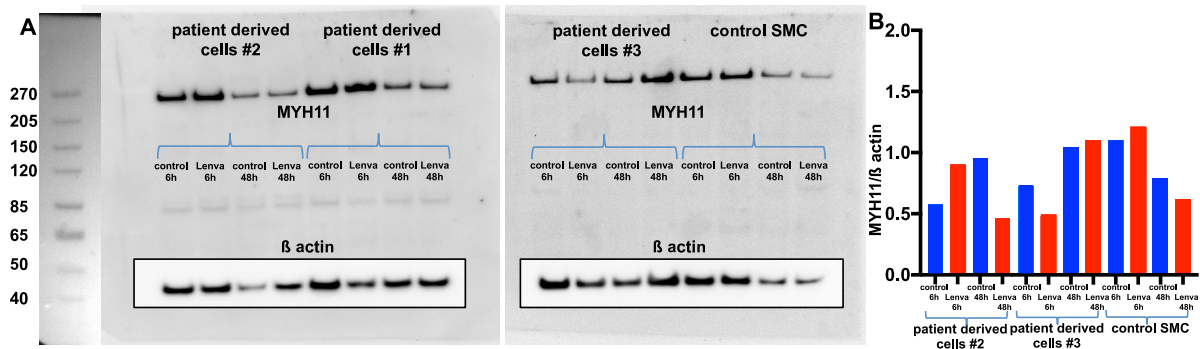
Fig.20: The two gels show the membranes experiment for MYH11 for the 3 primary human AAA cell lines (strain #1-3) and the commercial non-aneurysmatic aortic SMCs **(A)**. β-actin for loading control and for normalization is shown as inlay. A cell strain #1 blow-up is shown in **fig.4**. Additionally, the quantification of the staining intensity comparing MYH11/β-actin is shown for all conditions DMSO 6h/48h and Lenvatinib 6h/48h **(B)**.

4.1.6. Establishing a new Yucatan *LDLR*$^{-/-}$ mini-pig AAA model

To further test the potential of a local endovascular delivery of Lenvatinib to halt aneurysm growth, we established a novel large animal model with inducible AAA in hypercholesterolemic *LDLR*$^{-/-}$ Yucatan mini-pigs (**fig.21**). The animals show severe atherosclerosis throughout the vascular system, with the infrarenal aorta mimicking an "aged" vascular phenotype compared to wildtype littermates, and thus perfectly matching prototypical human AAA disease.[351]
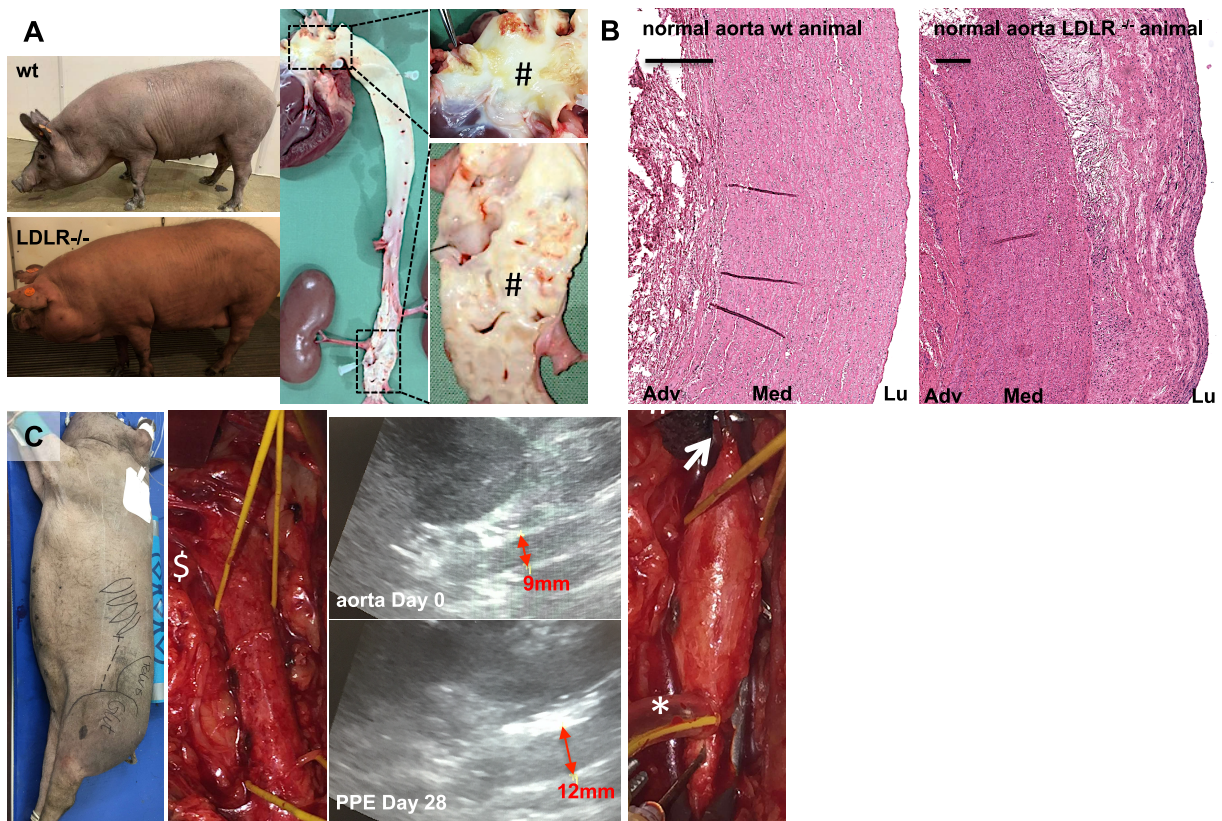

Fig.21: 12 months old *LDLR*$^{-/-}$ (bottom) and wildtype (top) Yucatan minipigs demonstrating an obese phenotype upon gross appearance **(A)**. On an en face preparation, the aorta shows severs atherosclerosis at the branching sites at the supra-aortic level and at the aortic trifurcation (blow-ups).

HE staining shows a plaque formation with foam cells and cholesterol depositions in the endothelium and media in an *LDLR$^{-/-}$* compared to a wildtype aorta **(B)**. Note the cell-rich infiltrate at the border of plaques. Pigs are lying on their right side and a left retroperitoneal approach is used to expose the infrarenal aorta form the lower renal artery ($) to the aortic trifurcation **(C)**. After ligation of the lumbar arteries, a Satinsky clamp (arrow) is applied, and the isolated segment is pressure-perfused with elastase via a blunt 5G needle (#) secured by an additional vessel loop tourniquet (asterisk). Abdominal ultrasound is used to follow-up the diameter of the infrarenal aorta based on leading-edge measurement at baseline (top) and at 1 and 4 weeks after aneurysm induction (bottom; 4 weeks). (scale bar 200µm; Adv=adventitia; Lu=lumen; Med=Media)

The PPE procedure resulted in a significant increase of the aortic diameter at 1 and 4 weeks (week1: 21±15%, p=0.0004; week4: 56±21%, p=0.000002; N=12; **fig.22; s. 6.5.1.**) compared to the sham-operation (saline instead of elastase perfusion; at week 4: 10±9% diameter increase). Compared to non-dilated *LDR$^{-/-}$* mini-pig aortas, PPE-induced aneurysms showed reduced MYH11 expression and CD31 positive neovessels in the aortic media of the dilated vessel (**fig.22**).
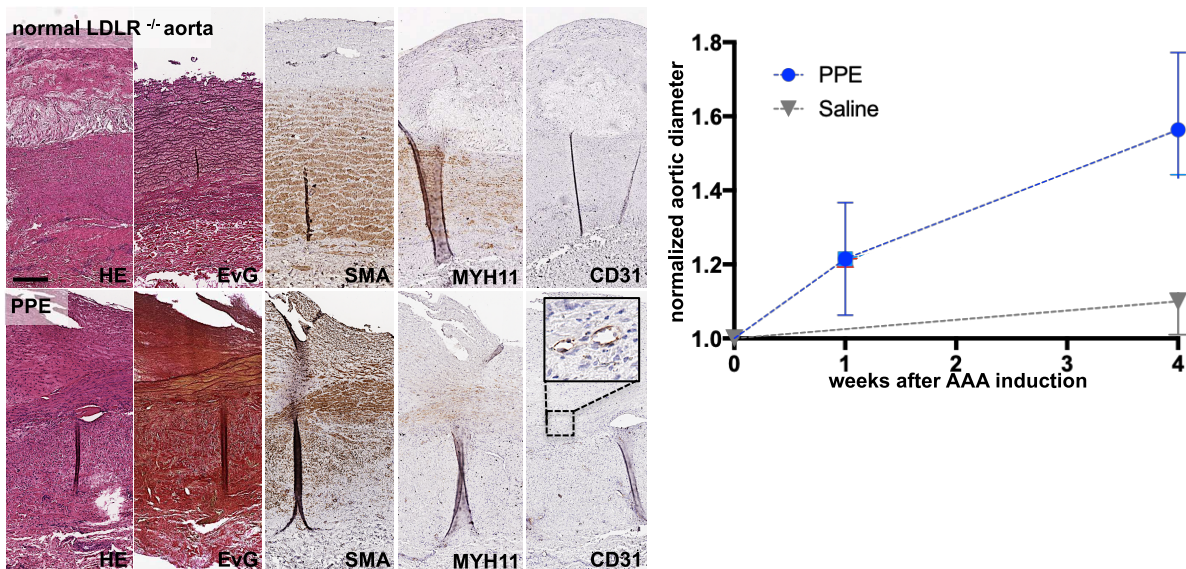

Fig.22: The aorta of *LDLR$^{-/-}$* knockout pigs shows an aortic wall with parallel-orientated elastic fibers in the media and plaque formation in the intima/media in HE and EvG stains **(upper row)**. The VSMCs in the media are positive for SMA and MYH11 but don't show any CD31 positivity. After PPE treatment, the elastic fibers are mostly disrupted, and the parallel-layered structure of the media vanished **(lower row)**. Vast positivity for SMA remains, whereas only a few cells show MYH11. CD31 positive neovessels are seen in the media and the thickened adventitia **(C blow-up)**. The PPE procedure results in a 56% diameter increase of the treated aorta compared to untreated animals. Intraluminal saline perfusion (grey) instead of PPE (dark blue) does not lead to aortic diameter enlargement. (magnification 5x; scale bar 100µm)

4.1.7. Lenvatinib coated balloon angioplasty blocks aneurysm progression

The development of AAA was put to halt with a Lenvatinib coated balloon treatment at day 7, significantly reducing the aortic diameter after 4 weeks (58±24% vs. 23±8%, p=0.001; N=4) (**fig.23A,B**). Histological and immunohistochemical analysis revealed again abundance of MYH11 co-localizing with SMA in the aortic media. Consistently, a similar trend was confirmed by western blot: Lenvatinib-treated pig aortas seem to

have a higher MYH11 protein amount as compared to untreated animals (DMSO only) **(fig.23C,D; fig.24)**. Animals' weights remained stable over time and no alterations in blood parameters (cell count; liver, kidney function) were detected (**s. 6.5.1.**). Control treatment with a vehicle (DMSO) coated balloon did not show a significant effect on the aortic diameter (data not shown).
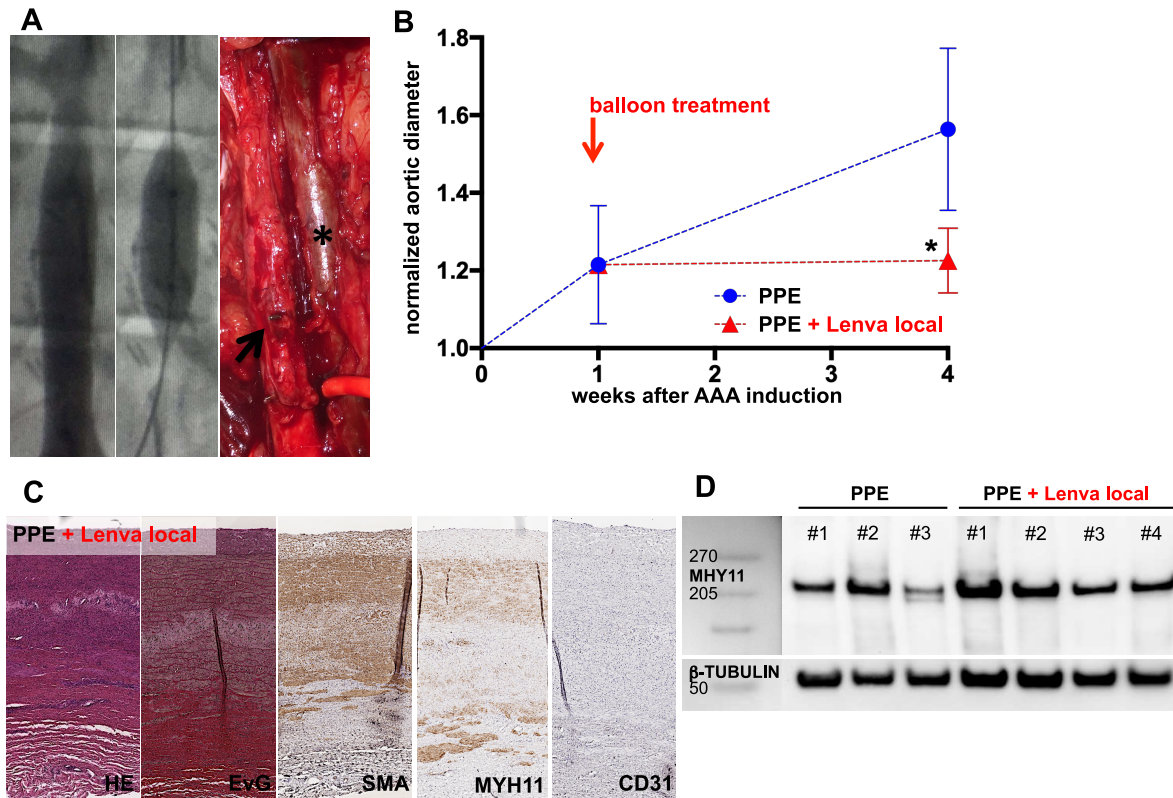

Fig.23: Transfemoral angiography of the infrarenal aorta (right renal artery seen on upper end) shows a dilated segment of the aorta. Radiopaque markers guide the coated balloon (12x20mm) to the lesion. Note the surgical clips from the aneurysm induction procedure sealing the lumbar vessels. The photo shows the dilated part of the aorta (arrow) at the time of sacrifice (no more blood circulation) next to the caval vein (asterisk) **(A)**. Treatment with a Lenvatinib-coated balloon on day seven after AAA induction showed significant diameter reduction and halt of aneurysm growth at sacrifice on day 24 upon ultrasound assessment (red; N=4) compared to non-treated control animals (blue; N=12) **(B)**. Upon Lenvatinib treatment, MYH11 positivity is restored **(C)**. Of note, CD31 stains positive only the endothelial layer. A similar trend was confirmed by western blot: Lenvatinib-treated pig aortas seem to have a higher MYH11 protein amount as compared to untreated animals (DMSO only) **(D)**. (*: $p < 0.05$; magnification 5x/20x/40x; scale bar 200µm; vessel lumen oriented upwards)
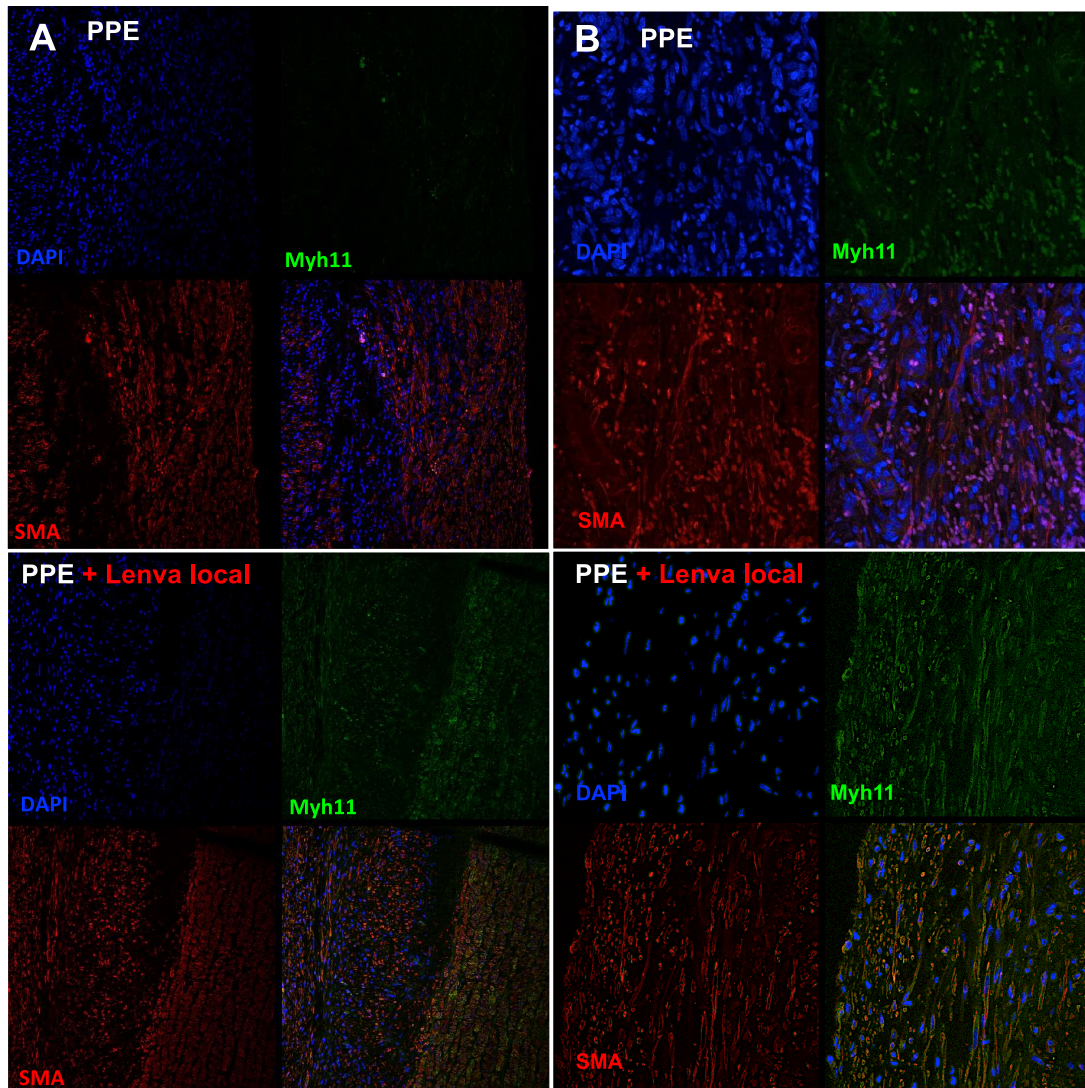
Fig.24: Double immunofluorescence reveals the distribution pattern of the two filaments SMA and MYH11 in the aortic media of the pig aorta and the disruption of this co-localization in AAA in comparison in low **(A)** and high magnification **(B)**. (Lu=Lumen; Adv=Adventitia; Med=Media; Th=Thrombus; magnification 2.5x/40x in IHC; 63x in IF; scale bar 200μm; *=p<0.05)

4.2. Part II: Long non-coding RNA H19 in AAA formation

The majority of data presented in this section has been published already in a paper by our group in 2018 (s. supplement **6.5.3.** for the published paper).[352] The doctoral student performed a variety of experiments as part of his PhD thesis that are presented here. Section **4.2.4.** contains data that is currently followed up on for a possible additional publication.

4.2.1. Murine AAA tissues for RNA profiling

For the purpose of screening for lncRNA candidates in mouse AAA tissues, infrarenal aortic tissue of PPE or Angiotensin II induced AAAs and the respective control tissues were provided by the doctoral student (**fig.25**).
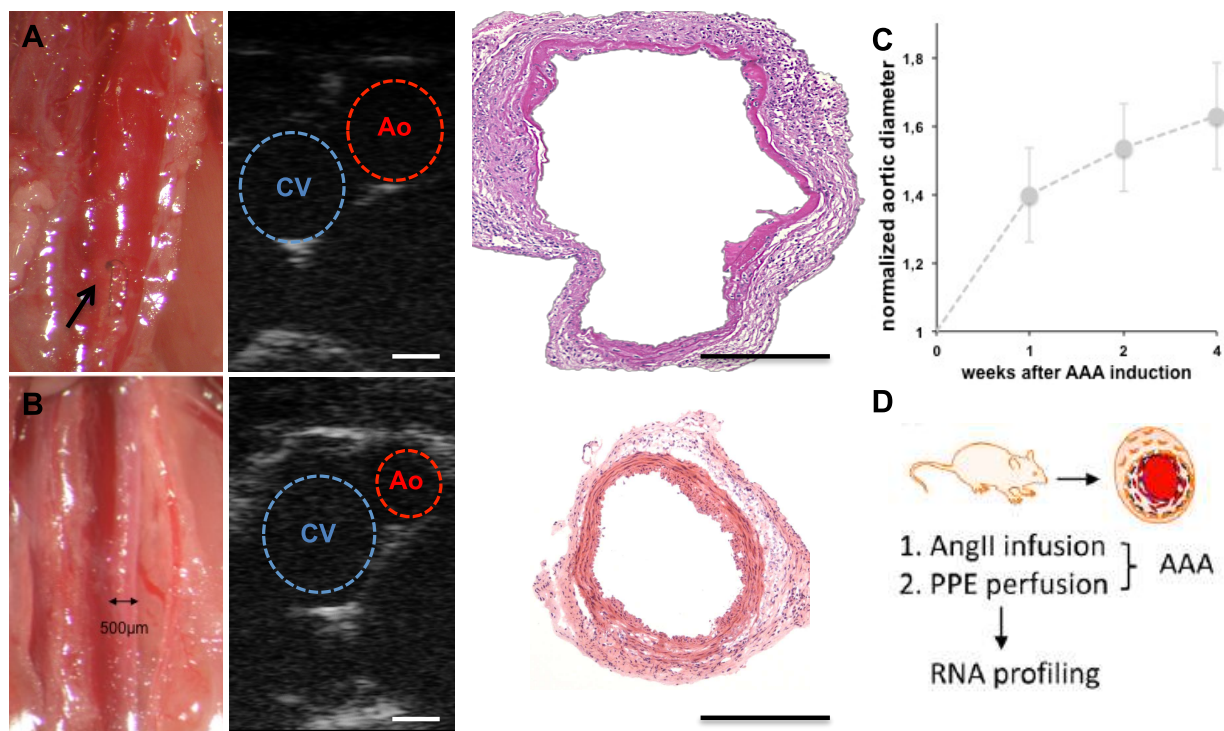

Fig.25: The murine infrarenal aorta is exposed 4 weeks after the PPE procedure **(A)** (arrow indicates the suture for closure of the catheter perfusion). The aorta is significantly dilated at 1, 2 and 4 weeks after the procedure **(B)**. Ultrasound is used to follow up the dilation (Ao = aorta; CV = caval vein). Normalized to the baseline diameter at day 0, the treated part of the aorta dilates by 40±14% at week 1 (N=22 animals), 54±13% at week 2 and 63±16% at week 4 **(C)**. Of note is the completely altered histomorphology of a PPE-induced AAA in comparison to a normal untreated aorta. The aortic media, typically consisting of 4-5 layers of elastic fibers becomes a fibrotic layer after the procedure. The adventitia consists of collagenous tissue with only little cellular content and also shows fibrosis and inflammatory infiltrates after the procedure. Carefully dissected and flushed tissue to rinse away debris and intraluminal blood cells from the PPE aneurysm model was provided for RNA profiling in this project **(D)** (modified from Li et al.[72]). Similarly, tissue from the Angiotensin II model (**s. 3.1.3.**) was provided. This is a standard model in our group and has been described and published various times before.[307, 308, 310] (scale bar 500µm; HE staining; own unpublished data and pictures)

4.2.2. Modifying H19 expression in experimental murine AAA models

To test the hypothesis of H19 knockdown limiting aneurysm growth in the PPE model, a knockdown experiment using specific LNA–anti-H19 GapmeR (intervention) or scr-GapmeR (negative control) was designed (**s. 3.1.4.**). Treatment was started immediately after aneurysm induction (1st injection) and was continued at days 7 (2nd injection) and 14 (3rd injection) after the procedure before ultrasound examination.
While animals injected with scr-GapmeR (week 1: 46±9%, p=0.14; week 2: 50±8%, p=0.85; week 4: 64±15%, p=0.5) did not show a significant difference in aortic diameter compared to standard PPE only animals (week 1: 40±14%; week 2: 54±13%; week 4: 63±14%), injection of LNA–anti-H19 GapmeR did (**fig.26**). Normalized baseline ultrasound diameters were 20±12% (week 1: p=0.04), 25±15% (week 2: p=0.06) and 27±16% (week 4: p=0.03).
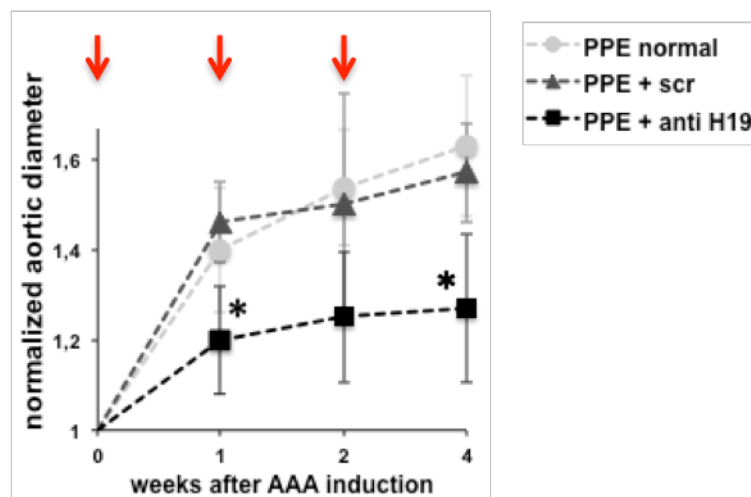

Fig.26: The infrarenal aortic diameter displayed normalized to the baseline diameter does not show a difference for the control experiment (scr-GapmeR injection) compared to the standard PPE procedure. Injection of LNA–anti-H19 GapmeR (red arrows) at three consecutive time points resulted in a significant decrease of the aortic diameter. (*= p<0.05; N= 22 for standard PPE; N=5 for scr control; N=7 for LNA–anti-H19 GapmeR)

To confirm sufficient H19 knockdown in the LNA–anti-H19 GapmeR group, qPCR (data not shown – not performed by the doctoral student) and in situ hybridization (ISH) were performed. H19 was not detected in the aorta of animals treated with a H19 knockdown (**fig.27**). This was confirmed by qPCR results.[72] Using standard immunohistochemistry, the co-localization with αSMA and HIF1α was investigated. Whereas co-localization with αSMA positive cells confirmed medial VSMCs as the major cellular effector of H19 under both conditions, HIF1α was not detected in the absence of H19 in the knockdown aortic tissue (**fig.27**).
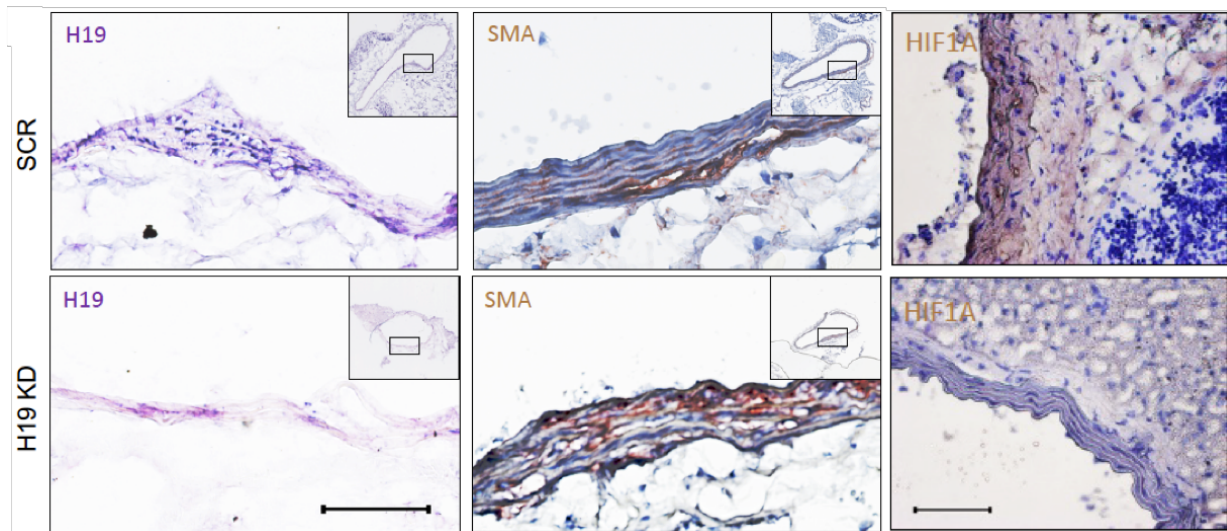
Fig.27: In situ hybridization of H19 (purple) and immunochemistry staining of smooth muscle cell a-actin (SMA, brown) and HIF1α (brown) shows abundant H19 located in the aortic media after injection of scr-GapmeR (control) in comparison to LNA–anti-H19 GapmeR (intervention: H19 knockdown). The number of SMA positive cells in the aortic media does not differ, but HIF1α in the media and the surrounding adventitia is markedly reduced in the absence of H19. (magnification 10x/45x; scale bar=100 µm; modified from Li et al.[72])

4.2.3. H19 and HIF1 in an experimental pig AAA model

Our new pre-clinical AAA model in Yucatan LDLR$^{-/-}$ pigs has been extensively introduced in Part I of the results section (**s. 4.1.6.**). Tissue from these animals has also been used to confirm the role H19 in aneurysm formation across species.

Here, qPCR confirmed the significant up-regulation of H19 and HIF1α in animals, where the PPE procedure was performed and showed aneurysmatic dilation of the infrarenal aorta (**fig.28**). The control group consisted of sham-operated pigs (perfusion with saline instead of elastase) (**fig.22**). Hence H19 was present in AAAs in mice, pigs and humans.[72]
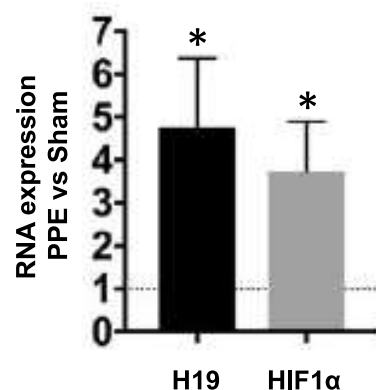

Fig.28: qPCR results show a significant up-regulation of H19 and HIF1α after the PPE procedure instead of the sham procedure. (*= p<0.05; N=4 sham procedures and N=8 PPE procedures; additional information is provided in the online supplement of our paper on this subject[72])

4.2.4. PPE aneurysm induction in H19 knockout mice

An additional, so far unpublished, experiment included the PPE aneurysm induction in H19 knockout mice for confirmation of the results using a systemic H19 knockdown by GapmeR injection (**s. 3.1.5.** and **4.2.2.**).

Here, markedly reduced aneurysm formation was seen after the procedure in comparison to PPE AAA induction in a standard C57BL/6J animal (**fig.29**) (values s. figure legend).
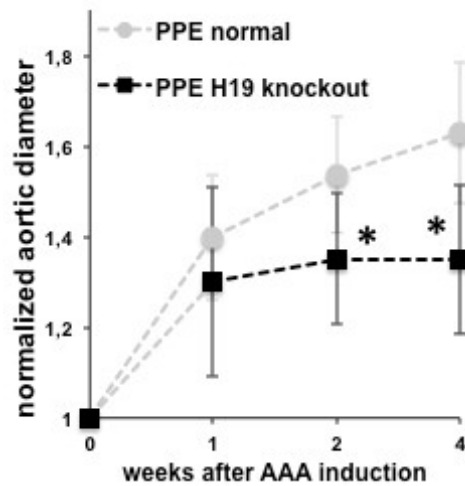

Fig.29: In comparison to normal wildtype animals, performance of the PPE procedure in H19 knockout animals resulted in a significant decrease of the aortic diameter at weeks 2 and 4 (week 1: 30±21%, p = 0.32; week 2: 35±14%, p = 0.04; week 4: 35±16%, p = 0.03; N=22 animals for standard wildtype PPE, N=10 H19 knockout animals)

5.   Summary and concluding remarks

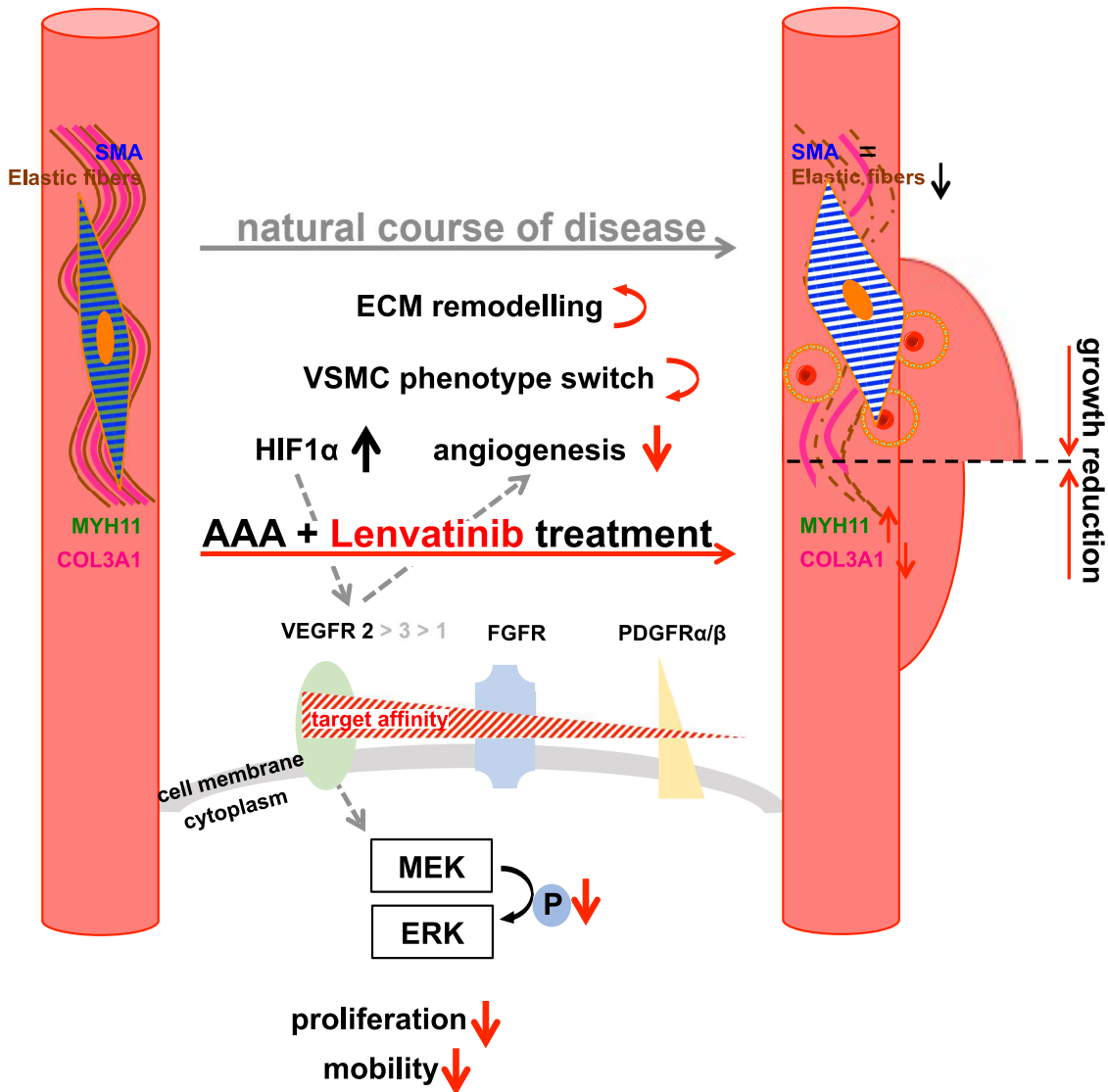## 5.1.   Discussion Part I: Repurposing Lenvatinib®

Fig.30: Graphic abstract: Treatment of AAA with Lenvatinib© significantly changes the course of disease. The multityrosine kinase inhibitor has the highest affinity to the VEGFR2 and reduces angiogenesis and influences ECM remodeling with preservation of MYH11 and the contractile phenotype of VSMCs in the aortic wall. Intracellularly this happens via reduced phosphorylation of ERK1-2.

In this current study, we successfully "re-purpose" the anti-cancer drug Lenvatinib to halt growth of experimental abdominal aortic aneurysms in two species and patient-derived primary human cells via reconstitution of VSMC contractility (**fig.30**).

Our study provides evidence for the first non-cancer application of Lenvatinib.[335, 353] We further successfully for the first time treat animals with an already existing AAA, 7 days after aneurysm induction (**fig.9A,11B,23B**). Previous drug interaction studies start treatment with the time of aneurysm induction (day 0), which tremendously counteracts inflammatory processes seen in the most initial phases of all animal AAA models.[170, 222, 308] As such, Imatinib and Erlotinib, both tyrosine kinase inhibitors with

different target receptors (c-abl and epidermal growth factor receptor, respectively), have previously been shown to attenuate experimental aneurysm growth in the AngII dissection model in mice.[342, 343]

In cancer therapy, Lenvatinib is employed mainly for its anti-angiogenic effect.[353] Neo-angiogenesis in the aortic media is a feature commonly observed in human AAA, as well as in the murine PPE model (**fig.11,22**).[24, 74] We observed no CD31/CD34 positivity as a hallmark of reduced angiogenesis in all samples from treated animals and reduced expression of e.g. VEGFR2 in human primary cells (**fig.15-17**). Similarly, we have previously demonstrated aneurysm abrogation in the murine PPE and AngII model by blocking the long non-coding RNA H19, which represses HIF1α expression and subsequent angiogenesis.[77] Interference with the HIF1α-VEGF-VEGFRs axis has been shown multiple times to hinder aneurysm growth in mouse models.[74, 83, 354] Lenvatinib has the highest affinity for VEGFR2, found abundantly in both, human and experimental AAA.[24, 355, 356]

Despite angiogenesis, or perhaps in combination with, the fate of VSMCs in the aortic media seems to determine aneurysm expansion. HIF1α overexpression seems to link angiogenesis with VSMC phenotype fate.[77, 357] Along with fragmentation of the elastic fibers and reorganization of the collagen architecture, the number of VSMCs decreases in AAA compared to non-aneurysmatic aorta, while their turnover increases and cells lose their contractile phenotype.[1, 358] These effects are here strongly opposed by treatment with low dose Lenvatinib, both on a cellular level and in experimental AAA in mice and minipigs (**fig.9,11,23**). While apoptosis is not increased, mobility and proliferation are markedly decreased and many genes suggestive of the contractile phenotype (e.g. *TAGLN; CNN1; MYOCD; ITG8; CALD1*) are upregulated upon treatment (**fig.15-18; Table VIII**). However, *COL3A1*, a main fibrillar component of a non-diseased aorta appeared down-regulated upon Lenvatinib in all cell strains, suggesting a reconstitution different from the non-dilated phenotype (**fig.15-17**). MYH11 becomes substantially restored through the Lenvatinib application (**fig.9-11,13,20,23,24**). Its regulatory role and contribution to an intact aortic wall, other than being a marker of the contractile apparatus, is largely unknown. However, it is well established for being dysregulated in various aneurysmatic conditions via genetic and proteomic profiling approaches.[359-361]

Interestingly, the magnitude of differential gene expression and the responsiveness to Lenvatinib on cellular assays was markedly enhanced in diseased (patient-derived, primary) as compared to control (non-aneurysmatic donor) cells, suggesting the diseased state to be more susceptible to an external stimulus or treatment (**fig.15-17**). Hence, a higher extent of intracellular damage has been observed in primary AAA cell cultures.[348] This may support our initial attempt to start treatment not at the time of AAA induction, but with an established lesion.[170] Targeting VSMC by RNA-based therapies or chemotherapeutics to change the course of aneurysm growth has been proven to be effective in various animal models.[302, 362]

Apart from the systemic application, we demonstrate the effectiveness of a local endovascular application of Lenvatinib in mice and a novel atherosclerotic minipig model (**fig.9,11,23**). The PPE procedure in pigs has successfully been performed before.[238] However, by using the *LDLR*^{-/-} animals with severe atherosclerotic lesions

one can achieve a closer mimicry of advanced human vascular disease (**fig.21**).[351] While only male mice have been utilized to exclude sex-specific effects, a mixed group of female and castrated male pigs was used, however, a very uniform aneurysm formation was observed (**s. 6.5.1.**).[363]

From a translational point of view, the local treatment with a Lenvatinib-coated balloon or stent(-graft) could be an amendment to difficult AAA morphologies with problematic proximal or distal sealing zones, as well as for otherwise inoperable patients (**fig.32**).[364, 365] In ophthalmology, intraviteal bevacizumab, a monoclonal VEGF-blocker is already in common use for retinal artery aneurysm treatment.[366] We did not observe any side effects based on overall survival or organ function, as indicated by our blood tests, however, possible, currently not expected, side effects should be further evaluated in a more chronic experimental setup (6 months instead of 4 weeks) with greater sample size.[367]

In conclusion, the multityrosine kinase inhibitor Lenvatinib, administered orally or by local endovascular means, successfully abrogates aneurysm growth in elastase-induced aneurysmatic lesions in mice and a novel *LDLR*^{-/-} preclinical minipig model. Array analysis identified MYH11 as the most deregulated target. In primary human AAA cell culture, Lenvatinib reduces VSMC proliferation and migration and restores a contractile phenotype. Hence, MYH11 is restored upon Lenvatinib treatment in the aortic media in both animal models, along with reduced angiogenesis and marked fibrosis.

5.2. Discussion Part II: Long non-coding RNA H19 in AAA formation

Most of the results in this part have been published by our group in 2018, so a vivid peer review and discussion has been provided already (**s. 6.5.3.**). Hence, in the following section a more unifying discussion for a common theory and a further translational use of the results presented in part I and II of the result section is provided.

As for the data not previously published (**s. 4.2.4.**), additional experiments are needed before this singular result can be put into context.

5.3. Unifying theory

5.3.1. HIF1α signaling

As shown in the previous chapters, a special role for AAA development, but also for influencing aneurysm growth lies within the HIF1α – VEGF – VEGFR signaling axis (**s.3.1./2.**).

The expression of the transcription factor HIF1α or better the prevention from decay of HIF1α is triggered by hypoxia at the cellular level from the very embryologic beginning of vascular development.[368, 369] We and others have previously shown that AAA development is linked to a thickening of the aortic wall and hence up-regulation of HIF1α, responsible for angiogenesis.[24, 74, 370, 371] Similar results have been

demonstrated for other than the infrarenal aorta.[79] After nuclear translocation, HIF1α triggers VEGF expression (s.2.1.3.7.). This process is an immediate reaction after exposure to hypoxia and both mRNAs resume to normal levels upon re-establishing normoxia.[368] It was shown to be exerted by various cell types including VSMCs and ECs.[78, 368, 372] Additionally, a variety of genes have been demonstrated to be transcribed after HIF1α translocation, a large subset being involved in AAA pathogenesis (reviewed in detail e.g. by Lim et al. 2013).[78]
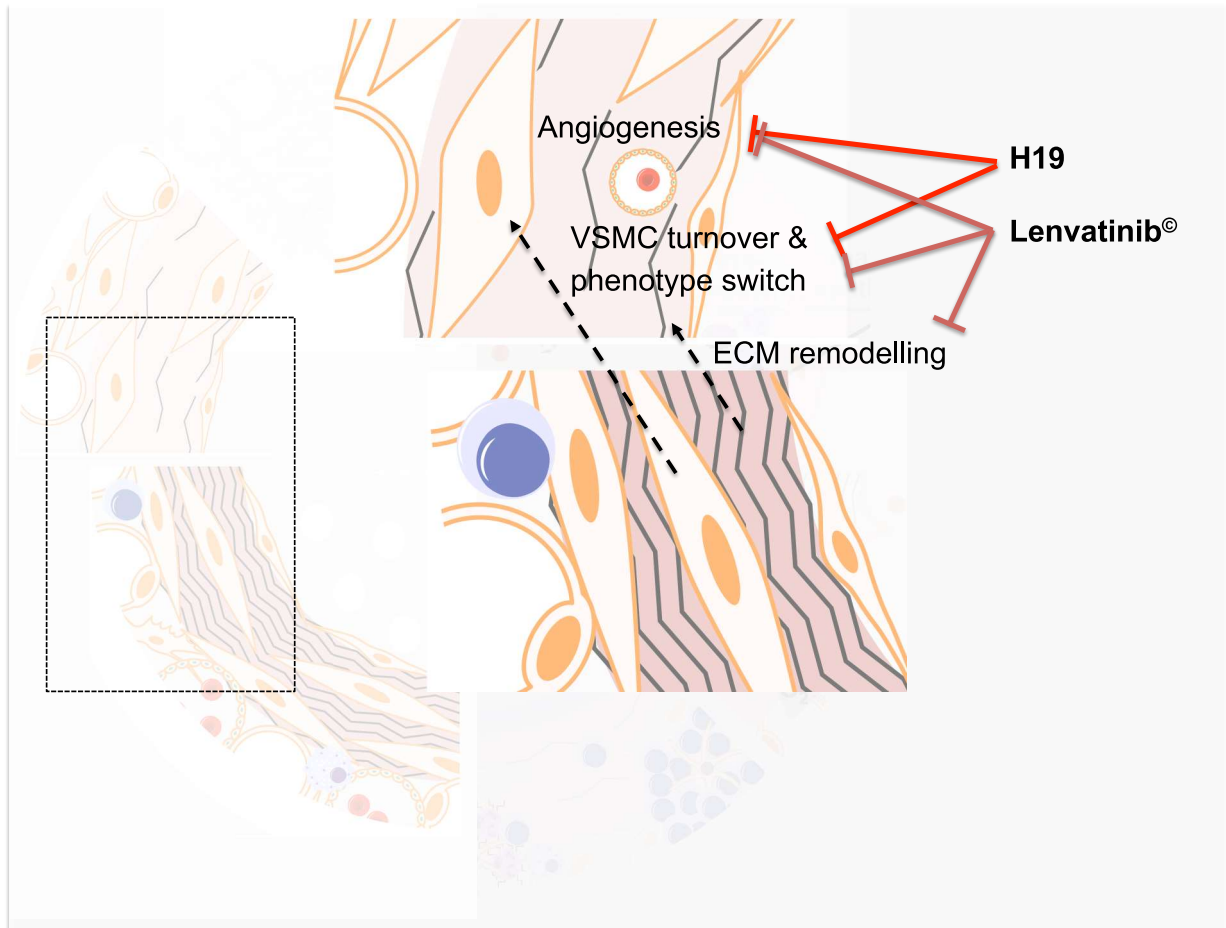

Fig.31: Graphic Summary: The figure summarizes the mechanisms elucidated in this thesis. Modified from **fig.4** and Busch et al. 2018 and Li et al. 2018.[72, 352]

Influencing HIF1α – VEGF – VEGFR signaling axis and studying the effects of such will provide valuable insights for future medical AAA therapy and basic translational research.

5.3.2. Angiogenesis and VSMC plasticity

In Part II of the results, we demonstrate the effect of H19-modification on VSMCs and in Part I, we show that Lenvatinib alters the VSMC phenotype and reduces angiogenesis upon treatment.

Apart from triggering angiogenesis or perhaps in close crosstalk with it, HIF1α was shown as a major inductor of VSMC phenotype switch, too.[357] Loss of HIF1α was even shown to increase VSMC contractility in pulmonary artery hypertension patients.[373] Up

regulation promotes VSMC migration and proliferation.[374, 375] Based on experimental data from Angiotensin II AAA model mice, HIF1α might also have an aneurysm-limiting effect.[376] This has, however, never been confirmed and HIF1α deficient mice are unable to develop experimental aneurysms.[377] Short-term additional supplementation of oxygen has even been suggested to reverse diseased vascular phenotypes by reducing VSMC proliferation.[378] VSMCs have been called "the broken bricks in the aortic wall".[379]

Similar as in Part I of this thesis, many tyrosine kinase inhibitors (TKIs) were shown to have different effects despite their original anti-angiogenic use (**s.2.3.2.1.**). Nilotinib has potent anti-inflammatory and immunomodulatory effects.[380] Imatinib has negative effects on worm physiology by influencing TGFβ signaling.[381] Apart from ECs and VSMCs, also different kinds of stromal cells, like pericytes and lymphatic tissue are affected by e.g. Sunitinib.[382]

In this matter, the use of anti-angiogenic treatments, such as cancer therapies affecting VEGF and its receptors have been shown to have pleiotropic effects and a variety of vessel-associated side effects, such as arterial hypertension, thrombo-embolic events and cardiac dysfunction.[383] However, most of this data again comes from cancer research and only little is known about the pleiotropic effects of e.g. TKIs on the vasculature.

The VSMCs in the aortic wall and their central role in important signaling pathways, such as angiogenesis, make them both, recipient and transmitter of pleiotropic acting drugs, such as RNA therapeutics or tyrosine kinase inhibitors.

5.3.3. Common denominators – a role for transforming growth factor β?

The transforming growth factor β (TGFβ) signaling pathway is involved in many cellular processes in both the adult organism and the developing embryo, including cell growth, cell differentiation, apoptosis, cellular homeostasis and other cellular functions.[384] Basically every cell is able to use this mechanism started by the binding of TGFβ to its receptor TGFβ R1 or R2 and thus starting a cascade of phosphorylated SMADs, transcription factors that activate transcription of TGFβ target genes.[385]

Most prominently, mutations in the TGFβR1 or R2 genes are held responsible for Loeys-Dietz syndrome, a novel rare disease entity characterized by fragile connective tissue and specifically aneurysm formation at any part of the aorta or the peripheral arteries.[121] Similar has been described for Marfan and Shprintzen–Goldberg syndrome (Aortic root aneurysms).[386] Despite these resulting loss-of-function mutations, TGFβ signaling and its downstream gene expression is activated in the aortas of such patients (TGFβ paradoxon).[387] In the classic canonical TGFβ signaling, phosphorylated SMADs lead to overexpression of e.g. MMPs and degradation of elastic fibers, enhanced proliferation and migration of VSMCs, and excessive collagen secretion and deposition.[388]

Hypoxia was shown to trigger epithelial-to-mesenchymal-transition, a key factor in VSMC differentiation, by HIF1α depending non-canonical TGFβ signaling.[389] Similarly, TGFβ can directly start the release of VEGFA from VSMCs.[390]

The very central implication of the TGFβ pathway in cellular homeostasis and the many proposed and proven connections to VSMC plasticity and angiogenesis along with the myriad of deregulated TGFβ genes in various aneurysm diseases and heritable aneurysm conditions suggest a crucial role for this pathway in future research.

5.4. Future translational aspect

Currently, not every patient is considered "fit for surgery". Some are too sick or too frail, especially when open surgery is planned.[391] Especially cardiac and pulmonary conditions and nutritional status are limitations.[392] Risk prediction models have been implicated to better stratify patients, however, these might not be perfect for the individual.[393, 394]

Additionally, the current surgical threshold for operating on AAAs is based on large population studies, showing that interventions on smaller diameters do not provide any benefit in terms of overall mortality (**s.2.1.2.**).[6, 395] However, these are based on the assumption of perioperative morbidity and mortality from OR and EVAR.

A new approach with a less invasive drug coated balloon treatment as suggested in Part I of this thesis might thus help to provide additional options in patients with smaller AAA diameters or those considered unfit for surgery. Additionally, based on personal experience, not every patient feels comfortable with waiting of treatment until reaching the surgical threshold.

Currently, there is an ongoing debate on the long-term effectiveness of drug-coated balloons in vascular surgery, due to the observation that Paclitaxel-coated devices used for PAOD interventions came with an increased risk of death following application in the femoro-popliteal artery.[327] This meta-analysis by Katsanos et al. gained huge impact, since the patency of target vessels was shown to be superior to non-coated balloons previously and has even gained acknowledgement in current guidelines.[86, 396]

Although being challenged by comparing different statistical models to estimate the relevant endpoints, it clearly raised the issue of long-term side effects, previously not considered.[397]

Our data cannot currently provide any answers on long-term side effects. Although RNA-therapeutics, as well as, e.g. local Lenvatinib at the lesion site, might have a short half-life, this needs to be considered. Today, already a large variety of RNA-therapeutics is under clinical consideration or even trial. Different forms of delivery have already been discussed (**s.2.3.1.3.**). The general assumption regarding off-target effects is a short-lived local interference at the site of interest, due to a specific set of genes, RNAs or ncRNAs, only presenting themselves to be altered at the very site.[398]

By contrast, Paclitaxel is a non-selective cytoskeleton inhibitor preventing cells from going into mitosis and thus, despite local delivery, can exert its function everywhere in the body, upon entering the blood stream.[399]

Another debate on AAA treatment does concern cost-effectiveness of screening and treatment. Despite the individual medical benefit, in many countries screening and treatment of AAA has been proven to be cost-effective.[400, 401] Additionally, in most countries, EVAR has proven to be more cost-effective than open repair.[402, 403] This

might, however, only be true for simple EVAR procedure, whereas due to the high manufacturing costs for a fenestrated or branched endograft, this advantage is completely lost.[404] These results have to be interpreted carefully, since healthcare systems differ from country to country.[405, 406] Generally, due to the specific complications following EVAR (**s.2.1.4.**) associated with serious follow-up intervention rates, in the long-term (<2 years), there is no difference in cost-effectiveness for the two procedures.[407-409] The cost of an anti-H19-coated balloon or a Lenvatinib-coated balloon is currently difficult to estimate, but since the procedure can be performed under local anesthesia in an ambulatory setting, it is pretty much determined by the drug cost.

Despite drug-coated balloon angioplasty, another way of local delivery would be drug-coated stentgrafts, especially at the sealing zones. Today a large proportion of EVAR procedures are performed in patients outside instructions for use (IFU), with only scarcely published results.[410, 411] They refer to neck length and diameter especially and imply complications of type I endoleaks and stentgraft dislocation.[412-414] But also the iliac sealing zones might be compromised when violating the IFUs.[415] Thus, having a stentgraft with an active biological inducing fibrosis at the sealing zones could help to provide additional sealing (**fig.31/32**).

drug coated balloon   **drug coated stentgraft**

off-target effects?

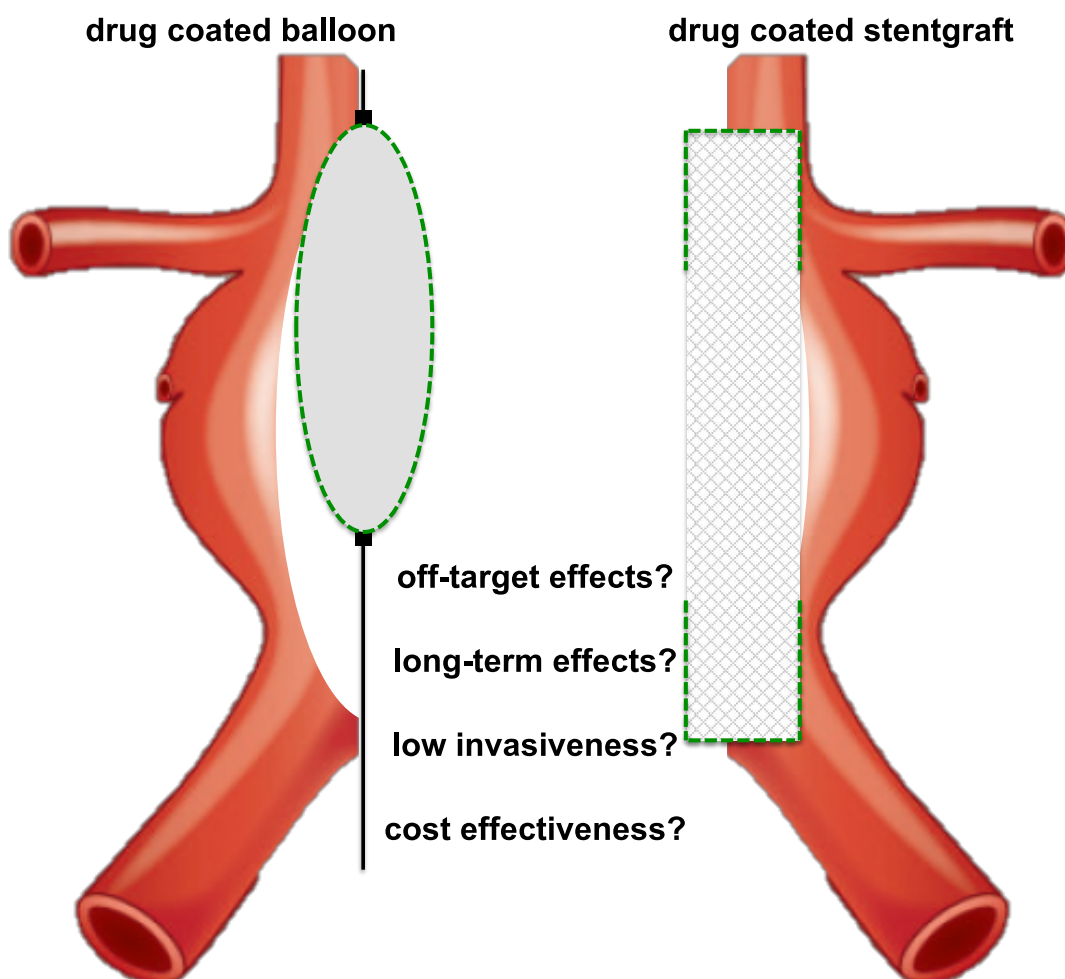long-term effects?

low invasiveness?

cost effectiveness?

Fig.32: Graphic abstract of translational use. For the AAA treatments proposed in this thesis, a future translational use in drug-coated devices, e.g. balloons or stentgrafts, is proposed (dotted green line = drug-coating). However, some major concerns remain with question marks.

In conclusion, novel non-surgical treatment strategies, especially considering minimally invasive, local endovascular delivery, will provide the vascular clinician with a valuable tool to treat their AAA patient. The future challenge and responsibility will be to identify those patients eligible for such treatments and those benefiting more from a classical surgical approach. For such, dedicated clinician scientists, overseeing both vascular surgery and experimental biology, will be able to tailor a patient-specific approach!

6. Supplement

6.1. Acknowledgement

Finally being able to finish this PhD, I want to first and foremost thank my doctoral committee. **Lars Maegdefessel** has gratefully taken me into his lab at CMM at the Karolinska Institute in Stockholm for my DFG-funded postdoc. Our time has transferred my personal research from the observational to the interventional level, climaxing in our joint field trips on the hunt for a reliable large animal mode. Thank you for your trust, effort and ongoing support. **Christoph Otto** not only took on the duty to supervise this PhD but also accompanied my very first steps in animal research in our Würzburg facility. Despite our initial hind limb problems, he always supported my mouse research and also facilitated my initial access to E7080. **Andreas Rosenwald**, probably unknowingly, once put me to shame during a pathology internship in my 3rd year of medical school asking questions I should have been able to answer, yet couldn't. Ever since, I am more than grateful that he accepted my invitation to supervise this thesis.

Three very special ladies have helped to put this thesis to an end. Their constant lab and personal support as well as good ideas and most skilled assistance have helped to finalize all three papers. **Valentina Paloschi**, **Ekaterina Chernogubova** and **Renate Hegenloh**, my work and my scientific career has, is and will depend on you. I couldn't be more grateful.

My current boss, **Hans-Henning Eckstein** deserves a special mention for his constant support in the struggle between becoming and being a clinician scientist and an academic vascular surgeon despite a hostile environment with a severe workload.

A special thanks is to **Anna-Leonie Menges**, who has allowed me to grow.

The experiments for this very thesis have been carried out in three different labs in three different cities in 2 countries. Therefore, many many people have been involved and deserve to be thankworthy mentioned.

From our lab in Würzburg, Germany:

Monika Koospal, **Manuela Hofmann** and **Bettina Mühling** who have always been there and helpful with skilled technical assistance in the beginning of my basic research career and have named my one-man show "AG Aneurysma" on a little blue box containing the microsurgical gear. **Sven Flemming** who has always been a friend, a peer group role model and one to higher the bar of personal achievement. **Armin Wiegering** whose inevitable role in this was to first use Lenvatinib in his experiments on the bench next to me.

From our lab in Stockholm, Sweden:

Alexandra Bäcklund, who not only opened her house to me, but also the door to the animal house at 11pM, while KI was in lockdown. **Hong Jin**, who introduced me to vascular ultrasound and whose ID I borrowed traveling as a mouse operator. At the KI gym between lab sessions, **Anton Gisterå** helped to improve my deadlifts. **Yuhuang "Daniel" Li** was an office neighbor and special help with the H19 project. **Greg Winski**

6.2. Funding

6.3. Dissemination of results

<u>Publications:</u>
So far one manuscript was successfully published in Circulation.[77] At the time of finalization of this thesis, two more manuscripts are being submitted.

<u>Other presentations:</u>
The results shown here were content of various poster (P) and oral (O) presentations throughout the last three years. These include:

MAC, December 2017 (The Munich Vascular Conference)	O
ATVB, May 2018 (Annual Meeting)	P
The Vienna Vascular Symposium, June 2018, Vienna	O
The SVS Meeting, June 2018, Boston	P
The DZHK Summer School, July 2018, Munich	O
The ESC (European Society of Cardiology) Meeting, August 2018, Munich	P
The ESVS Meeting, September 2018, Valencia	P
DGG Jahreskongress, October 2018, Bonn	O
MAC, December 2018 (The Munich Vascular Conference)	P
The Young MHA Meeting, May 2019, Munich	O
The ESVS Meeting, September 2019, Hamburg	O
Dreiländertagung, October 2019 (DGG Jahreskongress), Mannheim	O
MAC, December 2019 (The Munich Vascular Conference)	O

6.4.   Curriculum Vitae

personal details

name	Busch, Albert Franz Jakob
date of birth	3. November 1983
place of birth	Weiden i.d. Opf., Germany

academic career

2003	university entrance diploma
2003 – 2004	civilian service
2004 – 2010	Medical School Julius-Maximilians-University Würzburg
2007 – 2010	German National Academic Foundation Scholar
2010	license to practice medicine
2012	medical doctorate
2018	UEMS Fellow of the European Board of Vascular Surgeons
2019	BLAEK specialist vascular surgery
2019	postdoctoral lecture qualification (Habilitation)
2011 – 2016	Department of Visceral, Vascular and Pediatric Surgery (Prof. C.-T. Germer), University Hospital Würzburg, Germany
2015 – 2016	DFG Research Fellow Karolinska Institute Stockholm (Prof. L. Maegdefessel), Sweden
from 2016	Department of Vascular and Endovascular Surgery (Prof. H.-H. Eckstein), Rechts der Isar Munich, Germany

additional qualifications

2012	FELASA B scientific animal surgery
2013	ATLS® Advanced Trauma Life Support
2013	DEGUM I vascular ultrasound
2014	DEGUM I abdominal ultrasound
2015	BLAEK technical qualification: genetic counseling surgery
2018	MediTUM certificate medical didactics

memberships

German Society of Vascular and Endovascular Surgery DGG
European Society for Vascular and Endovascular Surgery ESVS

scientific expertise

2008 – 2009   scientific internship:
„Stem Cell Therapy and Regenerative Medicine"
Karolinska Institute Stockholm (Prof. K. Spalding)

2007 – 2010   medical doctorate:
„Charakterisierung nukleärer Transportvorgänge bei Lamino-pathien"
University of Würzburg (PD Dr. S. Hübner)

2012 – 2019   postdoctoral lecture qualification (Habilitation):
„Deduktive Analyse arterieller Aneurysmen zur Translation spezifischer Pathomechanismen im Tierversuch"
Technical University Munich (Prof. H.-H. Eckstein)

2015 – 2016   DFG Research fellowship:
„The role of miR-19b, miR-194 and miR-362-3p in development, expansion and rupture of abdominal aortic aneurysm"
Karolinska Institute Stockholm (Prof. L. Maegdefessel)

funds granted by third-party donors

2013 – 2014   Starting Grant IZKF Würzburg: *„Identifikation neuer Mechanismen bei der Entstehung von Bauchaorten-aneurysmen"*

2014   Research grant DGG: *„Die Rolle des TGFß Signalweges für die Pathogenese von Aortenaneurysma und Poplitealaneurysma"*

2014   Clinical Trial Support Eva Luise und Horst Köhler Foundation: *„Blutgerinnung bei EDS-Patienten"*

6.5. Supplement Material

6.5.1. Supplement data on Part I

Ultrasound measurements mice

	Day 0		Day 7		Day 14		Day 28		
	absolut	normalized	absolut	normalized	absolut	normalized	absolut	normalized	
stan PPE	0,58	1,00	0,93	1,59	0,85	1,47	0,98	1,69	N=22
stan PPE	0,55	1,00	0,90	1,64	0,86	1,56	0,89	1,61	
stan PPE	0,62	1,00	0,87	1,39	0,87	1,39	1,00	1,60	
stan PPE	0,60	1,00	0,87	1,46	0,96	1,62	0,89	1,49	
stan PPE	0,57	1,00	0,79	1,38	0,84	1,47	0,85	1,48	
stan PPE	0,62	1,00	0,76	1,23	0,94	1,53	0,97	1,57	
stan PPE	0,64	1,00	0,68	1,06	0,76	1,18	0,79	1,23	
stan PPE	0,62	1,00	0,87	1,40	0,93	1,50	1,07	1,73	
stan PPE	0,62	1,00	0,81	1,31	0,91	1,47	0,87	1,40	
stan PPE	0,56	1,00	0,76	1,36	0,83	1,48	0,93	1,66	
stan PPE	0,55	1,00	0,83	1,51	0,99	1,80	0,99	1,80	
stan PPE	0,62	1,00	0,80	1,29	1,03	1,66	1,10	1,77	
stan PPE	0,57	1,00			0,92	1,63	0,98	1,72	
stan PPE	0,58	1,00	0,71	1,23	0,91	1,57	0,92	1,60	
stan PPE	0,60	1,00	0,79	1,32	0,95	1,59	1,03	1,71	
stan PPE	0,61	1,00	0,81	1,33	0,87	1,42	0,91	1,50	
stan PPE	0,59	1,00	0,86	1,45	0,99	1,67	1,04	1,75	
stan PPE	0,61	1,00	0,98	1,59	0,95	1,55	0,99	1,62	
stan PPE	0,53	1,00	0,81	1,52	0,91	1,71	0,98	1,83	
stan PPE	0,62	1,00	0,91	1,46	0,90	1,44	0,93	1,49	
stan PPE	0,61	1,00	0,87	1,43	0,93	1,53	1,17	1,93	
stan PPE	0,50	1,00							

	Day 0		Day 7		Day 14		Day 28	
	absolut	normalized	absolut	normalized	absolut	normalized	absolut	normalized
mean	0,59	1,00	0,83	1,40	0,91	1,54	0,97	1,63
std dev	0,03	0,00	0,07	0,14	0,06	0,13	0,09	0,16

	Day 0		Day 7		Day 14		Day 28		
	absolut	normalized	absolut	normalized	absolut	normalized	absolut	normalized	
Lenva syst	0,58	1,00	0,85	1,45	0,89	1,53	0,86	1,48	N=7
Lenva syst	0,61	1,00	0,75	1,23	0,94	1,54	0,95	1,55	
Lenva syst	0,63	1,00	0,87	1,39	0,80	1,27	0,94	1,50	
Lenva syst	0,59	1,00	0,70	1,18	0,78	1,31	0,67	1,13	
Lenva syst	0,56	1,00	0,80	1,43	0,77	1,38	0,81	1,44	
Lenva syst	0,61	1,00	0,78	1,28	0,82	1,35	0,87	1,43	
Lenva syst	0,65	1,00	0,81	1,24	0,71	1,09	0,73	1,12	

	Day 0		Day 7		Day 14		Day 28	
	absolut	normalized	absolut	normalized	absolut	normalized	absolut	normalized
mean	0,60	1,00	0,79	1,32	0,81	1,35	0,83	1,38
std dev	0,03	0,00	0,05	0,10	0,07	0,14	0,10	0,16

Lenva local	0,58	1,00	0,75	1,29	0,79	1,37	0,75	1,29	N=5
Lenva local	0,53	1,00	0,83	1,57					
Lenva local	0,61	1,00	0,88	1,45	0,78	1,28	0,90	1,48	
Lenva local	0,63	1,00	0,83	1,33	0,79	1,26	0,89	1,41	
Lenva local	0,47	1,00	0,78	1,66	0,88	1,87	0,75	1,60	
mean	0,56	1,00	0,81	1,46	0,81	1,44	0,82	1,45	
std dev	0,06	0,00	0,05	0,14	0,04	0,25	0,07	0,11	
Sham-ReOP	0,52	1,00	0,84	1,61	0,93	1,80	1,04	2,01	N=3
Sham-ReOP	0,58	1,00	0,83	1,44	0,92	1,59	0,88	1,52	
Sham-ReOP	0,49	1,00	0,76	1,55	0,82	1,66	0,89	1,80	
mean	0,53	1,00	0,81	1,53	0,89	1,68	0,94	1,78	
std dev	0,03	0,00	0,03	0,07	0,05	0,09	0,08	0,20	

Laboratory Analysis mice

stan PPE	4,4	3,4	0,1	0,9	727	8,6
stan PPE	3,6	2,9	0,1	0,6	818	8,6
stan PPE	2,3	1,7	0,1	0,5	350	10,6
stan PPE	3,9	2,9	0,1	0,9	576	9,4
mean	3,55	2,73	0,10	0,73	617,75	9,3
std dev	0,78	0,63	0,00	0,18	177,11	0,82

	white cell	lymphocytes	monocytes	granulocytes	platelets	hemoglobin
normal x10^9/µl	3.0-15.0	1.2-3.2	0.3-0.8	1.2-6.8	140-600	6.9-11,2mmol/l
Lenva syst	6,3	4,2	0,2	1,9	637	9,6
Lenva syst	4,6	3,1	0,2	1,3	937	9,2
Lenva syst	4,2	2,9	0,1	1,2	798	9,2
Lenva syst	8,8	6,2	0,3	2,3	669	9,9
Lenva syst	4,7	3,5	0,2	1	835	9,1
Lenva syst	4,7	3,7	0,1	0,9	855	8,8
Lenva syst	4,4	3,3	0,1	1	788	9,5
mean	5,39	3,84	0,17	1,37	788,43	9,33
std dev	1,53	1,04	0,07	0,49	97,07	0,34

Ultrasound measurements pigs

	Day 0		Day 7		Day 28		
	absolut	normalized	absolut	normalized	absolut	normalized	
stan PPE	10,82	1			15,60	1,44	N=12
stan PPE	8,28	1			12,73	1,54	
stan PPE	8,59	1			10,19	1,19	
stan PPE	8,59	1			17,19	2,00	
stan PPE	6,63	1	9,50	1,43	12,70	1,92	
stan PPE	5,60	1	8,20	1,46	8,60	1,54	
stan PPE	6,80	1	8,60	1,26	10,60	1,56	
stan PPE	6,63	1	9,50	1,43	10,40	1,57	
stan PPE	6,40	1	7,60	1,19	9,60	1,50	
stan PPE	8,20	1	9,80	1,20	11,60	1,41	
stan PPE	7,20	1	8,60	1,19	12,00	1,67	
stan PPE	7,00	1	9,30	1,33	10,10	1,44	
mean	7,56	1	9,48	1,21	11,78	1,56	
std dev	1,34	0	1,07	0,15	2,40	0,21	

	Day 0		Day 7		Day 28		
Lenva 1	7,10	1	10,00	1,41	9,70	1,37	N=4
Lenva 2	8,00	1	10,80	1,35	9,70	1,21	
Lenva 3	8,50	1	10,50	1,24	9,90	1,16	
Lenva 4	8,10	1	10,00	1,23	9,40	1,16	
mean	7,79	1	10,68	1,38	9,68	1,23	
std dev	0,56	0	0,89	0,13	0,18	0,08	

	Day 0		Day 7		Day 28		
DMSO 9	7,70	1	11,00	1,43	11,30	1,47	N=3
DMSO 11	7,90	1	12,20	1,54	10,60	1,34	
DMSO 12	8,10	1	10,40	1,28	10,80	1,33	
mean	7,79	1	10,68	1,38	10,90	1,38	
std dev	0,56	0	0,89	0,13	0,29	0,06	

Laboratory analysis pigs

		Day 0						
Animal		1	2	3	4	9	11	12
treatment		Lenva	Lenva	Lenva	Lenva	DMSO	DMSO	DMSO
Blood count	normal range							
WBC (G/L)	11,0-22,0	6,7	7,7	5,9	6,7	15	7,2	8
RBC (T/L)	5,8-6,1	5,89	5,11	6,3	5,89	4,76	6,18	5,57
HGB (g/L)	120-160	123	105	133	123	106	135	117
HCT (L/L)	0,36-0,50	0,38	0,32	0,38	0,38	0,33	0,42	0,36
MCV (fL)	50-65	64,7	63,1	60,7	64,7	68,9	67,5	65,2
MCH (pg)	17-21	20,9	20,5	21,1	20,9	22,3	21,8	21
MCHC (g/dL)	30-35	32,3	32,6	34,8	32,3	32,3	32,4	32,2
PLT (G/L)	220-620	334	370	289	334	301	202	156
Liver								
alcalic phosphatase	< 156	56	78	48	56	73	46	114
AST (U/L)	< 59	32	67	29	32	29	31	22
ALT (U/L)	< 68	31	56	31	31	20	43	31
γ-GT	< 54	71	69	76	71	55	58	65
GLDH (U/L)	-6,4	< 2,0	5,4	<2,0	<2,0	<2,0	<2,0	<2,2
Bilirubin (µmol/L)	< 4,3	6,84	3,42	3,42	6,84	11,97	5,13	8,55
CK (U/L)	< 4000	390	375	410	390	361	361	177
Kidney								
creatinine (µmol/L)	< 160	147,6	116,7	101,7	147,6	157,4	123,8	115,8
urea (mmol/L)	2,5-6,7	4,00	4,66	2,33	4	9,49	4,66	2,83
sodium (mmol/L)	135-150	144	142	139	144	144	140	141
potassium (mmol/L)	4,2-5,6	3,8	3,9	4,3	3,8	3,1	4,1	4
Calcium(mmol/L)	1,80-2,90	2,49	2,4	2,44	2,49	2,52	2,52	2,52
Magnesium (mmol/L)	0,50-1,30	0,75	0,84	0,79	0,75	0,88	0,78	0,76
chloride (mmol/L)	102-106	101	101	101	101	99	99	99
Phosphat (mmol/L)	1,90-3,20	1,94	1,97	1,86	1,94	2,05	2,15	2,04
other								
total iron (µmol/L)	> 18	28,7	14	19,9	28,7	31,2	29,6	20,2
glucose (mmol/L)	4,05-6,60	10,38	7,16	10,16	10,38	5	9,99	9,32
Albumin(g/L)	28-40	33,9	30,2	33,5	33,9	36,6	32,9	33,4
total protein(g/L)	65-85	79	72	74	79	78	80	80

Day 7						
1 Lenva	2 Lenva	3 Lenva	4 Lenva	9 DMSO	11 DMSO	12 DMSO
9,2	9,1	10,5	7,7	9,8	9,6	7,6
3,08	4,67	4,04	3,47	4,02	4,68	5,31
70	96	84	74	89	102	110
0,21	0,3	0,25	0,23	0,28	0,31	0,34
68,3	64	61,7	66	68,6	64,6	64,8
22,7	20,6	20,8	21,3	22,1	21,8	20,7
33,3	32,1	33,7	32,3	32,3	33,2	32
542	346	316	536	151	223	83
62	47	33	35	59	35	73
34	35	29	33	37	40	26
31	35	30	34	33	34	31
53	75	34	59	50	65	52
15,6	15,9	<2,0	15,8	<2,0	<2,0	<2,0
5,13	5,13	5,13	6,84	6,84	6,84	5,13
692	649	496	613	505	511	536
96,4	122	105,2	120,2	118,5	146,7	107,9
4,5	3,16	2,16	4	2,33	4,16	3,5
142	144	143	145	141	138	140
4	3,9	3,2	3,8	3,3	3,5	4
2,45	2,38	2,32	2,39	2,46	2,5	2,54
0,98	0,86	0,78	0,93	0,9	1,05	0,97
103	102	101	102	98	100	101
2,23	1,94	1,87	2,15	2,3	2,09	2,09
21,5	10,6	12	27,4	16,8	16,3	19,3
4	4,22	5,44	5,44	7,16	7,38	11,1
31,7	25,4	23,7	27,4	32,1	30	30,8
64	63	54	63	72	72	69

1 Lenva	2 Lenva	3 Lenva	4 Lenva	9 DMSO	11 DMSO	12 DMSO
			Day 28			
5,8	7	6,3	5,8	6,7	6,3	8,4
5,32	6	5,71	5,32	5,03	6,13	5,1
116	126	118	116	110	134	112
0,36	0,39	0,37	0,36	0,33	0,4	0,34
67,5	64,8	64,9	67,5	65,8	64,7	66,2
21,8	21	20,7	21,8	21,9	21,9	22
32,3	32,4	31,8	32,3	33,2	33,8	33,2
431	263	256	431	415	298	403
64	61	61	64	105	67	103
31	29	33	31	33	28	12
34	41	33	34	29	42	29
56	63	48	56	49	43	44
<2,0	<2,0	<2,0	<2,0	<2,0	<2,0	<2,0
3,42	3,42	3,42	3,42	3,42	3,42	5,13
120	157	339	120	185	124	56
91,1	122,9	108,7	91,1	97,2	112,3	103,4
4,83	4	3,66	4,83	3	3,83	2,33
143	141	146	143	140	139	139
3,6	3,6	3,3	3,6	3,5	4	3,3
2,5	2,57	2,45	2,5	2,51	2,48	2,55
0,76	0,76	0,83	0,76	0,71	0,79	0,83
103	100	103	103	103	104	99
1,9	1,67	1,84	1,9	1,91	1,87	1,79
42,8	18,3	22,7	42,8	25,4	21,9	9,1
4,83	6,83	6,6	4,83	4,66	7,16	9,82
34,7	33,4	31,7	34,7	35,9	33	34,8
79	82	73	79	75	76	78

Selleck becomes a licensed supplier of Pfizer's bioactive compounds.

Selleckchem.com

Lenvatinib (E7080)

Catalog No.S1164

Lenvatinib (E7080) Chemical Structure

Technical Data

Molecular Weight (MW)	426.85		Storage	3 years -20°C powder
Formula	$C_{21}H_{19}ClN_4O_4$			6 months -80°C in solvent
CAS No.	417716-92-8		Synonyms	N/A

		DMSO	40 mg/mL warming (93.7 mM)
Solubility (25°C) *	*In vitro*	Water	<1 mg/mL (<1 mM)
		Ethanol	<1 mg/mL (<1 mM)
	In vivo	0.5% methylcellulose	30 mg/mL

* <1 mg/ml means slightly soluble or insoluble.
* Please note that Selleck tests the solubility of all compounds in-house, and the actual solubility may differ slightly from published values. This is normal and is due to slight batch-to-batch variations.

Chemical Name	1-(4-(6-carbamoyl-7-methoxyquinolin-4-yloxy)-2-chlorophenyl)-3-cyclopropylurea

Preparing Stock Solutions
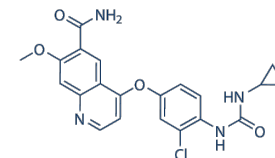
	1 mg	5 mg	10 mg
1 mM	2.3427 mL	11.7137 mL	23.4274 mL
5 mM	0.4685 mL	2.3427 mL	4.6855 mL
10 mM	0.2343 mL	1.1714 mL	2.3427 mL
50 mM	0.0469 mL	0.2343 mL	0.4685 mL

Biological Activity

Description	Lenvatinib (E7080) is a multi-target inhibitor, mostly for **VEGFR2(KDR)/VEGFR3(Flt-4)** with **IC50** of 4 nM/5.2 nM, less potent against VEGFR1/Flt-1, ~10-fold more selective for VEGFR2/3 against FGFR1, PDGFRα/β in cell-free assays. Phase 3.					
Targets	VEGFR2	VEGFR3	VEGFR1	FGFR1	PDGFRα	PDGFRβ
IC50	4 nM	5.2 nM	22 nM [1]	46 nM [1]	51 nM [1]	39 nM [1]

In vitro	E7080, as a potent inhibitor of in vitro angiogenesis, shows a significantly inhibitory effect on VEGF/KDR and SCF/Kit signaling. According to the in vitro receptor tyrosine and serine/threonine kinase assays, E7080 inhibits Flt-1, KDR, Flt-4 with IC50 of 22, 4.0 and 5.2 nM, respectively. In addition to these kinases, E7080 also inhibits FGFR1 and PDGFR tyrosine kinases with IC50 value of 46, 51 and 100 nM for FGFR1, PDGFRα and PDGFRβ, respectively. [1] E7080 potently inhibits phosphorylation of VEGFR2 (IC50, 0.83 nM) and VEGFR3 (IC50, 0.36 nM) in HUVECs which is stimulated by VEGF and VEGF-C, respectively. [2] A recent study shows that E7080 treatment (both at 1 μM and 10 μM) results in a significant inhibition of cell migration and invasion by inhibiting FGFR and PDGFR signaling. [3]
In vivo	When orally administrated in a H146 xenograft model, E7080 inhibits the growth of H146 tumor at 30 and 100 mg/kg in a dose-dependent manner and leads to tumor regression at 100 mg/kg. Furthermore, E7080 at 100 mg/kg decreases microvessel density more than anti-VEGF antibody and imatinib treatment. [1] E7080 significantly inhibits local tumor growth in a MDA-MB-231 mammary fat pad (m.f.p.) model with RTVs (calculated tumor volume on day 8/tumor volume on day 1) of 0.81, and reduces both angiogenesis and lymphangiogenesis of established metastatic nodules of MDA-MB-231 tumor in the lymph nodes. [2]
Features	

Protocol (Only for Reference)

Return Policy

Selleck Chemical's Unconditional Return Policy ensures a smooth online shopping experience for our customers. If you are in any way unsatisfied with your purchase, you may return any item(s) within 365 days of its original purchase date.

Toll Free:
(877) 796-6397
-- USA and Canada only --

Fax:
+1-713-796-9816

Orders:
+1-832-582-8158
sales@selleckchem.com

Tech Support:
+1-832-582-8158 Ext:3
tech@selleckchem.com
(Please provide your Order Number in the email. We strive to reply to all email inquiries within one business day.)

Website:
www.selleckchem.com

Kinase Assay: [1]

In vitro kinase assay [1]	Tyrosine kinase assays are performed by HTRF (KDR, VEGFR1, FGFR1, c-Met, EGFR) and ELISA (PDGFRβ), using the recombinant kinase domains of receptors. In both assays, 4 µL of serial dilutions of E7080 are mixed in a 96-well round plate with 10 µL of enzyme, 16 µL of poly (GT) solution (250 ng) and 10 µL of ATP solution (1 µM ATP) (final concentration of DMSO is 0.1%). In wells for blanks, no enzyme is added. In control wells no test article is added. The kinase reaction is initiated by adding ATP solution to each well. After 30-minute incubation at 30°C, the reaction is stopped by adding 0.5 M EDTA (10 µL/well) to the reaction mixture in each well. Dilution buffer adequate to each kinase assay is added to the reaction mixture. In the HTRF assay, 50 µL of the reaction mixture is transferred to a 96-well 1/2 area black EIA/RIA plate, HTRF solution (50 µL/well) is added to the reaction mixture, and then kinase activity is determined by measurement of fluorescence with a time-resolved fluorescence detector at an excitation wavelength of 337 nm and an emission wavelengths of 620 and 665 nm. In the ELISA, 50 µL of the reaction mixture is incubated in avidin coated 96-well polystyrene plates at room temperature for 30 minutes. After washing with wash buffer, PY20-HRP solution (70 µL/well) is added and the reaction mixture is incubated at room temperature for 30 minutes. After washing with wash buffer, TMB reagent (100 µL/well) is added to each well. After several minutes (10–30 minutes), 1 M H_3PO_4 (100 µL/well) is added to each well. Kinase activity is determined by measurement of absorbance at 450 nm with a microplate reader.

Cell Assay: [2]

Cell lines	HUVECs
Concentrations	0-10 µM
Incubation Time	72 hours
Method	HUVECs (1,000 cells in each well in serum-free medium containing 2% fetal bovine serum) and L6 rat skeletal muscle myoblasts (5,000 cells in each well in serum-free DMEM) are dispensed in a 96-well plate and incubated overnight. E7080 and either VEGF (20 ng/mL) or FGF-2 (20 ng/mL) containing 2% fetal bovine serum and PDGFβ (40 ng/mL) are added to each well. Cells are incubated for 3 days and then the ratios of surviving cells are measured by WST-1 reagent. For proliferation assay, samples are duplicated and three separate experiments are done.

Animal Study: [1]

Animal Models	H146 tumor cells are implanted subcutaneously (s.c.) into the flank region of female BALB/c nude mice.
Formulation	E7080 is dissolved in suspended in 0.5% methylcellulose.
Dosages	≤100 mg/kg
Administration	Administered via p.o.

Conversion of different model animals based on BSA (Value based on data from FDA Draft Guidelines)

Species	Mouse	Rat	Rabbit	Guinea pig	Hamster	Dog
Weight (kg)	0.02	0.15	1.8	0.4	0.08	10
Body Surface Area (m^2)	0.007	0.025	0.15	0.05	0.02	0.5
K_m factor	3	6	12	8	5	20

$$\text{Animal A (mg/kg) = Animal B (mg/kg) multiplied by } \frac{\text{Animal B } K_m}{\text{Animal A } K_m}$$

For example, to modify the dose of resveratrol used for a mouse (22.4 mg/kg) to a dose based on the BSA for a rat, multiply 22.4 mg/kg by the K_m factor for a mouse and then divide by the K_m factor for a rat. This calculation results in a rat equivalent dose for resveratrol of 11.2 mg/kg.

$$\text{Rat dose (mg/kg) = mouse dose (22.4 mg/kg)} \times \frac{\text{mouse } K_m(3)}{\text{rat } K_m(6)} = 11.2 \text{ mg/kg}$$

References

[1] Matsui J, et al. Int J Cancer. 2008, 122(3), 664-671.

[2] Matsui J, et al. Clin Cancer Res. 2008, 14(17),5459-5465.

[3] Glen H, et al. BMC Cancer. 2011, 11, 309.

Customer Product Validation

Data from [Data independently produced by **Asian Pac J Cancer Prev**, 2014, 15(7), 3113-21]
Lenvatinib (E7080) purchased from **Selleck**
Dot Plot Distribution of Live, Preapoptotic and Apoptotic Cells after Administration of DuP-697 and E7080 Combination.
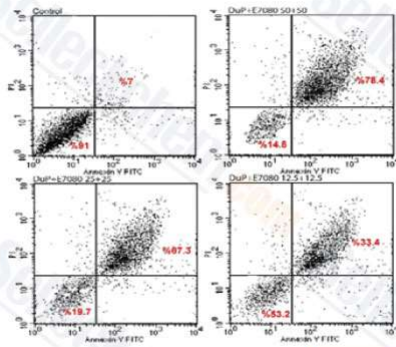
S1164Y0120141211
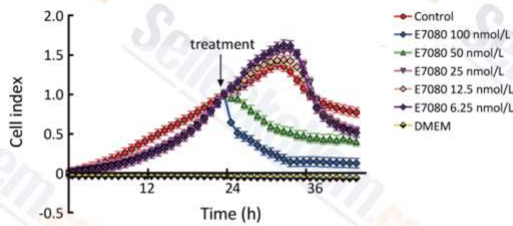
Data from [**Chin J Cancer Res**, 2013, 25(5), 572-84]
Lenvatinib (E7080) purchased from **Selleck**
Real-time monitoring of cytotoxic effect on HT29 cells using RTCA. (A) E7080

S116401X0120140126

Lenvatinib (E7080) has been referenced in 5 publications.

BRAF Inhibition Stimulates Melanoma-Associated Macrophages to Drive Tumor Growth [Wang T, et al. Clin Cancer Res, 2015, 21(7):1652-64]	PubMed: 25617424
E7080 (lenvatinib), a multi-targeted tyrosine kinase inhibitor, demonstrates antitumor activities against colorectal cancer xenografts [Wiegering A, et al. Neoplasia, 2014, 16(11):972-81]	PubMed: 25425971
Activation of coagulation by lenalidomide-based regimens for the treatment of multiple myeloma. [Isozumi Y, et al. PLoS One, 2013, 8(5):e64369]	PubMed: 23696885
Anticancer Effect of COX-2 Inhibitor DuP-697 Alone and in Combination with Tyrosine Kinase Inhibitor (E7080) on Colon Cancer Cell Lines. [Altun A, et al. Asian Pac J Cancer Prev, 2014, 5(7):3113-21]	PubMed: 24815456
Effects of tyrosine kinase inhibitor E7080 and eNOS inhibitor L-NIO on colorectal cancer alone and in combination. [Altun A, et al. Chin J Cancer Res, 2013, 25(5):572-84]	PubMed: 24255582

PLEASE KEEP THE PRODUCT UNDER -20°C FOR LONG-TERM STORAGE.

NOT FOR HUMAN, VETERINARY DIAGNOSTIC OR THERAPEUTIC USE

   Specific storage and handling information for each product is indicated on the product datasheet. Most Selleck products are stable under the recommended conditions. Products are sometimes shipped at a temperature that differs from the recommended storage temperature. Short-term storage of many products are stable in the short-term at temperatures that differ from that required for long-term storage.
We ensure that the product is shipped under conditions that will maintain the quality of the reagents. Upon receipt of the product, follow the storage recommendations on the product data sheet.

6.6. References

Own references from original work, reviews and co-authorships cited here are highlighted **bold** in the following list.

1.   Michel JB, Martin-Ventura JL, Egido J, Sakalihasan N, Treska V, Lindholt J, et al. Novel aspects of the pathogenesis of aneurysms of the abdominal aorta in humans. Cardiovascular research. 2011;90(1):18-27.
2.   Li K, Zhang K, Li T, Zhai S. Primary results of abdominal aortic aneurysm screening in the at-risk residents in middle China. BMC Cardiovasc Disord. 2018;18(1):60.
3.   Brady AR, Thompson SG, Fowkes FG, Greenhalgh RM, Powell JT, Participants UKSAT. Abdominal aortic aneurysm expansion: risk factors and time intervals for surveillance. Circulation. 2004;110(1):16-21.
4.   Sweeting MJ, Thompson SG, Brown LC, Powell JT. Meta-analysis of individual patient data to examine factors affecting growth and rupture of small abdominal aortic aneurysms. The British journal of surgery. 2012;99(5):655-65.
5.   Oliver-Williams C, Sweeting MJ, Turton G, Parkin D, Cooper D, Rodd C, et al. Lessons learned about prevalence and growth rates of abdominal aortic aneurysms from a 25-year ultrasound population screening programme. The British journal of surgery. 2018;105(1):68-74.
6.   Wanhainen A, Verzini F, Van Herzeele I, Allaire E, Bown M, Cohnert T, et al. Editor's Choice - European Society for Vascular Surgery (ESVS) 2019 Clinical Practice Guidelines on the Management of Abdominal Aorto-iliac Artery Aneurysms. European journal of vascular and endovascular surgery : the official journal of the European Society for Vascular Surgery. 2019;57(1):8-93.
7.   Chaikof EL, Dalman RL, Eskandari MK, Jackson BM, Lee WA, Mansour MA, et al. The Society for Vascular Surgery practice guidelines on the care of patients with an abdominal aortic aneurysm. Journal of vascular surgery : official publication, the Society for Vascular Surgery [and] International Society for Cardiovascular Surgery, North American Chapter. 2018;67(1):2-77 e2.
8.   Cosford PA, Leng GC. Screening for abdominal aortic aneurysm. The Cochrane database of systematic reviews. 2007(2):CD002945.
9.   Mohan IV, Stephen MS. Peripheral arterial aneurysms: open or endovascular surgery? Progress in cardiovascular diseases. 2013;56(1):36-56.
10.   Carr SC, Mahvi DM, Hoch JR, Archer CW, Turnipseed WD. Visceral artery aneurysm rupture. Journal of vascular surgery : official publication, the Society for Vascular Surgery [and] International Society for Cardiovascular Surgery, North American Chapter. 2001;33(4):806-11.
11.   Messina LM, Shanley CJ. Visceral artery aneurysms. The Surgical clinics of North America. 1997;77(2):425-42.
12.   Trickett JP, Scott RA, Tilney HS. Screening and management of asymptomatic popliteal aneurysms. J Med Screen. 2002;9(2):92-3.
13.   Tuveson V, Lofdahl HE, Hultgren R. Patients with abdominal aortic aneurysm have a high prevalence of popliteal artery aneurysms. Vasc Med. 2016.
14.   Chandra V, Trang K, Virgin-Downey W, Tran K, Harris EJ, Dalman RL, et al. Management and outcomes of symptomatic abdominal aortic aneurysms during the past 20 years. Journal of vascular surgery : official publication, the Society for Vascular Surgery [and] International Society for Cardiovascular Surgery, North American Chapter. 2017;66(6):1679-85.

15. Chandra V, Trang K, Virgin-Downey W, Dalman RL, Mell MW. Long-term outcomes after repair of symptomatic abdominal aortic aneurysms. Journal of vascular surgery : official publication, the Society for Vascular Surgery [and] International Society for Cardiovascular Surgery, North American Chapter. 2018;68(5):1360-6.

16. Soden PA, Zettervall SL, Ultee KH, Darling JD, Buck DB, Hile CN, et al. Outcomes for symptomatic abdominal aortic aneurysms in the American College of Surgeons National Surgical Quality Improvement Program. Journal of vascular surgery : official publication, the Society for Vascular Surgery [and] International Society for Cardiovascular Surgery, North American Chapter. 2016;64(2):297-305.

17. Khosla S, Morris DR, Moxon JV, Walker PJ, Gasser TC, Golledge J. Meta-analysis of peak wall stress in ruptured, symptomatic and intact abdominal aortic aneurysms. The British journal of surgery. 2014;101(11):1350-7; discussion 7.

18. Erhart P, Hyhlik-Durr A, Geisbusch P, Kotelis D, Muller-Eschner M, Gasser TC, et al. Finite element analysis in asymptomatic, symptomatic, and ruptured abdominal aortic aneurysms: in search of new rupture risk predictors. European journal of vascular and endovascular surgery : the official journal of the European Society for Vascular Surgery. 2015;49(3):239-45.

19. Chaikof EL, Brewster DC, Dalman RL, Makaroun MS, Illig KA, Sicard GA, et al. SVS practice guidelines for the care of patients with an abdominal aortic aneurysm: executive summary. Journal of vascular surgery : official publication, the Society for Vascular Surgery [and] International Society for Cardiovascular Surgery, North American Chapter. 2009;50(4):880-96.

20. Detlev D. Anatomie. München: Elsevier; 2002.

21. Kumar VAAKFN. Pathologic Basis of Disease. Philadelphi: Elsevier Saunders; 2005.

22. Harkness ML, Harkness RD, Mc DD. The collagen and elastin content of the arterial wall. J Physiol. 1955;127(2):33-4P.

23. Mei CC, Zhang J, Jing HX. Fluid mechanics of Windkessel effect. Med Biol Eng Comput. 2018;56(8):1357-66.

24. Busch A, Hartmann E, Grimm C, Ergun S, Kickuth R, Otto C, et al. Heterogeneous histomorphology, yet homogeneous vascular smooth muscle cell dedifferentiation, characterize human aneurysm disease. Journal of vascular surgery : official publication, the Society for Vascular Surgery [and] International Society for Cardiovascular Surgery, North American Chapter. 2016.

25. Schwartz SM, Virmani R, Majesky MW. An update on clonality: what smooth muscle cell type makes up the atherosclerotic plaque? F1000Res. 2018;7.

26. Lacolley P, Regnault V, Nicoletti A, Li Z, Michel JB. The vascular smooth muscle cell in arterial pathology: a cell that can take on multiple roles. Cardiovascular research. 2012;95(2):194-204.

27. Rijbroek A, Moll FL, von Dijk HA, Meijer R, Jansen JW. Inflammation of the abdominal aortic aneurysm wall. European journal of vascular surgery. 1994;8(1):41-6.

28. Butcovan D, Mocanu V, Haliga RE, Ioan BG, Danciu M, Tinica G. Sub-classification of non-inflammatory and inflammatory surgical aortic aneurysms and the association of histological characteristics with potential risk factors. Exp Ther Med. 2019;18(4):3046-52.

29. Villard C, Eriksson P, Hanemaaijer R, Lindeman JH, Hultgren R. The composition of collagen in the aneurysm wall of men and women. Journal of vascular surgery : official publication, the Society for Vascular Surgery [and] International Society for Cardiovascular Surgery, North American Chapter. 2017;66(2):579-85 e1.

30.   Niestrawska JA, Regitnig P, Viertler C, Cohnert TU, Babu AR, Holzapfel GA. The role of tissue remodeling in mechanics and pathogenesis of abdominal aortic aneurysms. Acta Biomater. 2019;88:149-61.

31.   Meekel JP, Mattei G, Costache VS, Balm R, Blankensteijn JD, Yeung KK. A multilayer micromechanical elastic modulus measuring method in ex vivo human aneurysmal abdominal aortas. Acta Biomater. 2019;96:345-53.

32.   Wilson KA, Lindholt JS, Hoskins PR, Heickendorff L, Vammen S, Bradbury AW. The relationship between abdominal aortic aneurysm distensibility and serum markers of elastin and collagen metabolism. European journal of vascular and endovascular surgery : the official journal of the European Society for Vascular Surgery. 2001;21(2):175-8.

33.   Tavares Monteiro JA, da Silva ES, Raghavan ML, Puech-Leao P, de Lourdes Higuchi M, Otoch JP. Histologic, histochemical, and biomechanical properties of fragments isolated from the anterior wall of abdominal aortic aneurysms. Journal of vascular surgery : official publication, the Society for Vascular Surgery [and] International Society for Cardiovascular Surgery, North American Chapter. 2014;59(5):1393-401 e1-2.

34.   Kazi M, Thyberg J, Religa P, Roy J, Eriksson P, Hedin U, et al. Influence of intraluminal thrombus on structural and cellular composition of abdominal aortic aneurysm wall. Journal of vascular surgery : official publication, the Society for Vascular Surgery [and] International Society for Cardiovascular Surgery, North American Chapter. 2003;38(6):1283-92.

35.   Adolph R, Vorp DA, Steed DL, Webster MW, Kameneva MV, Watkins SC. Cellular content and permeability of intraluminal thrombus in abdominal aortic aneurysm. Journal of vascular surgery : official publication, the Society for Vascular Surgery [and] International Society for Cardiovascular Surgery, North American Chapter. 1997;25(5):916-26.

36.   Houard X, Rouzet F, Touat Z, Philippe M, Dominguez M, Fontaine V, et al. Topology of the fibrinolytic system within the mural thrombus of human abdominal aortic aneurysms. J Pathol. 2007;212(1):20-8.

37.   Maguire EM, Pearce SWA, Xiao R, Oo AY, Xiao Q. Matrix Metalloproteinase in Abdominal Aortic Aneurysm and Aortic Dissection. Pharmaceuticals (Basel). 2019;12(3).

38.   Lindquist Liljeqvist M, Silveira A, Hultgren R, Frebelius S, Lengquist M, Engstrom J, et al. Neutrophil Elastase-Derived Fibrin Degradation Products Indicate Presence of Abdominal Aortic Aneurysms and Correlate with Intraluminal Thrombus Volume. Thrombosis and haemostasis. 2018;118(2):329-39.

39.   Behr Andersen C, Lindholt JS, Urbonavicius S, Halekoh U, Jensen PS, Stubbe J, et al. Abdominal Aortic Aneurysms Growth Is Associated With High Concentrations of Plasma Proteins in the Intraluminal Thrombus and Diseased Arterial Tissue. Arteriosclerosis, thrombosis, and vascular biology. 2018;38(9):2254-67.

40.   Haller SJ, Crawford JD, Courchaine KM, Bohannan CJ, Landry GJ, Moneta GL, et al. Intraluminal thrombus is associated with early rupture of abdominal aortic aneurysm. Journal of vascular surgery : official publication, the Society for Vascular Surgery [and] International Society for Cardiovascular Surgery, North American Chapter. 2018;67(4):1051-8 e1.

41.   Wiernicki I, Parafiniuk M, Kolasa-Wolosiuk A, Gutowska I, Kazimierczak A, Clark J, et al. Relationship between aortic wall oxidative stress/proteolytic enzyme expression and intraluminal thrombus thickness indicates a novel pathomechanism in the progression of human abdominal aortic aneurysm. FASEB J. 2019;33(1):885-95.

42.   Folkesson M, Silveira A, Eriksson P, Swedenborg J. Protease activity in the multi-layered intra-luminal thrombus of abdominal aortic aneurysms. Atherosclerosis. 2011;218(2):294-9.

43.   Siennicka A, Drozdzynska M, Chelstowski K, Cnotliwy M, Jastrzebska M. Haemostatic factors and intraluminal thrombus thickness in abdominal aortic aneurysm. Is secondary fibrinolysis relevant? Journal of physiology and pharmacology : an official journal of the Polish Physiological Society. 2013;64(3):321-30.

44.   Koole D, Zandvoort HJ, Schoneveld A, Vink A, Vos JA, van den Hoogen LL, et al. Intraluminal abdominal aortic aneurysm thrombus is associated with disruption of wall integrity. Journal of vascular surgery : official publication, the Society for Vascular Surgery [and] International Society for Cardiovascular Surgery, North American Chapter. 2013;57(1):77-83.

45.   Martufi G, Lindquist Liljeqvist M, Sakalihasan N, Panuccio G, Hultgren R, Roy J, et al. Local Diameter, Wall Stress, and Thrombus Thickness Influence the Local Growth of Abdominal Aortic Aneurysms. Journal of endovascular therapy : an official journal of the International Society of Endovascular Specialists. 2016;23(6):957-66.

46.   van Noort K, Schuurmann RC, Wermelink B, Slump CH, Kuijpers KC, de Vries JP. Fluid displacement from intraluminal thrombus of abdominal aortic aneurysm as a result of uniform compression. Vascular. 2017;25(5):542-8.

47.   Polzer S, Gasser TC, Markert B, Bursa J, Skacel P. Impact of poroelasticity of intraluminal thrombus on wall stress of abdominal aortic aneurysms. Biomed Eng Online. 2012;11:62.

48.   Metaxa E, Kontopodis N, Tzirakis K, Ioannou CV, Papaharilaou Y. Effect of intraluminal thrombus asymmetrical deposition on abdominal aortic aneurysm growth rate. Journal of endovascular therapy : an official journal of the International Society of Endovascular Specialists. 2015;22(3):406-12.

49.   Dua MM, Dalman RL. Hemodynamic influences on abdominal aortic aneurysm disease: Application of biomechanics to aneurysm pathophysiology. Vascul Pharmacol. 2010;53(1-2):11-21.

50.   Zhang Z, Deng X, Fan Y, Guidoin R. The effects of recirculation flows on mass transfer from the arterial wall to flowing blood. ASAIO J. 2008;54(1):37-43.

51.   Sangha GS, Busch A, Acuna A, Berman AG, Phillips EH, Trenner M, et al. Effects of Iliac Stenosis on Abdominal Aortic Aneurysm Formation in Mice and Humans. J Vasc Res. 2019;56(5):217-29.

52.   Vollmar JF, Paes E, Pauschinger P, Henze E, Friesch A. Aortic aneurysms as late sequelae of above-knee amputation. Lancet. 1989;2(8667):834-5.

53.   Joly F, Soulez G, Lessard S, Kauffmann C, Vignon-Clementel I. A Cohort Longitudinal Study Identifies Morphology and Hemodynamics Predictors of Abdominal Aortic Aneurysm Growth. Ann Biomed Eng. 2020;48(2):606-23.

54.   Zambrano BA, Gharahi H, Lim C, Jaberi FA, Choi J, Lee W, et al. Association of Intraluminal Thrombus, Hemodynamic Forces, and Abdominal Aortic Aneurysm Expansion Using Longitudinal CT Images. Ann Biomed Eng. 2016;44(5):1502-14.

55.   Suh GY, Les AS, Tenforde AS, Shadden SC, Spilker RL, Yeung JJ, et al. Hemodynamic changes quantified in abdominal aortic aneurysms with increasing exercise intensity using mr exercise imaging and image-based computational fluid dynamics. Ann Biomed Eng. 2011;39(8):2186-202.

56.   Jana S, Hu M, Shen M, Kassiri Z. Extracellular matrix, regional heterogeneity of the aorta, and aortic aneurysm. Exp Mol Med. 2019;51(12):160.

57.   Riches K, Angelini TG, Mudhar GS, Kaye J, Clark E, Bailey MA, et al. Exploring smooth muscle phenotype and function in a bioreactor model of abdominal aortic aneurysm. Journal of translational medicine. 2013;11:208.

58.   Chang TW, Gracon AS, Murphy MP, Wilkes DS. Exploring autoimmunity in the pathogenesis of abdominal aortic aneurysms. American journal of physiology Heart and circulatory physiology. 2015;309(5):H719-27.

59.   Swedenborg J, Mayranpaa MI, Kovanen PT. Mast cells: important players in the orchestrated pathogenesis of abdominal aortic aneurysms. Arteriosclerosis, thrombosis, and vascular biology. 2011;31(4):734-40.

60.   Shimizu K, Mitchell RN, Libby P. Inflammation and cellular immune responses in abdominal aortic aneurysms. Arteriosclerosis, thrombosis, and vascular biology. 2006;26(5):987-94.

61.   Clement M, Chappell J, Raffort J, Lareyre F, Vandestienne M, Taylor AL, et al. Vascular Smooth Muscle Cell Plasticity and Autophagy in Dissecting Aortic Aneurysms. Arteriosclerosis, thrombosis, and vascular biology. 2019;39(6):1149-59.

62.   Raffort J, Lareyre F, Clement M, Hassen-Khodja R, Chinetti G, Mallat Z. Monocytes and macrophages in abdominal aortic aneurysm. Nature reviews Cardiology. 2017;14(8):457-71.

63.   Boytard L, Spear R, Chinetti-Gbaguidi G, Acosta-Martin AE, Vanhoutte J, Lamblin N, et al. Role of proinflammatory CD68(+) mannose receptor(-) macrophages in peroxiredoxin-1 expression and in abdominal aortic aneurysms in humans. Arteriosclerosis, thrombosis, and vascular biology. 2013;33(2):431-8.

64.   Zhang L, Wang Y. B lymphocytes in abdominal aortic aneurysms. Atherosclerosis. 2015;242(1):311-7.

65.   Lindholt JS, Shi GP. Chronic inflammation, immune response, and infection in abdominal aortic aneurysms. European journal of vascular and endovascular surgery : the official journal of the European Society for Vascular Surgery. 2006;31(5):453-63.

66.   Bobryshev YV, Lord RS. Vascular-associated lymphoid tissue (VALT) involvement in aortic aneurysm. Atherosclerosis. 2001;154(1):15-21.

67.   Spear R, Boytard L, Blervaque R, Chwastyniak M, Hot D, Vanhoutte J, et al. Adventitial Tertiary Lymphoid Organs as Potential Source of MicroRNA Biomarkers for Abdominal Aortic Aneurysm. International journal of molecular sciences. 2015;16(5):11276-93.

68.   Curci JA, Thompson RW. Adaptive cellular immunity in aortic aneurysms: cause, consequence, or context? The Journal of clinical investigation. 2004;114(2):168-71.

69.   Centa M, Jin H, Hofste L, Hellberg S, Busch A, Baumgartner R, et al. Germinal Center-Derived Antibodies Promote Atherosclerosis Plaque Size and Stability. Circulation. 2019;139(21):2466-82.

70.   Sakalihasan N, Michel JB, Katsargyris A, Kuivaniemi H, Defraigne JO, Nchimi A, et al. Abdominal aortic aneurysms. Nat Rev Dis Primers. 2018;4(1):34.

71.   Anzai T. Inflammatory Mechanisms of Cardiovascular Remodeling. Circulation journal : official journal of the Japanese Circulation Society. 2018;82(3):629-35.

72.   Busch A. Die Pathophysiologie des abdominalen Aortenaneurysmas. Gefäßchirurgie. 2018;23(3):130-5.

73.   Holmes DR, Liao S, Parks WC, Thompson RW. Medial neovascularization in abdominal aortic aneurysms: a histopathologic marker of aneurysmal degeneration with pathophysiologic implications. Journal of vascular surgery : official publication, the Society for Vascular Surgery [and] International Society for Cardiovascular Surgery, North American Chapter. 1995;21(5):761-71; discussion 71-2.

74.   Wang W, Xu B, Xuan H, Ge Y, Wang Y, Wang L, et al. Hypoxia-inducible factor 1 in clinical and experimental aortic aneurysm disease. Journal of vascular surgery : official publication, the Society for Vascular Surgery [and] International Society for Cardiovascular Surgery, North American Chapter. 2018;68(5):1538-50 e2.

75. Kaneko H, Anzai T, Takahashi T, Kohno T, Shimoda M, Sasaki A, et al. Role of vascular endothelial growth factor-A in development of abdominal aortic aneurysm. Cardiovascular research. 2011;91(2):358-67.

76. Gabel G, Northoff BH, Weinzierl I, Ludwig S, Hinterseher I, Wilfert W, et al. Molecular Fingerprint for Terminal Abdominal Aortic Aneurysm Disease. Journal of the American Heart Association. 2017;6(12).

77. Li DY, Busch A, Jin H, Chernogubova E, Pelisek J, Karlsson J, et al. H19 Induces Abdominal Aortic Aneurysm Development and Progression. Circulation. 2018.

78. Lim CS, Kiriakidis S, Sandison A, Paleolog EM, Davies AH. Hypoxia-inducible factor pathway and diseases of the vascular wall. Journal of vascular surgery : official publication, the Society for Vascular Surgery [and] International Society for Cardiovascular Surgery, North American Chapter. 2013;58(1):219-30.

79. Billaud M, Hill JC, Richards TD, Gleason TG, Phillippi JA. Medial Hypoxia and Adventitial Vasa Vasorum Remodeling in Human Ascending Aortic Aneurysm. Front Cardiovasc Med. 2018;5:124.

80. Kessler K, Borges LF, Ho-Tin-Noe B, Jondeau G, Michel JB, Vranckx R. Angiogenesis and remodelling in human thoracic aortic aneurysms. Cardiovascular research. 2014;104(1):147-59.

81. Forsythe RO, Newby DE, Robson JM. Monitoring the biological activity of abdominal aortic aneurysms Beyond Ultrasound. Heart. 2016;102(11):817-24.

82. Lukasiewicz A, Reszec J, Kowalewski R, Chyczewski L, Lebkowska U. Assessment of inflammatory infiltration and angiogenesis in the thrombus and the wall of abdominal aortic aneurysms on the basis of histological parameters and computed tomography angiography study. Folia Histochem Cytobiol. 2012;50(4):547-53.

83. Xu B, Iida Y, Glover KJ, Ge Y, Wang Y, Xuan H, et al. Inhibition of VEGF (Vascular Endothelial Growth Factor)-A or its Receptor Activity Suppresses Experimental Aneurysm Progression in the Aortic Elastase Infusion Model. Arteriosclerosis, thrombosis, and vascular biology. 2019;39(8):1652-66.

84. Sano M, Sasaki T, Hirakawa S, Sakabe J, Ogawa M, Baba S, et al. Lymphangiogenesis and angiogenesis in abdominal aortic aneurysm. PloS one. 2014;9(3):e89830.

85. Scott DJ, Allen CJ, Honstvet CA, Hanby AM, Hammond C, Johnson AB, et al. Lymphangiogenesis in abdominal aortic aneurysm. The British journal of surgery. 2013;100(7):895-903.

86. Aboyans V, Ricco JB, Bartelink MEL, Bjorck M, Brodmann M, Cohnert T, et al. Editor's Choice - 2017 ESC Guidelines on the Diagnosis and Treatment of Peripheral Arterial Diseases, in collaboration with the European Society for Vascular Surgery (ESVS). European journal of vascular and endovascular surgery : the official journal of the European Society for Vascular Surgery. 2018;55(3):305-68.

87. Palazzuoli A, Gallotta M, Guerrieri G, Quatrini I, Franci B, Campagna MS, et al. Prevalence of risk factors, coronary and systemic atherosclerosis in abdominal aortic aneurysm: comparison with high cardiovascular risk population. Vascular health and risk management. 2008;4(4):877-83.

88. Oderich GS, Karkkainen JM, Reed NR, Tenorio ER, Sandri GA. Penetrating Aortic Ulcer and Intramural Hematoma. Cardiovascular and interventional radiology. 2019;42(3):321-34.

89. Shteinberg D, Halak M, Shapiro S, Kinarty A, Sobol E, Lahat N, et al. Abdominal aortic aneurysm and aortic occlusive disease: a comparison of risk factors and inflammatory response. European journal of vascular and endovascular surgery : the official journal of the European Society for Vascular Surgery. 2000;20(5):462-5.

90.   Ketelhuth DF, Hansson GK. Adaptive Response of T and B Cells in Atherosclerosis. Circulation research. 2016;118(4):668-78.
91.   Gomez D, Owens GK. Smooth muscle cell phenotypic switching in atherosclerosis. Cardiovascular research. 2012;95(2):156-64.
92.   Yamagishi M, Higashikata T, Ishibashi-Ueda H, Sasaki H, Ogino H, Iihara K, et al. Sustained upregulation of inflammatory chemokine and its receptor in aneurysmal and occlusive atherosclerotic disease: results form tissue analysis with cDNA macroarray and real-time reverse transcriptional polymerase chain reaction methods. Circulation journal : official journal of the Japanese Circulation Society. 2005;69(12):1490-5.
93.   Davis VA, Persidskaia RN, Baca-Regen LM, Fiotti N, Halloran BG, Baxter BT. Cytokine pattern in aneurysmal and occlusive disease of the aorta. The Journal of surgical research. 2001;101(2):152-6.
94.   Pearce WH, Sweis I, Yao JS, McCarthy WJ, Koch AE. Interleukin-1 beta and tumor necrosis factor-alpha release in normal and diseased human infrarenal aortas. Journal of vascular surgery : official publication, the Society for Vascular Surgery [and] International Society for Cardiovascular Surgery, North American Chapter. 1992;16(5):784-9.
95.   McMillan WD, Pearce WH. Increased plasma levels of metalloproteinase-9 are associated with abdominal aortic aneurysms. Journal of vascular surgery : official publication, the Society for Vascular Surgery [and] International Society for Cardiovascular Surgery, North American Chapter. 1999;29(1):122-7; discussion 7-9.
96.   Shireman PK, McCarthy WJ, Pearce WH, Shively VP, Cipollone M, Kwaan HC. Elevations of tissue-type plasminogen activator and differential expression of urokinase-type plasminogen activator in diseased aorta. Journal of vascular surgery : official publication, the Society for Vascular Surgery [and] International Society for Cardiovascular Surgery, North American Chapter. 1997;25(1):157-64.
97.   Grytsan A, Eriksson TSE, Watton PN, Gasser TC. Growth Description for Vessel Wall Adaptation: A Thick-Walled Mixture Model of Abdominal Aortic Aneurysm Evolution. Materials (Basel). 2017;10(9).
98.   Walburn F, Stein P. Flow characteristics in symmetrically branched tubes simulating the human aortic bifurcation. J Biomech Eng. 1980;102(4):340-2.
99.   Bennett PC, Silverman SH, Gill PS, Lip GY. Peripheral arterial disease and Virchow's triad. Thrombosis and haemostasis. 2009;101(6):1032-40.
100.   Airhart N, Brownstein BH, Cobb JP, Schierding W, Arif B, Ennis TL, et al. Smooth muscle cells from abdominal aortic aneurysms are unique and can independently and synergistically degrade insoluble elastin. Journal of vascular surgery : official publication, the Society for Vascular Surgery [and] International Society for Cardiovascular Surgery, North American Chapter. 2014;60(4):1033-41; discussion 41-2.
101.   Ailawadi G, Moehle CW, Pei H, Walton SP, Yang Z, Kron IL, et al. Smooth muscle phenotypic modulation is an early event in aortic aneurysms. The Journal of thoracic and cardiovascular surgery. 2009;138(6):1392-9.
102.   Ruddy JM, Jones JA, Ikonomidis JS. Pathophysiology of thoracic aortic aneurysm (TAA): is it not one uniform aorta? Role of embryologic origin. Progress in cardiovascular diseases. 2013;56(1):68-73.
103.   Ruddy JM, Jones JA, Spinale FG, Ikonomidis JS. Regional heterogeneity within the aorta: relevance to aneurysm disease. The Journal of thoracic and cardiovascular surgery. 2008;136(5):1123-30.
104.   Lindsay ME, Dietz HC. Lessons on the pathogenesis of aneurysm from heritable conditions. Nature. 2011;473(7347):308-16.

105.   Meijer CA, Stijnen T, Wasser MN, Hamming JF, van Bockel JH, Lindeman JH. Doxycycline for stabilization of abdominal aortic aneurysms: a randomized trial. Annals of internal medicine. 2013;159(12):815-23.

106.   Nakano K, Nemoto H, Nomura R, Inaba H, Yoshioka H, Taniguchi K, et al. Detection of oral bacteria in cardiovascular specimens. Oral Microbiol Immunol. 2009;24(1):64-8.

107.   Myllyharju J, Kivirikko KI. Collagens and collagen-related diseases. Ann Med. 2001;33(1):7-21.

108.   Holsti M, Wanhainen A, Lundin C, Bjorck M, Tegler G, Svensson J, et al. Circulating Vascular Basement Membrane Fragments are Associated with the Diameter of the Abdominal Aorta and Their Expression Pattern is Altered in AAA Tissue. European journal of vascular and endovascular surgery : the official journal of the European Society for Vascular Surgery. 2018;56(1):110-8.

109.   Carmeliet P, Moons L, Lijnen R, Baes M, Lemaitre V, Tipping P, et al. Urokinase-generated plasmin activates matrix metalloproteinases during aneurysm formation. Nature genetics. 1997;17(4):439-44.

110.   Itoga NK, Rothenberg KA, Suarez P, Ho TV, Mell MW, Xu B, et al. Metformin prescription status and abdominal aortic aneurysm disease progression in the U.S. veteran population. Journal of vascular surgery : official publication, the Society for Vascular Surgery [and] International Society for Cardiovascular Surgery, North American Chapter. 2019;69(3):710-6 e3.

111.   Golledge J, Moxon J, Pinchbeck J, Anderson G, Rowbotham S, Jenkins J, et al. Association between metformin prescription and growth rates of abdominal aortic aneurysms. The British journal of surgery. 2017;104(11):1486-93.

112.   Larsson E, Granath F, Swedenborg J, Hultgren R. A population-based case-control study of the familial risk of abdominal aortic aneurysm. Journal of vascular surgery : official publication, the Society for Vascular Surgery [and] International Society for Cardiovascular Surgery, North American Chapter. 2009;49(1):47-50; discussion 1.

113.   Verloes A, Sakalihasan N, Koulischer L, Limet R. Aneurysms of the abdominal aorta: familial and genetic aspects in three hundred thirteen pedigrees. Journal of vascular surgery : official publication, the Society for Vascular Surgery [and] International Society for Cardiovascular Surgery, North American Chapter. 1995;21(4):646-55.

114.   Elmore JR, Obmann MA, Kuivaniemi H, Tromp G, Gerhard GS, Franklin DP, et al. Identification of a genetic variant associated with abdominal aortic aneurysms on chromosome 3p12.3 by genome wide association. Journal of vascular surgery : official publication, the Society for Vascular Surgery [and] International Society for Cardiovascular Surgery, North American Chapter. 2009;49(6):1525-31.

115.   Gretarsdottir S, Baas AF, Thorleifsson G, Holm H, den Heijer M, de Vries JP, et al. Genome-wide association study identifies a sequence variant within the DAB2IP gene conferring susceptibility to abdominal aortic aneurysm. Nature genetics. 2010;42(8):692-7.

116.   Bown MJ, Jones GT, Harrison SC, Wright BJ, Bumpstead S, Baas AF, et al. Abdominal aortic aneurysm is associated with a variant in low-density lipoprotein receptor-related protein 1. Am J Hum Genet. 2011;89(5):619-27.

117.   Bradley DT, Hughes AE, Badger SA, Jones GT, Harrison SC, Wright BJ, et al. A variant in LDLR is associated with abdominal aortic aneurysm. Circulation Cardiovascular genetics. 2013;6(5):498-504.

118.   Jones GT, Tromp G, Kuivaniemi H, Gretarsdottir S, Baas AF, Giusti B, et al. Meta-Analysis of Genome-Wide Association Studies for Abdominal Aortic Aneurysm

Identifies Four New Disease-Specific Risk Loci. Circulation research. 2017;120(2):341-53.

119. van Laarhoven C, van Setten J, van Herwaarden JA, Pasterkamp G, de Kleijn DPV, de Borst GJ, et al. Polygenic Susceptibility of Aortic Aneurysms Associates to the Diameter of the Aneurysm Sac: the Aneurysm-Express Biobank Cohort. Sci Rep. 2019;9(1):19844.

120. Seo GH, Kim YM, Kang E, Kim GH, Seo EJ, Lee BH, et al. The phenotypic heterogeneity of patients with Marfan-related disorders and their variant spectrums. Medicine (Baltimore). 2018;97(20):e10767.

121. Loeys BL, Chen J, Neptune ER, Judge DP, Podowski M, Holm T, et al. A syndrome of altered cardiovascular, craniofacial, neurocognitive and skeletal development caused by mutations in TGFBR1 or TGFBR2. Nature genetics. 2005;37(3):275-81.

122. Bergqvist D, Bjorck M, Wanhainen A. Treatment of vascular Ehlers-Danlos syndrome: a systematic review. Annals of surgery. 2013;258(2):257-61.

123. Kakafika AI, Mikhailidis DP. Smoking and aortic diseases. Circulation journal : official journal of the Japanese Circulation Society. 2007;71(8):1173-80.

124. Wagenhauser MU, Schellinger IN, Yoshino T, Toyama K, Kayama Y, Deng A, et al. Chronic Nicotine Exposure Induces Murine Aortic Remodeling and Stiffness Segmentation-Implications for Abdominal Aortic Aneurysm Susceptibility. Front Physiol. 2018;9:1459.

125. Sweeting MJ, Thompson SG, Brown LC, Powell JT, collaborators R. Meta-analysis of individual patient data to examine factors affecting growth and rupture of small abdominal aortic aneurysms. The British journal of surgery. 2012;99(5):655-65.

126. Telomeres Mendelian Randomization C, Haycock PC, Burgess S, Nounu A, Zheng J, Okoli GN, et al. Association Between Telomere Length and Risk of Cancer and Non-Neoplastic Diseases: A Mendelian Randomization Study. JAMA Oncol. 2017;3(5):636-51.

127. Davis FM, Rateri DL, Daugherty A. Abdominal aortic aneurysm: novel mechanisms and therapies. Current opinion in cardiology. 2015;30(6):566-73.

128. Bhamidipati CM, Whatling CA, Mehta GS, Meher AK, Hajzus VA, Su G, et al. 5-Lipoxygenase pathway in experimental abdominal aortic aneurysms. Arteriosclerosis, thrombosis, and vascular biology. 2014;34(12):2669-78.

129. Hurks R, Pasterkamp G, Vink A, Hoefer IE, Bots ML, van de Pavoordt HD, et al. Circumferential heterogeneity in the abdominal aortic aneurysm wall composition suggests lateral sides to be more rupture prone. Journal of vascular surgery : official publication, the Society for Vascular Surgery [and] International Society for Cardiovascular Surgery, North American Chapter. 2012;55(1):203-9.

130. Wilson WR, Anderton M, Schwalbe EC, Jones JL, Furness PN, Bell PR, et al. Matrix metalloproteinase-8 and -9 are increased at the site of abdominal aortic aneurysm rupture. Circulation. 2006;113(3):438-45.

131. Wilson WR, Anderton M, Choke EC, Dawson J, Loftus IM, Thompson MM. Elevated plasma MMP1 and MMP9 are associated with abdominal aortic aneurysm rupture. European journal of vascular and endovascular surgery : the official journal of the European Society for Vascular Surgery. 2008;35(5):580-4.

132. Wilson WR, Wills J, Furness PN, Loftus IM, Thompson MM. Abdominal aortic aneurysm rupture is not associated with an up-regulation of inflammation within the aneurysm wall. European journal of vascular and endovascular surgery : the official journal of the European Society for Vascular Surgery. 2010;40(2):191-5.

133. Choke E, Cockerill GW, Laing K, Dawson J, Wilson WR, Loftus IM, et al. Whole genome-expression profiling reveals a role for immune and inflammatory response in

abdominal aortic aneurysm rupture. European journal of vascular and endovascular surgery : the official journal of the European Society for Vascular Surgery. 2009;37(3):305-10.

134. Erhart P, Grond-Ginsbach C, Hakimi M, Lasitschka F, Dihlmann S, Bockler D, et al. Finite element analysis of abdominal aortic aneurysms: predicted rupture risk correlates with aortic wall histology in individual patients. Journal of endovascular therapy : an official journal of the International Society of Endovascular Specialists. 2014;21(4):556-64.

135. Barrett HE, Cunnane EM, Hidayat H, O'Brien JM, Moloney MA, Kavanagh EG, et al. On the influence of wall calcification and intraluminal thrombus on prediction of abdominal aortic aneurysm rupture. Journal of vascular surgery : official publication, the Society for Vascular Surgery [and] International Society for Cardiovascular Surgery, North American Chapter. 2018;67(4):1234-46 e2.

136. Choke E, Cockerill GW, Dawson J, Wilson RW, Jones A, Loftus IM, et al. Increased angiogenesis at the site of abdominal aortic aneurysm rupture. Annals of the New York Academy of Sciences. 2006;1085:315-9.

137. Choke E, Cockerill GW, Dawson J, Chung YL, Griffiths J, Wilson RW, et al. Hypoxia at the site of abdominal aortic aneurysm rupture is not associated with increased lactate. Annals of the New York Academy of Sciences. 2006;1085:306-10.

138. English SJ, Piert MR, Diaz JA, Gordon D, Ghosh A, D'Alecy LG, et al. Increased 18F-FDG uptake is predictive of rupture in a novel rat abdominal aortic aneurysm rupture model. Annals of surgery. 2015;261(2):395-404.

139. Hasan D, Chalouhi N, Jabbour P, Hashimoto T. Macrophage imbalance (M1 vs. M2) and upregulation of mast cells in wall of ruptured human cerebral aneurysms: preliminary results. J Neuroinflammation. 2012;9:222.

140. Busch A, Grimm C, Hartmann E, Paloschi V, Kickuth R, Lengquist M, et al. Vessel wall morphology is equivalent for different artery types and localizations of advanced human aneurysms. Histochemistry and cell biology. 2017.

141. Choke E, Cockerill G, Wilson WR, Sayed S, Dawson J, Loftus I, et al. A review of biological factors implicated in abdominal aortic aneurysm rupture. European journal of vascular and endovascular surgery : the official journal of the European Society for Vascular Surgery. 2005;30(3):227-44.

142. Bobadilla JL. From Ebers to EVARs: A Historical Perspective on Aortic Surgery. Aorta (Stamford). 2013;1(2):89-95.

143. Livesay JJ, Messner GN, Vaughn WK. Milestones in the treatment of aortic aneurysm: Denton A. Cooley, MD, and the Texas Heart Institute. Texas Heart Institute journal / from the Texas Heart Institute of St Luke's Episcopal Hospital, Texas Children's Hospital. 2005;32(2):130-4.

144. Westaby S BC. Landmarks in cardiac surgery: Oxford:
Isis Medical Media; 1997.

145. Crafoord C NG. Congenital coarctation of the aorta and its surgical treatment. J Thorac Surg. 1945;14:347-61.

146. Wilton A. The history of abdominal aortic repair: from Egypt to EVAR. Australian Medical Student Journal. 2012.

147. Thompson JE. Early history of aortic surgery. Journal of vascular surgery : official publication, the Society for Vascular Surgery [and] International Society for Cardiovascular Surgery, North American Chapter. 1998;28(4):746-52.

148. Debakey ME, Crawford ES, Cooley DA, Morris GC, Jr., Royster TS, Abbott WP. Aneurysm of Abdominal Aorta Analysis of Results of Graft Replacement Therapy One to Eleven Years after Operation. Annals of surgery. 1964;160:622-39.

149.   Kline RG, D'Angelo AJ, Chen MH, Halpern VJ, Cohen JR. Laparoscopically assisted abdominal aortic aneurysm repair: first 20 cases. Journal of vascular surgery : official publication, the Society for Vascular Surgery [and] International Society for Cardiovascular Surgery, North American Chapter. 1998;27(1):81-7; discussion 8.
150.   Matsumoto Y, Nishimori H, Yamada H, Yamamoto A, Okazaki Y, Kusume K, et al. Laparoscopy-assisted abdominal aortic aneurysm repair: first case reports from Japan. Circulation journal : official journal of the Japanese Circulation Society. 2003;67(1):99-101.
151.   Friedman SG. Charles Dotter: interventional radiologist. Radiology. 1989;172(3 Pt 2):921-4.
152.   [Munchener Medizinische Wochenschrift/20 March 1931 Contrast representation of the cavities of the living right half of the heart by Werner Forssmann, Eberswalde]. MMW Munch Med Wochenschr. 1978;120(14):489.
153.   Parodi JC, Palmaz JC, Barone HD. Transfemoral intraluminal graft implantation for abdominal aortic aneurysms. Annals of vascular surgery. 1991;5(6):491-9.
154.   Greenberg RK. Abdominal aortic endografting: fixation and sealing. Journal of the American College of Surgeons. 2002;194(1 Suppl):S79-87.
155.   Vatakencherry G, Molloy C, Sheth N, Liao M, Lam CK. Percutaneous access planning, techniques and considerations for endovascular aortic repair (EVAR). Cardiovasc Diagn Ther. 2018;8(Suppl 1):S184-S90.
156.   Kuhnl A, Erk A, Trenner M, Salvermoser M, Schmid V, Eckstein HH. Incidence, Treatment and Mortality in Patients with Abdominal Aortic Aneurysms. Deutsches Arzteblatt international. 2017;114(22-23):391-8.
157.   Eckstein HH, Bockler D, Flessenkamper I, Schmitz-Rixen T, Debus S, Lang W. Ultrasonographic screening for the detection of abdominal aortic aneurysms. Deutsches Arzteblatt international. 2009;106(41):657-63.
158.   Sidloff D, Stather P, Dattani N, Bown M, Thompson J, Sayers R, et al. Aneurysm global epidemiology study: public health measures can further reduce abdominal aortic aneurysm mortality. Circulation. 2014;129(7):747-53.
159.   Peacock A, Leung J, Larney S, Colledge S, Hickman M, Rehm J, et al. Global statistics on alcohol, tobacco and illicit drug use: 2017 status report. Addiction. 2018.
160.   Kotz DB, M; Kastaun, S. The Use of Tobacco, E-Cigarettes, and Methods to Quit Smoking in Germany. Deutsches Arzteblatt international. 2018.
161.   Sampson UK, Norman PE, Fowkes FG, Aboyans V, Song Y, Harrell FE, Jr., et al. Estimation of global and regional incidence and prevalence of abdominal aortic aneurysms 1990 to 2010. Glob Heart. 2014;9(1):159-70.
162.   National Center for Health Statistics. Deaths, percent of total deaths, and death rates for the 15 leading causes of death in selected age groups, by race and sex. 2007.
163.   D'Oria M, Hanson KT, Shermerhorn M, Bower TC, Mendes BC, Shuja F, et al. Short Term and Long Term Outcomes After Endovascular or Open Repair for Ruptured Infrarenal Abdominal Aortic Aneurysms in the Vascular Quality Initiative. European journal of vascular and endovascular surgery : the official journal of the European Society for Vascular Surgery. 2020.
164.   Trenner M, Kuehnl A, Salvermoser M, Reutersberg B, Geisbuesch S, Schmid V, et al. Editor's Choice - High Annual Hospital Volume is Associated with Decreased in Hospital Mortality and Complication Rates Following Treatment of Abdominal Aortic Aneurysms: Secondary Data Analysis of the Nationwide German DRG Statistics from 2005 to 2013. European journal of vascular and endovascular surgery : the official journal of the European Society for Vascular Surgery. 2018;55(2):185-94.

165. Paolini D, Chahwan S, Wojnarowski D, Pigott JP, LaPorte F, Comerota AJ. Elective endovascular and open repair of abdominal aortic aneurysms in octogenarians. Journal of vascular surgery : official publication, the Society for Vascular Surgery [and] International Society for Cardiovascular Surgery, North American Chapter. 2008;47(5):924-7.

166. Patel R, Sweeting MJ, Powell JT, Greenhalgh RM, investigators Et. Endovascular versus open repair of abdominal aortic aneurysm in 15-years' follow-up of the UK endovascular aneurysm repair trial 1 (EVAR trial 1): a randomised controlled trial. Lancet. 2016;388(10058):2366-74.

167. Antoniou GA, Antoniou SA, Torella F. Endovascular vs. Open Repair for Abdominal Aortic Aneurysm: Systematic Review and Meta-analysis of Updated Peri-operative and Long Term Data of Randomised Controlled Trials. European journal of vascular and endovascular surgery : the official journal of the European Society for Vascular Surgery. 2019.

168. Kontopodis N, Tavlas E, Ioannou CV, Giannoukas AD, Geroulakos G, Antoniou GA. Prognosis Systematic Review and Meta-Analysis of Outcomes of Open and Endovascular Repair of Ruptured Abdominal Aortic Aneurysm in Patients with Hostile vs. Friendly Aortic Anatomy. European journal of vascular and endovascular surgery : the official journal of the European Society for Vascular Surgery. 2020.

169. Lindeman JH, Matsumura JS. Pharmacologic Management of Aneurysms. Circulation research. 2019;124(4):631-46.

170. Busch A, Chernogubova E, Jin H, Meurer F, Eckstein HH, Kim M, et al. Four Surgical Modifications to the Classic Elastase Perfusion Aneurysm Model Enable Haemodynamic Alterations and Extended Elastase Perfusion. European journal of vascular and endovascular surgery : the official journal of the European Society for Vascular Surgery. 2018.

171. Trachet B, Fraga-Silva RA, Jacquet PA, Stergiopulos N, Segers P. Incidence, severity, mortality, and confounding factors for dissecting AAA detection in angiotensin II-infused mice: a meta-analysis. Cardiovascular research. 2015;108(1):159-70.

172. Propanolol Aneurysm Trial I. Propranolol for small abdominal aortic aneurysms: results of a randomized trial. Journal of vascular surgery : official publication, the Society for Vascular Surgery [and] International Society for Cardiovascular Surgery, North American Chapter. 2002;35(1):72-9.

173. Lindholt JS, Henneberg EW, Juul S, Fasting H. Impaired results of a randomised double blinded clinical trial of propranolol versus placebo on the expansion rate of small abdominal aortic aneurysms. International angiology : a journal of the International Union of Angiology. 1999;18(1):52-7.

174. Sweeting MJ, Thompson SG, Brown LC, Greenhalgh RM, Powell JT. Use of angiotensin converting enzyme inhibitors is associated with increased growth rate of abdominal aortic aneurysms. Journal of vascular surgery : official publication, the Society for Vascular Surgery [and] International Society for Cardiovascular Surgery, North American Chapter. 2010;52(1):1-4.

175. Hackam DG, Thiruchelvam D, Redelmeier DA. Angiotensin-converting enzyme inhibitors and aortic rupture: a population-based case-control study. Lancet. 2006;368(9536):659-65.

176. Bicknell CD, Kiru G, Falaschetti E, Powell JT, Poulter NR, Collaborators A. An evaluation of the effect of an angiotensin-converting enzyme inhibitor on the growth rate of small abdominal aortic aneurysms: a randomized placebo-controlled trial (AARDVARK). Eur Heart J. 2016;37(42):3213-21.

177.	Ferguson CD, Clancy P, Bourke B, Walker PJ, Dear A, Buckenham T, et al. Association of statin prescription with small abdominal aortic aneurysm progression. Am Heart J. 2010;159(2):307-13.

178.	Lindholt JS, Sorensen HT, Michel JB, Thomsen HF, Henneberg EW. Low-dose aspirin may prevent growth and later surgical repair of medium-sized abdominal aortic aneurysms. Vascular and endovascular surgery. 2008;42(4):329-34.

179.	Bhak RH, Wininger M, Johnson GR, Lederle FA, Messina LM, Ballard DJ, et al. Factors associated with small abdominal aortic aneurysm expansion rate. JAMA Surg. 2015;150(1):44-50.

180.	Meijer CA, Stijnen T, Wasser MN, Hamming JF, van Bockel JH, Lindeman JH, et al. Doxycycline for stabilization of abdominal aortic aneurysms: a randomized trial. Annals of internal medicine. 2013;159(12):815-23.

181.	Baxter BT, Pearce WH, Waltke EA, Littooy FN, Hallett JW, Jr., Kent KC, et al. Prolonged administration of doxycycline in patients with small asymptomatic abdominal aortic aneurysms: report of a prospective (Phase II) multicenter study. Journal of vascular surgery : official publication, the Society for Vascular Surgery [and] International Society for Cardiovascular Surgery, North American Chapter. 2002;36(1):1-12.

182.	Sillesen H, Eldrup N, Hultgren R, Lindeman J, Bredahl K, Thompson M, et al. Randomized clinical trial of mast cell inhibition in patients with a medium-sized abdominal aortic aneurysm. The British journal of surgery. 2015;102(8):894-901.

183.	Nishijo N, Sugiyama F, Kimoto K, Taniguchi K, Murakami K, Suzuki S, et al. Salt-sensitive aortic aneurysm and rupture in hypertensive transgenic mice that overproduce angiotensin II. Lab Invest. 1998;78(9):1059-66.

184.	Daugherty A, Manning MW, Cassis LA. Angiotensin II promotes atherosclerotic lesions and aneurysms in apolipoprotein E-deficient mice. The Journal of clinical investigation. 2000;105(11):1605-12.

185.	Daugherty A, Cassis LA, Lu H. Complex pathologies of angiotensin II-induced abdominal aortic aneurysms. J Zhejiang Univ Sci B. 2011;12(8):624-8.

186.	Deng GG, Martin-McNulty B, Sukovich DA, Freay A, Halks-Miller M, Thinnes T, et al. Urokinase-type plasminogen activator plays a critical role in angiotensin II-induced abdominal aortic aneurysm. Circulation research. 2003;92(5):510-7.

187.	Daugherty A, Manning MW, Cassis LA. Antagonism of AT2 receptors augments angiotensin II-induced abdominal aortic aneurysms and atherosclerosis. Br J Pharmacol. 2001;134(4):865-70.

188.	Cassis LA, Rateri DL, Lu H, Daugherty A. Bone marrow transplantation reveals that recipient AT1a receptors are required to initiate angiotensin II-induced atherosclerosis and aneurysms. Arteriosclerosis, thrombosis, and vascular biology. 2007;27(2):380-6.

189.	Rateri DL, Moorleghen JJ, Balakrishnan A, Owens AP, 3rd, Howatt DA, Subramanian V, et al. Endothelial cell-specific deficiency of Ang II type 1a receptors attenuates Ang II-induced ascending aortic aneurysms in LDL receptor-/- mice. Circulation research. 2011;108(5):574-81.

190.	Saraff K, Babamusta F, Cassis LA, Daugherty A. Aortic dissection precedes formation of aneurysms and atherosclerosis in angiotensin II-infused, apolipoprotein E-deficient mice. Arteriosclerosis, thrombosis, and vascular biology. 2003;23(9):1621-6.

191.	Cassis LA, Helton MJ, Howatt DA, King VL, Daugherty A. Aldosterone does not mediate angiotensin II-induced atherosclerosis and abdominal aortic aneurysms. Br J Pharmacol. 2005;144(3):443-8.

192.	Cassis LA, Gupte M, Thayer S, Zhang X, Charnigo R, Howatt DA, et al. ANG II infusion promotes abdominal aortic aneurysms independent of increased blood

pressure in hypercholesterolemic mice. American journal of physiology Heart and circulatory physiology. 2009;296(5):H1660-5.

193. Police SB, Putnam K, Thatcher S, Batifoulier-Yiannikouris F, Daugherty A, Cassis LA. Weight loss in obese C57BL/6 mice limits adventitial expansion of established angiotensin II-induced abdominal aortic aneurysms. American journal of physiology Heart and circulatory physiology. 2010;298(6):H1932-8.

194. Police SB, Thatcher SE, Charnigo R, Daugherty A, Cassis LA. Obesity promotes inflammation in periaortic adipose tissue and angiotensin II-induced abdominal aortic aneurysm formation. Arteriosclerosis, thrombosis, and vascular biology. 2009;29(10):1458-64.

195. Rateri DL, Davis FM, Balakrishnan A, Howatt DA, Moorleghen JJ, O'Connor WN, et al. Angiotensin II induces region-specific medial disruption during evolution of ascending aortic aneurysms. The American journal of pathology. 2014;184(9):2586-95.

196. Manning MW, Cassis LA, Daugherty A. Differential effects of doxycycline, a broad-spectrum matrix metalloproteinase inhibitor, on angiotensin II-induced atherosclerosis and abdominal aortic aneurysms. Arteriosclerosis, thrombosis, and vascular biology. 2003;23(3):483-8.

197. Gavrila D, Li WG, McCormick ML, Thomas M, Daugherty A, Cassis LA, et al. Vitamin E inhibits abdominal aortic aneurysm formation in angiotensin II-infused apolipoprotein E-deficient mice. Arteriosclerosis, thrombosis, and vascular biology. 2005;25(8):1671-7.

198. Xie X, Lu H, Moorleghen JJ, Howatt DA, Rateri DL, Cassis LA, et al. Doxycycline does not influence established abdominal aortic aneurysms in angiotensin II-infused mice. PloS one. 2012;7(9):e46411.

199. Chen X, Rateri DL, Howatt DA, Balakrishnan A, Moorleghen JJ, Morris AJ, et al. Amlodipine reduces AngII-induced aortic aneurysms and atherosclerosis in hypercholesterolemic mice. PloS one. 2013;8(11):e81743.

200. Tanaka A, Hasegawa T, Chen Z, Okita Y, Okada K. A novel rat model of abdominal aortic aneurysm using a combination of intraluminal elastase infusion and extraluminal calcium chloride exposure. Journal of vascular surgery : official publication, the Society for Vascular Surgery [and] International Society for Cardiovascular Surgery, North American Chapter. 2009;50(6):1423-32.

201. Busch A, Holm A, Wagner N, Ergun S, Rosenfeld M, Otto C, et al. Extra- and Intraluminal Elastase Induce Morphologically Distinct Abdominal Aortic Aneurysms in Mice and Thus Represent Specific Subtypes of Human Disease. J Vasc Res. 2016;53(1-2):49-57.

202. Prescott MF, Sawyer WK, Von Linden-Reed J, Jeune M, Chou M, Caplan SL, et al. Effect of matrix metalloproteinase inhibition on progression of atherosclerosis and aneurysm in LDL receptor-deficient mice overexpressing MMP-3, MMP-12, and MMP-13 and on restenosis in rats after balloon injury. Annals of the New York Academy of Sciences. 1999;878:179-90.

203. Barisione C, Charnigo R, Howatt DA, Moorleghen JJ, Rateri DL, Daugherty A. Rapid dilation of the abdominal aorta during infusion of angiotensin II detected by noninvasive high-frequency ultrasonography. Journal of vascular surgery : official publication, the Society for Vascular Surgery [and] International Society for Cardiovascular Surgery, North American Chapter. 2006;44(2):372-6.

204. Allaire E, Guettier C, Bruneval P, Plissonnier D, Michel JB. Cell-free arterial grafts: morphologic characteristics of aortic isografts, allografts, and xenografts in rats. Journal of vascular surgery : official publication, the Society for Vascular Surgery [and] International Society for Cardiovascular Surgery, North American Chapter. 1994;19(3):446-56.

205. Senemaud J, Caligiuri G, Etienne H, Delbosc S, Michel JB, Coscas R. Translational Relevance and Recent Advances of Animal Models of Abdominal Aortic Aneurysm. Arteriosclerosis, thrombosis, and vascular biology. 2017;37(3):401-10.

206. Allaire E, Bruneval P, Mandet C, Becquemin JP, Michel JB. The immunogenicity of the extracellular matrix in arterial xenografts. Surgery. 1997;122(1):73-81.

207. Schneider F, Saucy F, de Blic R, Dai J, Mohand F, Rouard H, et al. Bone marrow mesenchymal stem cells stabilize already-formed aortic aneurysms more efficiently than vascular smooth muscle cells in a rat model. European journal of vascular and endovascular surgery : the official journal of the European Society for Vascular Surgery. 2013;45(6):666-72.

208. Alsac JM, Delbosc S, Rouer M, Journe C, Louedec L, Meilhac O, et al. Fucoidan interferes with Porphyromonas gingivalis-induced aneurysm enlargement by decreasing neutrophil activation. Journal of vascular surgery : official publication, the Society for Vascular Surgery [and] International Society for Cardiovascular Surgery, North American Chapter. 2013;57(3):796-805.

209. Gertz SD, Kurgan A, Eisenberg D. Aneurysm of the rabbit common carotid artery induced by periarterial application of calcium chloride in vivo. The Journal of clinical investigation. 1988;81(3):649-56.

210. Gertz SD, Mintz Y, Beeri R, Rubinstein C, Gilon D, Gavish L, et al. Lessons from Animal Models of Arterial Aneurysm. Aorta (Stamford). 2013;1(5):244-54.

211. Chiou AC, Chiu B, Pearce WH. Murine aortic aneurysm produced by periarterial application of calcium chloride. The Journal of surgical research. 2001;99(2):371-6.

212. Yamanouchi D, Morgan S, Stair C, Seedial S, Lengfeld J, Kent KC, et al. Accelerated aneurysmal dilation associated with apoptosis and inflammation in a newly developed calcium phosphate rodent abdominal aortic aneurysm model. Journal of vascular surgery : official publication, the Society for Vascular Surgery [and] International Society for Cardiovascular Surgery, North American Chapter. 2012;56(2):455-61.

213. Bhamidipati CM, Mehta GS, Lu G, Moehle CW, Barbery C, DiMusto PD, et al. Development of a novel murine model of aortic aneurysms using peri-adventitial elastase. Surgery. 2012;152(2):238-46.

214. Tyerman Z, Dahl J, Shannon A, Johnston WF, Pope NH, Lu G, et al. Murine Surgical Model of Topical Elastase Induced Descending Thoracic Aortic Aneurysm. Journal of visualized experiments : JoVE. 2019(150).

215. Nuki Y, Tsou TL, Kurihara C, Kanematsu M, Kanematsu Y, Hashimoto T. Elastase-induced intracranial aneurysms in hypertensive mice. Hypertension. 2009;54(6):1337-44.

216. Anidjar S, Salzmann JL, Gentric D, Lagneau P, Camilleri JP, Michel JB. Elastase-induced experimental aneurysms in rats. Circulation. 1990;82(3):973-81.

217. Pyo R, Lee JK, Shipley JM, Curci JA, Mao D, Ziporin SJ, et al. Targeted gene disruption of matrix metalloproteinase-9 (gelatinase B) suppresses development of experimental abdominal aortic aneurysms. The Journal of clinical investigation. 2000;105(11):1641-9.

218. Azuma J, Asagami T, Dalman R, Tsao PS. Creation of murine experimental abdominal aortic aneurysms with elastase. Journal of visualized experiments : JoVE. 2009(29).

219. Halpern VJ, Nackman GB, Gandhi RH, Irizarry E, Scholes JV, Ramey WG, et al. The elastase infusion model of experimental aortic aneurysms: synchrony of induction of endogenous proteinases with matrix destruction and inflammatory cell response. Journal of vascular surgery : official publication, the Society for Vascular Surgery [and]

International Society for Cardiovascular Surgery, North American Chapter. 1994;20(1):51-60.

220. Yamaguchi T, Yokokawa M, Suzuki M, Higashide S, Katoh Y, Sugiyama S, et al. The time course of elastin fiber degeneration in a rat aneurysm model. Surg Today. 2000;30(8):727-31.

221. DiMusto PD, Lu G, Ghosh A, Roelofs KJ, Su G, Zhao Y, et al. Increased PAI-1 in females compared with males is protective for abdominal aortic aneurysm formation in a rodent model. American journal of physiology Heart and circulatory physiology. 2012;302(7):H1378-86.

222. Di Gennaro A, Araujo AC, Busch A, Jin H, Wagsater D, Vorkapic E, et al. Cysteinyl leukotriene receptor 1 antagonism prevents experimental abdominal aortic aneurysm. Proceedings of the National Academy of Sciences of the United States of America. 2018;115(8):1907-12.

223. Wei Z, Wang Y, Zhang K, Liao Y, Ye P, Wu J, et al. Inhibiting the Th17/IL-17A-related inflammatory responses with digoxin confers protection against experimental abdominal aortic aneurysm. Arteriosclerosis, thrombosis, and vascular biology. 2014;34(11):2429-38.

224. Zhang Q, Huang JH, Xia RP, Duan XH, Jiang YB, Jiang Q, et al. Suppression of experimental abdominal aortic aneurysm in a rat model by the phosphodiesterase 3 inhibitor cilostazol. The Journal of surgical research. 2011;167(2):e385-93.

225. Bartoli MA, Parodi FE, Chu J, Pagano MB, Mao D, Baxter BT, et al. Localized administration of doxycycline suppresses aortic dilatation in an experimental mouse model of abdominal aortic aneurysm. Annals of vascular surgery. 2006;20(2):228-36.

226. Jin J, Arif B, Garcia-Fernandez F, Ennis TL, Davis EC, Thompson RW, et al. Novel mechanism of aortic aneurysm development in mice associated with smoking and leukocytes. Arteriosclerosis, thrombosis, and vascular biology. 2012;32(12):2901-9.

227. Lysgaard Poulsen J, Stubbe J, Lindholt JS. Animal Models Used to Explore Abdominal Aortic Aneurysms: A Systematic Review. European journal of vascular and endovascular surgery : the official journal of the European Society for Vascular Surgery. 2016;52(4):487-99.

228. Yoo YS, Park HS, Choi GH, Lee T. Recent Advances in the Development of Experimental Animal Models Mimicking Human Aortic Aneurysms. Vasc Specialist Int. 2015;31(1):1-10.

229. Andrews EJ, White WJ, Bullock LP. Spontaneous aortic aneurysms in blotchy mice. The American journal of pathology. 1975;78(2):199-210.

230. Rowe DW, McGoodwin EB, Martin GR, Grahn D. Decreased lysyl oxidase activity in the aneurysm-prone, mottled mouse. The Journal of biological chemistry. 1977;252(3):939-42.

231. Maki JM, Rasanen J, Tikkanen H, Sormunen R, Makikallio K, Kivirikko KI, et al. Inactivation of the lysyl oxidase gene Lox leads to aortic aneurysms, cardiovascular dysfunction, and perinatal death in mice. Circulation. 2002;106(19):2503-9.

232. Tangirala RK, Rubin EM, Palinski W. Quantitation of atherosclerosis in murine models: correlation between lesions in the aortic origin and in the entire aorta, and differences in the extent of lesions between sexes in LDL receptor-deficient and apolipoprotein E-deficient mice. Journal of lipid research. 1995;36(11):2320-8.

233. Gifford SM, Duncan AA, Greiten LE, Gloviczki P, Oderich GS, Kalra M, et al. The natural history and outcomes for thoracic and abdominal penetrating aortic ulcers. Journal of vascular surgery : official publication, the Society for Vascular Surgery [and] International Society for Cardiovascular Surgery, North American Chapter. 2016;63(5):1182-8.

234. Silence J, Collen D, Lijnen HR. Reduced atherosclerotic plaque but enhanced aneurysm formation in mice with inactivation of the tissue inhibitor of metalloproteinase-1 (TIMP-1) gene. Circulation research. 2002;90(8):897-903.

235. Whitbread T, Birch P, Rogers S, Majeed A, Rochester J, Beard JD, et al. A new animal model for abdominal aortic aneurysms:initial results using a multiple-wire stent. European journal of vascular and endovascular surgery : the official journal of the European Society for Vascular Surgery. 1996;11(1):90-7.

236. Vos AW, Linsen MA, Wisselink W, Rauwerda JA. Endovascular grafting of complex aortic aneurysms with a modular side branch stent-graft system in a porcine model. European journal of vascular and endovascular surgery : the official journal of the European Society for Vascular Surgery. 2004;27(5):492-7.

237. Riber SS, Ali M, Bergseth SH, Stubbe J, Stenger M, Behr-Rasmussen C, et al. Induction of autoimmune abdominal aortic aneurysm in pigs - A novel large animal model. Ann Med Surg (Lond). 2017;20:26-31.

238. Hynecek RL, DeRubertis BG, Trocciola SM, Zhang H, Prince MR, Ennis TL, et al. The creation of an infrarenal aneurysm within the native abdominal aorta of swine. Surgery. 2007;142(2):143-9.

239. Molacek J, Treska V, Kobr J, Certik B, Skalicky T, Kuntscher V, et al. Optimization of the model of abdominal aortic aneurysm--experiment in an animal model. J Vasc Res. 2009;46(1):1-5.

240. Kloster BO, Lund L, Lindholt JS. Induction of continuous expanding infrarenal aortic aneurysms in a large porcine animal model. Ann Med Surg (Lond). 2015;4(1):30-5.

241. Houdek K, Molacek J, Treska V, Krizkova V, Eberlova L, Boudova L, et al. Focal histopathological progression of porcine experimental abdominal aortic aneurysm is mitigated by atorvastatin. International angiology : a journal of the International Union of Angiology. 2013;32(3):291-306.

242. Czerski A, Bujok J, Gnus J, Hauzer W, Ratajczak K, Nowak M, et al. Experimental methods of abdominal aortic aneurysm creation in swine as a large animal model. Journal of physiology and pharmacology : an official journal of the Polish Physiological Society. 2013;64(2):185-92.

243. Lederman A, Saliture Neto FT, Ferreira R, de Figueiredo LF, Otoch JP, Aun R, et al. Endovascular model of abdominal aortic aneurysm induction in swine. Vasc Med. 2014;19(3):167-74.

244. Tian Y, Zhang W, Sun J, Zhai H, Yu Y, Qi X, et al. A reproducible swine model of proximal descending thoracic aortic aneurysm created with intra-adventitial application of elastase. Journal of vascular surgery : official publication, the Society for Vascular Surgery [and] International Society for Cardiovascular Surgery, North American Chapter. 2018;67(1):300-8 e2.

245. Shannon AH, Cullen JM, Dahl JJ, Scott EJ, Tyerman Z, Spinosa MD, et al. Porcine Model of Infrarenal Abdominal Aortic Aneurysm. Journal of visualized experiments : JoVE. 2019(153).

246. Lin JB, Phillips EH, Riggins TE, Sangha GS, Chakraborty S, Lee JY, et al. Imaging of small animal peripheral artery disease models: recent advancements and translational potential. International journal of molecular sciences. 2015;16(5):11131-77.

247. Goergen CJ, Johnson BL, Greve JM, Taylor CA, Zarins CK. Increased anterior abdominal aortic wall motion: possible role in aneurysm pathogenesis and design of endovascular devices. Journal of endovascular therapy : an official journal of the International Society of Endovascular Specialists. 2007;14(4):574-84.

248. Gandhi R, Cawthorne C, Craggs LJL, Wright JD, Domarkas J, He P, et al. Cell proliferation detected using [(18)F]FLT PET/CT as an early marker of abdominal aortic aneurysm. J Nucl Cardiol. 2019.

249. Botnar RM, Wiethoff AJ, Ebersberger U, Lacerda S, Blume U, Warley A, et al. In vivo assessment of aortic aneurysm wall integrity using elastin-specific molecular magnetic resonance imaging. Circ Cardiovasc Imaging. 2014;7(4):679-89.

250. Lu G, Su G, Davis JP, Schaheen B, Downs E, Roy RJ, et al. A novel chronic advanced stage abdominal aortic aneurysm murine model. Journal of vascular surgery : official publication, the Society for Vascular Surgery [and] International Society for Cardiovascular Surgery, North American Chapter. 2017;66(1):232-42 e4.

251. Simpson CF, Kling JM, Robbins RC, Harms RH. Beta-aminopropionitrile-induced aortic ruptures in turkeys: inhibition by reserpine and enhancement by monoamine oxidase inhibitors. Toxicol Appl Pharmacol. 1968;12(1):48-59.

252. Fashandi AZ, Hawkins RB, Salmon MD, Spinosa MD, Montgomery WG, Cullen JM, et al. A novel reproducible model of aortic aneurysm rupture. Surgery. 2018;163(2):397-403.

253. Fashandi AZ, Spinosa M, Salmon M, Su G, Montgomery W, Mast A, et al. Female Mice Exhibit Abdominal Aortic Aneurysm Protection in an Established Rupture Model. The Journal of surgical research. 2019.

254. Henriques TA, Huang J, D'Souza SS, Daugherty A, Cassis LA. Orchidectomy, but not ovariectomy, regulates angiotensin II-induced vascular diseases in apolipoprotein E-deficient mice. Endocrinology. 2004;145(8):3866-72.

255. Zhang X, Thatcher S, Wu C, Daugherty A, Cassis LA. Castration of male mice prevents the progression of established angiotensin II-induced abdominal aortic aneurysms. Journal of vascular surgery : official publication, the Society for Vascular Surgery [and] International Society for Cardiovascular Surgery, North American Chapter. 2015;61(3):767-76.

256. Ailawadi G, Eliason JL, Roelofs KJ, Sinha I, Hannawa KK, Kaldjian EP, et al. Gender differences in experimental aortic aneurysm formation. Arteriosclerosis, thrombosis, and vascular biology. 2004;24(11):2116-22.

257. Wu XF, Zhang J, Paskauskas S, Xin SJ, Duan ZQ. The role of estrogen in the formation of experimental abdominal aortic aneurysm. American journal of surgery. 2009;197(1):49-54.

258. Zhang X, Thatcher SE, Rateri DL, Bruemmer D, Charnigo R, Daugherty A, et al. Transient exposure of neonatal female mice to testosterone abrogates the sexual dimorphism of abdominal aortic aneurysms. Circulation research. 2012;110(11):e73-85.

259. Patelis N, Moris D, Schizas D, Damaskos C, Perrea D, Bakoyiannis C, et al. Animal models in the research of abdominal aortic aneurysms development. Physiol Res. 2017;66(6):899-915.

260. Busch A, Eken SM, Maegdefessel L. Prospective and therapeutic screening value of non-coding RNA as biomarkers in cardiovascular disease. Ann Transl Med. 2016;4(12):236.

261. Pennisi E. Genomics. ENCODE project writes eulogy for junk DNA. Science. 2012;337(6099):1159, 61.

262. Liu G, Mattick JS, Taft RJ. A meta-analysis of the genomic and transcriptomic composition of complex life. Cell Cycle. 2013;12(13):2061-72.

263. Arner E, Daub CO, Vitting-Seerup K, Andersson R, Lilje B, Drablos F, et al. Transcribed enhancers lead waves of coordinated transcription in transitioning mammalian cells. Science. 2015;347(6225):1010-4.

264.   Beaulieu CL, Majewski J, Schwartzentruber J, Samuels ME, Fernandez BA, Bernier FP, et al. FORGE Canada Consortium: outcomes of a 2-year national rare-disease gene-discovery project. Am J Hum Genet. 2014;94(6):809-17.

265.   Manolio TA, Brooks LD, Collins FS. A HapMap harvest of insights into the genetics of common disease. The Journal of clinical investigation. 2008;118(5):1590-605.

266.   Parasramka MA, Maji S, Matsuda A, Yan IK, Patel T. Long non-coding RNAs as novel targets for therapy in hepatocellular carcinoma. Pharmacol Ther. 2016;161:67-78.

267.   Lee RC, Feinbaum RL, Ambros V. The C. elegans heterochronic gene lin-4 encodes small RNAs with antisense complementarity to lin-14. Cell. 1993;75(5):843-54.

268.   Londin E, Loher P, Telonis AG, Quann K, Clark P, Jing Y, et al. Analysis of 13 cell types reveals evidence for the expression of numerous novel primate- and tissue-specific microRNAs. Proceedings of the National Academy of Sciences of the United States of America. 2015;112(10):E1106-15.

269.   Friedman RC, Farh KK, Burge CB, Bartel DP. Most mammalian mRNAs are conserved targets of microRNAs. Genome Res. 2009;19(1):92-105.

270.   Guil S, Esteller M. RNA-RNA interactions in gene regulation: the coding and noncoding players. Trends Biochem Sci. 2015;40(5):248-56.

271.   Jalali S, Bhartiya D, Lalwani MK, Sivasubbu S, Scaria V. Systematic transcriptome wide analysis of lncRNA-miRNA interactions. PloS one. 2013;8(2):e53823.

272.   Zampetaki A, Willeit P, Tilling L, Drozdov I, Prokopi M, Renard JM, et al. Prospective study on circulating MicroRNAs and risk of myocardial infarction. Journal of the American College of Cardiology. 2012;60(4):290-9.

273.   Ledda B, Ottaggio L, Izzotti A, Sukkar SG, Miele M. Small RNAs in eucaryotes: new clues for amplifying microRNA benefits. Cell Biosci. 2020;10:1.

274.   Sontheimer EJ, Carthew RW. Silence from within: endogenous siRNAs and miRNAs. Cell. 2005;122(1):9-12.

275.   Wang WT, Han C, Sun YM, Chen TQ, Chen YQ. Noncoding RNAs in cancer therapy resistance and targeted drug development. J Hematol Oncol. 2019;12(1):55.

276.   Gangwar RS, Rajagopalan S, Natarajan R, Deiuliis JA. Noncoding RNAs in Cardiovascular Disease: Pathological Relevance and Emerging Role as Biomarkers and Therapeutics. Am J Hypertens. 2018;31(2):150-65.

277.   Shi Q, Yang X. Circulating MicroRNA and Long Noncoding RNA as Biomarkers of Cardiovascular Diseases. Journal of cellular physiology. 2015.

278.   Derrien T, Johnson R, Bussotti G, Tanzer A, Djebali S, Tilgner H, et al. The GENCODE v7 catalog of human long noncoding RNAs: analysis of their gene structure, evolution, and expression. Genome Res. 2012;22(9):1775-89.

279.   Qu Z, Adelson DL. Evolutionary conservation and functional roles of ncRNA. Front Genet. 2012;3:205.

280.   Li X, Yang L, Chen LL. The Biogenesis, Functions, and Challenges of Circular RNAs. Molecular cell. 2018;71(3):428-42.

281.   Vo JN, Cieslik M, Zhang Y, Shukla S, Xiao L, Zhang Y, et al. The Landscape of Circular RNA in Cancer. Cell. 2019;176(4):869-81 e13.

282.   Wilusz JE. A 360 degrees view of circular RNAs: From biogenesis to functions. Wiley Interdiscip Rev RNA. 2018;9(4):e1478.

283.   Dong R, Ma XK, Chen LL, Yang L. Increased complexity of circRNA expression during species evolution. RNA Biol. 2017;14(8):1064-74.

284.	Liang D, Tatomer DC, Luo Z, Wu H, Yang L, Chen LL, et al. The Output of Protein-Coding Genes Shifts to Circular RNAs When the Pre-mRNA Processing Machinery Is Limiting. Molecular cell. 2017;68(5):940-54 e3.

285.	Esteller M. Non-coding RNAs in human disease. Nature reviews Genetics. 2011;12(12):861-74.

286.	Wong NK, Huang CL, Islam R, Yip SP. Long non-coding RNAs in hematological malignancies: translating basic techniques into diagnostic and therapeutic strategies. J Hematol Oncol. 2018;11(1):131.

287.	Rupaimoole R, Slack FJ. MicroRNA therapeutics: towards a new era for the management of cancer and other diseases. Nature reviews Drug discovery. 2017;16(3):203-22.

288.	Li Z, Rana TM. Therapeutic targeting of microRNAs: current status and future challenges. Nature reviews Drug discovery. 2014;13(8):622-38.

289.	Khvorova A, Watts JK. The chemical evolution of oligonucleotide therapies of clinical utility. Nat Biotechnol. 2017;35(3):238-48.

290.	Han DK, Khaing ZZ, Pollock RA, Haudenschild CC, Liau G. H19, a marker of developmental transition, is reexpressed in human atherosclerotic plaques and is regulated by the insulin family of growth factors in cultured rabbit smooth muscle cells. The Journal of clinical investigation. 1996;97(5):1276-85.

291.	Tai W. Current Aspects of siRNA Bioconjugate for In Vitro and In Vivo Delivery. Molecules. 2019;24(12).

292.	Adams D, Gonzalez-Duarte A, O'Riordan WD, Yang CC, Ueda M, Kristen AV, et al. Patisiran, an RNAi Therapeutic, for Hereditary Transthyretin Amyloidosis. The New England journal of medicine. 2018;379(1):11-21.

293.	Beer TM, Hotte SJ, Saad F, Alekseev B, Matveev V, Flechon A, et al. Custirsen (OGX-011) combined with cabazitaxel and prednisone versus cabazitaxel and prednisone alone in patients with metastatic castration-resistant prostate cancer previously treated with docetaxel (AFFINITY): a randomised, open-label, international, phase 3 trial. Lancet Oncol. 2017;18(11):1532-42.

294.	Kurreck J, Wyszko E, Gillen C, Erdmann VA. Design of antisense oligonucleotides stabilized by locked nucleic acids. Nucleic acids research. 2002;30(9):1911-8.

295.	Sekhon HS, London CA, Sekhon M, Iversen PL, Devi GR. c-MYC antisense phosphosphorodiamidate morpholino oligomer inhibits lung metastasis in a murine tumor model. Lung Cancer. 2008;60(3):347-54.

296.	Huang JL, Chen HZ, Gao XL. Lipid-coated calcium phosphate nanoparticle and beyond: a versatile platform for drug delivery. J Drug Target. 2018;26(5-6):398-406.

297.	Foster DJ, Brown CR, Shaikh S, Trapp C, Schlegel MK, Qian K, et al. Advanced siRNA Designs Further Improve In Vivo Performance of GalNAc-siRNA Conjugates. Mol Ther. 2018;26(3):708-17.

298.	Lv H, Zhang S, Wang B, Cui S, Yan J. Toxicity of cationic lipids and cationic polymers in gene delivery. J Control Release. 2006;114(1):100-9.

299.	Baker AT, Aguirre-Hernandez C, Hallden G, Parker AL. Designer Oncolytic Adenovirus: Coming of Age. Cancers (Basel). 2018;10(6).

300.	Harries LW. RNA Biology Provides New Therapeutic Targets for Human Disease. Front Genet. 2019;10:205.

301.	Wu ZY, Trenner M, Boon RA, Spin JM, Maegdefessel L. Long noncoding RNAs in key cellular processes involved in aortic aneurysms. Atherosclerosis. 2020;292:112-8.

302.	Leeper NJ, Maegdefessel L. Non-coding RNAs: key regulators of smooth muscle cell fate in vascular disease. Cardiovascular research. 2018;114(4):611-21.

303. Li Y, Maegdefessel L. Non-coding RNA Contribution to Thoracic and Abdominal Aortic Aneurysm Disease Development and Progression. Front Physiol. 2017;8:429.

304. Zheng C, Niu H, Li M, Zhang H, Yang Z, Tian L, et al. Cyclic RNA hsacirc000595 regulates apoptosis of aortic smooth muscle cells. Mol Med Rep. 2015;12(5):6656-62.

305. Teng L, Chen Y, Chen H, He X, Wang J, Peng Y, et al. Circular RNA hsa_circ_0021001 in peripheral blood: a potential novel biomarker in the screening of intracranial aneurysm. Oncotarget. 2017;8(63):107125-33.

306. Wang Y, Wang Y, Li Y, Wang B, Miao Z, Liu X, et al. Decreased expression of circ_0020397 in intracranial aneurysms may be contributing to decreased vascular smooth muscle cell proliferation via increased expression of miR-138 and subsequent decreased KDR expression. Cell Adh Migr. 2019;13(1):220-8.

307. Maegdefessel L, Azuma J, Toh R, Deng A, Merk DR, Raiesdana A, et al. MicroRNA-21 blocks abdominal aortic aneurysm development and nicotine-augmented expansion. Science translational medicine. 2012;4(122):122ra22.

308. Maegdefessel L, Spin JM, Raaz U, Eken SM, Toh R, Azuma J, et al. miR-24 limits aortic vascular inflammation and murine abdominal aneurysm development. Nature communications. 2014;5:5214.

309. Boon RA, Seeger T, Heydt S, Fischer A, Hergenreider E, Horrevoets AJ, et al. MicroRNA-29 in aortic dilation: implications for aneurysm formation. Circulation research. 2011;109(10):1115-9.

310. Maegdefessel L, Azuma J, Toh R, Merk DR, Deng A, Chin JT, et al. Inhibition of microRNA-29b reduces murine abdominal aortic aneurysm development. The Journal of clinical investigation. 2012;122(2):497-506.

311. Biros E, Moran CS, Wang Y, Walker PJ, Cardinal J, Golledge J. microRNA profiling in patients with abdominal aortic aneurysms: the significance of miR-155. Clin Sci (Lond). 2014;126(11):795-803.

312. Zampetaki A, Attia R, Mayr U, Gomes RS, Phinikaridou A, Yin X, et al. Role of miR-195 in aortic aneurysmal disease. Circulation research. 2014;115(10):857-66.

313. Kim CW, Kumar S, Son DJ, Jang IH, Griendling KK, Jo H. Prevention of abdominal aortic aneurysm by anti-microRNA-712 or anti-microRNA-205 in angiotensin II-infused mice. Arteriosclerosis, thrombosis, and vascular biology. 2014;34(7):1412-21.

314. Zhang L, Cheng H, Yue Y, Li S, Zhang D, He R. H19 knockdown suppresses proliferation and induces apoptosis by regulating miR-148b/WNT/beta-catenin in ox-LDL -stimulated vascular smooth muscle cells. J Biomed Sci. 2018;25(1):11.

315. Sun Y, Zhong L, He X, Wang S, Lai Y, Wu W, et al. LncRNA H19 promotes vascular inflammation and abdominal aortic aneurysm formation by functioning as a competing endogenous RNA. Journal of molecular and cellular cardiology. 2019;131:66-81.

316. Zhang Z, Zou G, Chen X, Lu W, Liu J, Zhai S, et al. Knockdown of lncRNA PVT1 Inhibits Vascular Smooth Muscle Cell Apoptosis and Extracellular Matrix Disruption in a Murine Abdominal Aortic Aneurysm Model. Mol Cells. 2019;42(3):218-27.

317. Hodos RA, Kidd BA, Shameer K, Readhead BP, Dudley JT. In silico methods for drug repurposing and pharmacology. Wiley Interdiscip Rev Syst Biol Med. 2016;8(3):186-210.

318. Schüler J. Die Biotechnologie-Industrie
Ein Einführungs-, Übersichtsund Nachschlagewerk: Springer Spektrum.

319. Forstner M, Eilenberg W, Simon F, Trenner M, Eckstein HH, Maegdefessel L, et al. „Drug repurposing" und „orphan drug usage" Neue Konzepte für die Gefäßchirurgie? Gefässchirurgie. 2019;7/2019.

320. Pallotta MT, Tascini G, Crispoldi R, Orabona C, Mondanelli G, Grohmann U, et al. Wolfram syndrome, a rare neurodegenerative disease: from pathogenesis to future treatment perspectives. Journal of translational medicine. 2019;17(1):238.

321. Bissler JJ, Kingswood JC, Radzikowska E, Zonnenberg BA, Belousova E, Frost MD, et al. Everolimus long-term use in patients with tuberous sclerosis complex: Four-year update of the EXIST-2 study. PloS one. 2017;12(8):e0180939.

322. Zanin M, Chorbev I, Stres B, Stalidzans E, Vera J, Tieri P, et al. Community effort endorsing multiscale modelling, multiscale data science and multiscale computing for systems medicine. Brief Bioinform. 2019;20(3):1057-62.

323. Sun P, Guo J, Winnenburg R, Baumbach J. Drug repurposing by integrated literature mining and drug-gene-disease triangulation. Drug Discov Today. 2017;22(4):615-9.

324. Jin G, Wong ST. Toward better drug repositioning: prioritizing and integrating existing methods into efficient pipelines. Drug Discov Today. 2014;19(5):637-44.

325. Agrawal S, Vamadevan P, Mazibuko N, Bannister R, Swery R, Wilson S, et al. A New Method for Ethical and Efficient Evidence Generation for Off-Label Medication Use in Oncology (A Case Study in Glioblastoma). Front Pharmacol. 2019;10:681.

326. Burton M. "Repurposing" off-patent drugs offers big hopes of new treatments. The Economist. 2019.

327. Katsanos K, Spiliopoulos S, Kitrou P, Krokidis M, Karnabatidis D. Risk of Death Following Application of Paclitaxel-Coated Balloons and Stents in the Femoropopliteal Artery of the Leg: A Systematic Review and Meta-Analysis of Randomized Controlled Trials. Journal of the American Heart Association. 2018;7(24):e011245.

328. Fujimura N, Xiong J, Kettler EB, Xuan H, Glover KJ, Mell MW, et al. Metformin treatment status and abdominal aortic aneurysm disease progression. Journal of vascular surgery : official publication, the Society for Vascular Surgery [and] International Society for Cardiovascular Surgery, North American Chapter. 2016;64(1):46-54 e8.

329. Golledge J, Morris DR, Pinchbeck J, Rowbotham S, Jenkins J, Bourke M, et al. Editor's Choice - Metformin Prescription is Associated with a Reduction in the Combined Incidence of Surgical Repair and Rupture Related Mortality in Patients with Abdominal Aortic Aneurysm. European journal of vascular and endovascular surgery : the official journal of the European Society for Vascular Surgery. 2019;57(1):94-101.

330. Inoue K, Mizuo H, Kawaguchi S, Fukuda K, Kusano K, Yoshimura T. Oxidative metabolic pathway of lenvatinib mediated by aldehyde oxidase. Drug Metab Dispos. 2014;42(8):1326-33.

331. Wiegering A, Korb D, Thalheimer A, Kammerer U, Allmanritter J, Matthes N, et al. E7080 (lenvatinib), a multi-targeted tyrosine kinase inhibitor, demonstrates antitumor activities against colorectal cancer xenografts. Neoplasia. 2014;16(11):972-81.

332. Yamada K, Yamamoto N, Yamada Y, Nokihara H, Fujiwara Y, Hirata T, et al. Phase I dose-escalation study and biomarker analysis of E7080 in patients with advanced solid tumors. Clin Cancer Res. 2011;17(8):2528-37.

333. Agency EM. Lenvima Product sheet. 2015.

334. Motzer RJ, Hutson TE, Glen H, Michaelson MD, Molina A, Eisen T, et al. Lenvatinib, everolimus, and the combination in patients with metastatic renal cell carcinoma: a randomised, phase 2, open-label, multicentre trial. Lancet Oncol. 2015;16(15):1473-82.

335. Kudo M, Finn RS, Qin S, Han KH, Ikeda K, Piscaglia F, et al. Lenvatinib versus sorafenib in first-line treatment of patients with unresectable hepatocellular carcinoma: a randomised phase 3 non-inferiority trial. Lancet. 2018;391(10126):1163-73.

336. Haddad RI, Schlumberger M, Wirth LJ, Sherman EJ, Shah MH, Robinson B, et al. Incidence and timing of common adverse events in Lenvatinib-treated patients from the SELECT trial and their association with survival outcomes. Endocrine. 2017;56(1):121-8.

337. Baek Moller N, Budolfsen C, Grimm D, Kruger M, Infanger M, Wehland M, et al. Drug-Induced Hypertension Caused by Multikinase Inhibitors (Sorafenib, Sunitinib, Lenvatinib and Axitinib) in Renal Cell Carcinoma Treatment. International journal of molecular sciences. 2019;20(19).

338. Yu ST, Ge JN, Luo JY, Wei ZG, Sun BH, Lei ST. Treatment-related adverse effects with TKIs in patients with advanced or radioiodine refractory differentiated thyroid carcinoma: a systematic review and meta-analysis. Cancer Manag Res. 2019;11:1525-32.

339. Zhu C, Ma X, Hu Y, Guo L, Chen B, Shen K, et al. Safety and efficacy profile of lenvatinib in cancer therapy: a systematic review and meta-analysis. Oncotarget. 2016;7(28):44545-57.

340. Oshima Y, Tanimoto T, Yuji K, Tojo A. Association Between Aortic Dissection and Systemic Exposure of Vascular Endothelial Growth Factor Pathway Inhibitors in the Japanese Adverse Drug Event Report Database. Circulation. 2017;135(8):815-7.

341. Faughnan ME, Gossage JR, Chakinala MM, Oh SP, Kasthuri R, Hughes CCW, et al. Pazopanib may reduce bleeding in hereditary hemorrhagic telangiectasia. Angiogenesis. 2019;22(1):145-55.

342. Vorkapic E, Dugic E, Vikingsson S, Roy J, Mayranpaa MI, Eriksson P, et al. Imatinib treatment attenuates growth and inflammation of angiotensin II induced abdominal aortic aneurysm. Atherosclerosis. 2016;249:101-9.

343. Obama T, Tsuji T, Kobayashi T, Fukuda Y, Takayanagi T, Taro Y, et al. Epidermal growth factor receptor inhibitor protects against abdominal aortic aneurysm in a mouse model. Clin Sci (Lond). 2015;128(9):559-65.

344. Park KS, Mitra A, Rahat B, Kim K, Pfeifer K. Loss of imprinting mutations define both distinct and overlapping roles for misexpression of IGF2 and of H19 lncRNA. Nucleic acids research. 2017;45(22):12766-79.

345. Wickham H. ggplot2: Elegant Graphics for Data Analysis: Springer-Verlag New York; 2016.

346. Pelisek J, Hegenloh R, Bauer S, Metschl S, Pauli J, Glukha N, et al. Biobanking: Objectives, Requirements, and Future Challenges-Experiences from the Munich Vascular Biobank. J Clin Med. 2019;8(2).

347. Pfaffl MW. A new mathematical model for relative quantification in real-time RT-PCR. Nucleic acids research. 2001;29(9):e45.

348. Riches K, Clark E, Helliwell RJ, Angelini TG, Hemmings KE, Bailey MA, et al. Progressive Development of Aberrant Smooth Muscle Cell Phenotype in Abdominal Aortic Aneurysm Disease. J Vasc Res. 2018;55(1):35-46.

349. Sachdeva J, Mahajan A, Cheng J, Baeten JT, Lilly B, Kuivaniemi H, et al. Smooth muscle cell-specific Notch1 haploinsufficiency restricts the progression of abdominal aortic aneurysm by modulating CTGF expression. PloS one. 2017;12(5):e0178538.

350. Peng H, Zhang K, Liu Z, Xu Q, You B, Li C, et al. VPO1 Modulates Vascular Smooth Muscle Cell Phenotypic Switch by Activating Extracellular Signal-regulated Kinase 1/2 (ERK 1/2) in Abdominal Aortic Aneurysms. Journal of the American Heart Association. 2018;7(17):e010069.

351.   Davis BT, Wang XJ, Rohret JA, Struzynski JT, Merricks EP, Bellinger DA, et al. Targeted disruption of LDLR causes hypercholesterolemia and atherosclerosis in Yucatan miniature pigs. PloS one. 2014;9(4):e93457.

352.   Li Y, Busch A, Hong J, Bäcklund A, Chernogubova E, Eken S, et al. H19 induces abdominal aortic aneurysm development and progression. Circulation. 2018;CIRCULATIONAHA/2017/032184R2(in press).

353.   Cabanillas ME, Habra MA. Lenvatinib: Role in thyroid cancer and other solid tumors. Cancer Treat Rev. 2016;42:47-55.

354.   Choke E, Cockerill GW, Dawson J, Howe F, Wilson WR, Loftus IM, et al. Vascular endothelial growth factor enhances angiotensin II-induced aneurysm formation in apolipoprotein E-deficient mice. Journal of vascular surgery : official publication, the Society for Vascular Surgery [and] International Society for Cardiovascular Surgery, North American Chapter. 2010;52(1):159-66 e1.

355.   Tedesco MM, Terashima M, Blankenberg FG, Levashova Z, Spin JM, Backer MV, et al. Analysis of in situ and ex vivo vascular endothelial growth factor receptor expression during experimental aortic aneurysm progression. Arteriosclerosis, thrombosis, and vascular biology. 2009;29(10):1452-7.

356.   Miwa K, Nakashima H, Aoki M, Miyake T, Kawasaki T, Iwai M, et al. Inhibition of ets, an essential transcription factor for angiogenesis, to prevent the development of abdominal aortic aneurysm in a rat model. Gene Ther. 2005;12(14):1109-18.

357.   Liu K, Fang C, Shen Y, Liu Z, Zhang M, Ma B, et al. Hypoxia-inducible factor 1a induces phenotype switch of human aortic vascular smooth muscle cell through PI3K/AKT/AEG-1 signaling. Oncotarget. 2017;8(20):33343-52.

358.   Petsophonsakul P, Furmanik M, Forsythe R, Dweck M, Schurink GW, Natour E, et al. Role of Vascular Smooth Muscle Cell Phenotypic Switching and Calcification in Aortic Aneurysm Formation. Arteriosclerosis, thrombosis, and vascular biology. 2019;39(7):1351-68.

359.   Yokoyama U, Arakawa N, Ishiwata R, Yasuda S, Minami T, Goda M, et al. Proteomic analysis of aortic smooth muscle cell secretions reveals an association of myosin heavy chain 11 with abdominal aortic aneurysm. American journal of physiology Heart and circulatory physiology. 2018;315(4):H1012-H8.

360.   Kurtelius A, Vantti N, Rezai Jahromi B, Tahtinen O, Manninen H, Koskenvuo J, et al. Association of Intracranial Aneurysms With Aortic Aneurysms in 125 Patients With Fusiform and 4253 Patients With Saccular Intracranial Aneurysms and Their Family Members and Population Controls. Journal of the American Heart Association. 2019;8(18):e013277.

361.   Yeung KK, Bogunovic N, Keekstra N, Beunders AA, Pals J, van der Kuij K, et al. Transdifferentiation of Human Dermal Fibroblasts to Smooth Muscle-Like Cells to Study the Effect of MYH11 and ACTA2 Mutations in Aortic Aneurysms. Human mutation. 2017;38(4):439-50.

362.   Li G, Qin L, Wang L, Li X, Caulk AW, Zhang J, et al. Inhibition of the mTOR pathway in abdominal aortic aneurysm: implications of smooth muscle cell contractile phenotype, inflammation, and aneurysm expansion. American journal of physiology Heart and circulatory physiology. 2017;312(6):H1110-H9.

363.   Cho BS, Woodrum DT, Roelofs KJ, Stanley JC, Henke PK, Upchurch GR, Jr. Differential regulation of aortic growth in male and female rodents is associated with AAA development. The Journal of surgical research. 2009;155(2):330-8.

364.   Oliveira NFG, Goncalves FB, Ultee K, Pinto JP, Josee van Rijn M, Raa ST, et al. Patients with large neck diameter have a higher risk of type IA endoleaks and aneurysm rupture after standard endovascular aneurysm repair. Journal of vascular

surgery : official publication, the Society for Vascular Surgery [and] International Society for Cardiovascular Surgery, North American Chapter. 2019;69(3):783-91.

365. Bryce Y, Kim W, Katzen B, Benenati J, Samuels S. Outcomes over Time in Patients with Hostile Neck Anatomy Undergoing Endovascular Repair of Abdominal Aortic Aneurysm. Journal of vascular and interventional radiology : JVIR. 2018;29(7):1011-6.

366. Pichi F, Morara M, Torrazza C, Manzi G, Alkabes M, Balducci N, et al. Intravitreal bevacizumab for macular complications from retinal arterial macroaneurysms. Am J Ophthalmol. 2013;155(2):287-94 e1.

367. Xu L, Wang B, Ding W. Abdominal aortic dissection during sorafenib therapy for hepatocellular carcinoma. Clin Res Hepatol Gastroenterol. 2017;41(2):e24-e5.

368. Shweiki D, Itin A, Soffer D, Keshet E. Vascular endothelial growth factor induced by hypoxia may mediate hypoxia-initiated angiogenesis. Nature. 1992;359(6398):843-5.

369. Imanirad P, Dzierzak E. Hypoxia and HIFs in regulating the development of the hematopoietic system. Blood Cells Mol Dis. 2013;51(4):256-63.

370. Menges AL, Busch A, Reutersberg B, Trenner M, Kath P, Chernogubova E, et al. The structural atrophy of the aneurysm wall in secondary expanding aortic aneurysms with endoleak type II. Journal of vascular surgery : official publication, the Society for Vascular Surgery [and] International Society for Cardiovascular Surgery, North American Chapter. 2019.

371. Blassova T, Tonar Z, Tomasek P, Hosek P, Hollan I, Treska V, et al. Inflammatory cell infiltrates, hypoxia, vascularization, pentraxin 3 and osteoprotegerin in abdominal aortic aneurysms - A quantitative histological study. PloS one. 2019;14(11):e0224818.

372. Egger M, Schgoer W, Beer AG, Jeschke J, Leierer J, Theurl M, et al. Hypoxia up-regulates the angiogenic cytokine secretoneurin via an HIF-1alpha- and basic FGF-dependent pathway in muscle cells. FASEB J. 2007;21(11):2906-17.

373. Barnes EA, Chen CH, Sedan O, Cornfield DN. Loss of smooth muscle cell hypoxia inducible factor-1alpha underlies increased vascular contractility in pulmonary hypertension. FASEB J. 2017;31(2):650-62.

374. Shan F, Huang Z, Xiong R, Huang QY, Li J. HIF1alpha-induced upregulation of KLF4 promotes migration of human vascular smooth muscle cells under hypoxia. Journal of cellular physiology. 2020;235(1):141-50.

375. Kyotani Y, Takasawa S, Yoshizumi M. Proliferative Pathways of Vascular Smooth Muscle Cells in Response to Intermittent Hypoxia. International journal of molecular sciences. 2019;20(11).

376. Takahara Y, Tokunou T, Kojima H, Hirooka Y, Ichiki T. Deletion of hypoxia-inducible factor-1alpha in myeloid lineage exaggerates angiotensin II-induced formation of abdominal aortic aneurysm. Clin Sci (Lond). 2017;131(7):609-20.

377. Imanishi M, Chiba Y, Tomita N, Matsunaga S, Nakagawa T, Ueno M, et al. Hypoxia-Inducible Factor-1alpha in Smooth Muscle Cells Protects Against Aortic Aneurysms-Brief Report. Arteriosclerosis, thrombosis, and vascular biology. 2016;36(11):2158-62.

378. Wan J, Lata C, Santilli A, Green D, Roy S, Santilli S. Supplemental oxygen reverses hypoxia-induced smooth muscle cell proliferation by modulating HIF-alpha and VEGF levels in a rabbit arteriovenous fistula model. Annals of vascular surgery. 2014;28(3):725-36.

379. Perrucci GL, Rurali E, Gowran A, Pini A, Antona C, Chiesa R, et al. Vascular smooth muscle cells in Marfan syndrome aneurysm: the broken bricks in the aortic wall. Cell Mol Life Sci. 2017;74(2):267-77.

380.	Marinelli Busilacchi E, Costantini A, Viola N, Costantini B, Olivieri J, Butini L, et al. Immunomodulatory Effects of Tyrosine Kinase Inhibitor In Vitro and In Vivo Study. Biol Blood Marrow Transplant. 2018;24(2):267-75.

381.	Buro C, Beckmann S, Oliveira KC, Dissous C, Cailliau K, Marhofer RJ, et al. Imatinib treatment causes substantial transcriptional changes in adult Schistosoma mansoni in vitro exhibiting pleiotropic effects. PLoS Negl Trop Dis. 2014;8(6):e2923.

382.	Duignan IJ, Corcoran E, Pennello A, Plym MJ, Amatulli M, Claros N, et al. Pleiotropic stromal effects of vascular endothelial growth factor receptor 2 antibody therapy in renal cell carcinoma models. Neoplasia. 2011;13(1):49-59.

383.	Touyz RM, Herrmann SMS, Herrmann J. Vascular toxicities with VEGF inhibitor therapies-focus on hypertension and arterial thrombotic events. J Am Soc Hypertens. 2018;12(6):409-25.

384.	Wrana JL, Attisano L, Carcamo J, Zentella A, Doody J, Laiho M, et al. TGF beta signals through a heteromeric protein kinase receptor complex. Cell. 1992;71(6):1003-14.

385.	Wharton K, Derynck R. TGFbeta family signaling: novel insights in development and disease. Development. 2009;136(22):3691-7.

386.	MacFarlane EG, Haupt J, Dietz HC, Shore EM. TGF-beta Family Signaling in Connective Tissue and Skeletal Diseases. Cold Spring Harb Perspect Biol. 2017;9(11).

387.	Takeda N, Hara H, Fujiwara T, Kanaya T, Maemura S, Komuro I. TGF-beta Signaling-Related Genes and Thoracic Aortic Aneurysms and Dissections. International journal of molecular sciences. 2018;19(7).

388.	Jones A, Deb R, Torsney E, Howe F, Dunkley M, Gnaneswaran Y, et al. Rosiglitazone reduces the development and rupture of experimental aortic aneurysms. Circulation. 2009;119(24):3125-32.

389.	Tao J, Barnett JV, Watanabe M, Ramirez-Bergeron D. Hypoxia Supports Epicardial Cell Differentiation in Vascular Smooth Muscle Cells through the Activation of the TGFbeta Pathway. J Cardiovasc Dev Dis. 2018;5(2).

390.	Shi X, Guo LW, Seedial SM, Si Y, Wang B, Takayama T, et al. TGF-beta/Smad3 inhibit vascular smooth muscle cell apoptosis through an autocrine signaling mechanism involving VEGF-A. Cell Death Dis. 2014;5:e1317.

391.	Morisaki K, Furuyama T, Yoshiya K, Kurose S, Yoshino S, Nakayama K, et al. Frailty in patients with abdominal aortic aneurysm predicts prognosis after elective endovascular aneurysm repair. Journal of vascular surgery : official publication, the Society for Vascular Surgery [and] International Society for Cardiovascular Surgery, North American Chapter. 2019.

392.	De Martino RR, Brooke BS, Robinson W, Schanzer A, Indes JE, Wallaert JB, et al. Designation as "unfit for open repair" is associated with poor outcomes after endovascular aortic aneurysm repair. Circ Cardiovasc Qual Outcomes. 2013;6(5):575-81.

393.	Eslami MH, Rybin DV, Doros G, Siracuse JJ, Farber A. External validation of Vascular Study Group of New England risk predictive model of mortality after elective abdominal aorta aneurysm repair in the Vascular Quality Initiative and comparison against established models. Journal of vascular surgery : official publication, the Society for Vascular Surgery [and] International Society for Cardiovascular Surgery, North American Chapter. 2018;67(1):143-50.

394.	Grant SW, Hickey GL, Grayson AD, Mitchell DC, McCollum CN. National risk prediction model for elective abdominal aortic aneurysm repair. The British journal of surgery. 2013;100(5):645-53.

395.	Brown LC, Thompson SG, Greenhalgh RM, Powell JT, Participants UKSAT. Fit patients with small abdominal aortic aneurysms (AAAs) do not benefit from early

intervention. Journal of vascular surgery : official publication, the Society for Vascular Surgery [and] International Society for Cardiovascular Surgery, North American Chapter. 2008;48(6):1375-81.

396.   Rosenfield K, Jaff MR, White CJ, Rocha-Singh K, Mena-Hurtado C, Metzger DC, et al. Trial of a Paclitaxel-Coated Balloon for Femoropopliteal Artery Disease. The New England journal of medicine. 2015;373(2):145-53.

397.   Behrendt CA, Sedrakyan A, Peters F, Kreutzburg T, Schermerhorn M, Bertges DJ, et al. Long Term Survival after Femoropopliteal Artery Revascularisation with Paclitaxel Coated Devices: A Propensity Score Matched Cohort Analysis. European journal of vascular and endovascular surgery : the official journal of the European Society for Vascular Surgery. 2020.

398.   Crooke ST, Witztum JL, Bennett CF, Baker BF. RNA-Targeted Therapeutics. Cell Metab. 2018;27(4):714-39.

399.   Desai N, Trieu V, Yao Z, Louie L, Ci S, Yang A, et al. Increased antitumor activity, intratumor paclitaxel concentrations, and endothelial cell transport of cremophor-free, albumin-bound paclitaxel, ABI-007, compared with cremophor-based paclitaxel. Clin Cancer Res. 2006;12(4):1317-24.

400.   Zarrouk M, Lundqvist A, Holst J, Troeng T, Gottsater A. Cost-effectiveness of Screening for Abdominal Aortic Aneurysm in Combination with Medical Intervention in Patients with Small Aneurysms. European journal of vascular and endovascular surgery : the official journal of the European Society for Vascular Surgery. 2016;51(6):766-73.

401.   Nair N, Kvizhinadze G, Jones GT, Rush R, Khashram M, Roake J, et al. Health gains, costs and cost-effectiveness of a population-based screening programme for abdominal aortic aneurysms. The British journal of surgery. 2019;106(8):1043-54.

402.   Canning P, Tawfick W, Whelan N, Hynes N, Sultan S. Cost-effectiveness analysis of endovascular versus open repair of abdominal aortic aneurysm in a high-volume center. Journal of vascular surgery : official publication, the Society for Vascular Surgery [and] International Society for Cardiovascular Surgery, North American Chapter. 2019;70(2):485-96.

403.   Burgers LT, Vahl AC, Severens JL, Wiersema AM, Cuypers PW, Verhagen HJ, et al. Cost-effectiveness of Elective Endovascular Aneurysm Repair Versus Open Surgical Repair of Abdominal Aortic Aneurysms. European journal of vascular and endovascular surgery : the official journal of the European Society for Vascular Surgery. 2016;52(1):29-40.

404.   Michel M, Becquemin JP, Marzelle J, Quelen C, Durand-Zaleski I, participants WT. Editor's Choice - A Study of the Cost-effectiveness of Fenestrated/branched EVAR Compared with Open Surgery for Patients with Complex Aortic Aneurysms at 2 Years. European journal of vascular and endovascular surgery : the official journal of the European Society for Vascular Surgery. 2018;56(1):15-21.

405.   Lederle FA, Stroupe KT, Open Versus Endovascular Repair Veterans Affairs Cooperative Study G. Cost-effectiveness at two years in the VA Open Versus Endovascular Repair Trial. European journal of vascular and endovascular surgery : the official journal of the European Society for Vascular Surgery. 2012;44(6):543-8.

406.   Min SI, Min SK, Ahn S, Kim SM, Park D, Park T, et al. Comparison of costs of endovascular repair versus open surgical repair for abdominal aortic aneurysm in Korea. J Korean Med Sci. 2012;27(4):416-22.

407.   Lederle FA, Stroupe KT, Kyriakides TC, Ge L, Freischlag JA, Open vs Endovascular Repair Veterans Affairs Cooperative Study G. Long-term Cost-effectiveness in the Veterans Affairs Open vs Endovascular Repair Study of Aortic

Abdominal Aneurysm: A Randomized Clinical Trial. JAMA Surg. 2016;151(12):1139-44.

408.	Humphries MD, Suckow BD, Binks JT, McAdam-Marx C, Kraiss LW. Elective Endovascular Aortic Aneurysm Repair Continues to Cost More than Open Abdominal Aortic Aneurysm Repair. Annals of vascular surgery. 2017;39:111-8.

409.	Epstein D, Sculpher MJ, Powell JT, Thompson SG, Brown LC, Greenhalgh RM. Long-term cost-effectiveness analysis of endovascular versus open repair for abdominal aortic aneurysm based on four randomized clinical trials. The British journal of surgery. 2014;101(6):623-31.

410.	Oliveira-Pinto J, Oliveira N, Bastos-Goncalves F, Hoeks S, MJ VANR, Ten Raa S, et al. Long-term results of outside "instructions for use" EVAR. The Journal of cardiovascular surgery. 2017;58(2):252-60.

411.	Charbonneau P, Hongku K, Herman CR, Habib M, Girsowicz E, Doonan RJ, et al. Long-term survival after endovascular and open repair in patients with anatomy outside instructions for use criteria for endovascular aneurysm repair. Journal of vascular surgery : official publication, the Society for Vascular Surgery [and] International Society for Cardiovascular Surgery, North American Chapter. 2019;70(6):1823-30.

412.	Sirignano P, Mansour W, Capoccia L, Cuozzo S, Camparini S, de Donato G, et al. Immediate results of the expanding indications for treatment with standard EVAR in patients with challenging anatomies, a multi-centric prospective evaluation - EXTREME Study. EuroIntervention. 2019.

413.	O'Brien-Irr MS, Harris LM, Dosluoglu HH, Cherr GS, Rivero M, Noor S, et al. Factors that affect cost and clinical outcome of endovascular aortic repair for abdominal aortic aneurysm. Journal of vascular surgery : official publication, the Society for Vascular Surgery [and] International Society for Cardiovascular Surgery, North American Chapter. 2017;65(4):997-1005.

414.	AbuRahma AF, Yacoub M, Mousa AY, Abu-Halimah S, Hass SM, Kazil J, et al. Aortic Neck Anatomic Features and Predictors of Outcomes in Endovascular Repair of Abdominal Aortic Aneurysms Following vs Not Following Instructions for Use. Journal of the American College of Surgeons. 2016;222(4):579-89.

415.	Falkensammer J, Hakaim AG, Andrew Oldenburg W, Neuhauser B, Paz-Fumagalli R, McKinney JM, et al. Natural history of the iliac arteries after endovascular abdominal aortic aneurysm repair and suitability of ectatic iliac arteries as a distal sealing zone. Journal of endovascular therapy : an official journal of the International Society of Endovascular Specialists. 2007;14(5):619-24.